Activation of Natural Killer Cells by Oncolytic Viruses

Michelle Hannah Wantoch

Submitted in accordance with the requirements for the degree of
Doctor of Philosophy

The University of Leeds

Faculty of Medicine and Health

School of Medicine

April 2018

Acknowledgements

Abstract

Natural killer (NK) cells protect the host against intracellular infection and cancer. These properties are exploited in oncolytic virus (OV) therapy, where anti-viral responses result in enhanced anti-tumour immunity. This study investigated the mechanisms by which reovirus, an oncolytic dsRNA virus, modulates human NK cell activity, in an *in vitro* model. Activation of NK cells within PBMC was dependent on soluble type I interferons (IFN-I). Blocking experiments and signalling pathway analysis support a model in which IFN-I acts directly on NK cells to activate them, inducing phosphorylation of signal transducer and activator of transcription 1 (STAT1) and STAT4. Microarray transcriptome profiling revealed the upregulation of genes involved in several relevant pathways: IFN-I signalling, granule and granule independent NK cytotoxicity, migration and proliferation. However, despite upregulation of cell cycle associated genes, NK cells did not proliferate in response to reovirus. In fact, priming with reovirus inhibited NK cell proliferation in response to the mitogenic cytokine interleukin 15 (IL-15). Further analysis showed that reovirus priming blocked the IL-15 induced accumulation of cell cycle proteins and inhibited Akt signalling. Inhibition of proliferation was dependent on IFN-I, demonstrating that interferon can have both stimulatory and inhibitory effects on NK cells in the context of oncolytic virus therapy. The observed upregulation of cell cycle associated genes during reovirus treatment might be due to the activation of a separate, pro-proliferative pathway, which is opposed by high levels of IFN-I. These results define a pathway of NK cell activation during oncolytic reovirus treatment, and show that OV treatment acts on the spectrum of NK cell activity.

Table of Contents

List of Tables

List of Figures

Abbreviations

ADCC	Antibody-dependent cell-mediated cytotoxicity
AF	Alexa Fluor
ALL	Acute lymphoblastic leukaemia
ANOVA	Analysis of variance
APC	Antigen presenting cell
APS	Ammonium persulfate
BLD	Below limit of detection
BM-MSC	Bone marrow-derived mesenchymal stromal cells
BSA	Bovine serum albumin
CCNA/B	Gene for Cyclin A/B
CD	Cluster of differentiation
CDK	Cyclin dependent kinase
cDNA	Complementary DNA
CFSE	Carboxyfluorescein succinimidyl ester
CM	Conditioned media
Ct	Cycle threshold
DAP10	DNAX activation protein of 10kDa
DAP12	DNAX activation protein of 12kDa
DC	Dendritic cell
DMEM	Dulbecco's Modified Eagle Medium
DNAM-1	DNAX accessory molecule-1, CD226
dsRNA	Double stranded RNA
ECL	Enhanced chemiluminescence
EDTA	Ethylenediaminetetraacetic acid
ELISA	Enzyme-linked immunosorbent assay
FACS	Fluorescence-activated cell sorting
FasL	Fas ligand

FcR	Fc receptor
FBS/FCS	Foetal bovine serum/calf serum
FDA	Food and Drug Administration
FDR	False discovery rate
FITC	Fluorescein
FSC	Forward scatter
GM-CSF	Granulocyte macrophage colony stimulating factor
HCMV	Human cytomegalovirus
HEV	High endothelial venules
HLA	Human leukocyte antigen
HSC	Haematopoietic stem cell
HSV	Herpes simplex virus
HTA	Human transcriptome array
ICAM-1	Intracellular adhesion molecule 1
IFN	Interferon
IFN-I	Type I interferon
IFNAR	Interferon α/β receptor
Ig	Immunoglobulin
IL	Interleukin
ILC	Innate lymphoid cell
IRF9	Interferon regulatory factor 9
ISG	Interferon stimulated gene
ISGF3	Interferon stimulated gene factor 3
ITAM	Immunoreceptor tyrosine-based activation motif
ITIM	Immunoreceptor tyrosine-based inhibitory motif
IU	International unit
JAK	Janus-associated kinase
JAM-A	Junctional adhesion molecule-A
kDa	Kilodalton
KIR	Killer cell immunoglobulin receptor

LCMV	Lymphocytic choriomeningitis virus
LoB	Limit of blank
LoD	Limit of detection
LPS	Lipopolysaccharide
MAPK	Mitogen-activated protein kinase
MCM4	minichromosome maintenance complex 4
MCMV	Murine cytomegalovirus
MCP-1	Monocyte chemoattractant protein-1
MDA5	melanoma differentiation-associated 5
MDSC	Myeloid-derived suppressor cell
MFI	Median fluorescence intensity
MHC	Major histocompatibility complex
MIC A	MHC class I polypeptide-related sequence A
MIC B	MHC class I polypeptide-related sequence B
MIP-1α	Macrophage inflammatory protein 1 alpha
MOI	Multiplicity of infection
mRNA	Messenger RNA
mTOR	Mammalian target of rapamycin
MV	Measles virus
NS	Not significant
NIR	Near infrared
NK	Natural killer
NKp46	Natural cytotoxicity triggering receptor 1; NCR1, CD335
OV	Oncolytic virus
PAMP	Pathogen associated molecular pattern

PBMC	Peripheral blood mononuclear cells
PBNK	NK cells within PBMC
PBS	Phosphate buffered saline
PCNA	Proliferating cell nuclear antigen
PCR	Polymerase chain reaction
PE	Phycoerythrin
PI	Propidium iodide
PI3K	Phosphoinositide 3-kinase
Poly(I:C)	Polyinosinic:polycytidylic acid
PRR	Pattern recognition receptor
pSTAT	Phosphorylated STAT
PTEN	Phosphatase and tensin homolog
PVDF	Polyvinylidene difluoride
Reo	Reovirus
RIG-I	Retinoic acid-inducible gene 1
RIPA	Radioimmunoprecipitation assay buffer
RPMI	Roswell Park Memorial Institute medium
RT	Room temperature
S1P	Sphingosine 1 phosphate
S1PR	Sphingosine 1 phosphate receptor
SD	Standard deviation
SDS-PAGE	Sodium dodecyl sulphate polyacrylamide gel electrophoresis
SELL	L- selectin/CD62L gene
SH2	Src homology 2
SLE	Systemic lupus erythematosus
SOCS	Suppressor of cytokine signalling
SSC	Side scatter
SST-RMA	Signal Space Transformation-Robust Multi-Chip Analysis

STAT	Signal transducer and activator of transcription
TBS	Tris buffered saline
TBST	Tris buffered saline with tween
TCR	T-cell receptor
TEMED	Tetramethylethylenediamine
TGF-β	Transforming growth factor beta
TLR	Toll like receptor
TNF	Tumour necrosis factor
TRAIL	TNF-related apoptosis-inducing ligand
T-VEC	Talimogene laherparepvec
TYK2	Tyrosine kinase 2
ULBP	UL16 binding protein
v/v	Volume per volume
w/v	Weight per volume

Chapter 1. Introduction

1.1 Immune system

1.1.1 Innate and adaptive immunity

The mammalian immune system is complex, consisting of numerous specialised cell types, adapted for diverse roles within the body. These cell types are typically grouped into either the adaptive or the innate immune system. While the adaptive immune system responds to specific antigens from invading pathogens, the innate system can respond non-specifically, as the first line of defence. A rapid innate defence is especially important since the adaptive immune system takes several days to mount a response to a new pathogen.

The adaptive immune system consists of B lymphocytes (which mature in the bone marrow) and T lymphocytes (which mature in the thymus). Work by Jacques Miller first showed that antibody forming B cells and thymus derived T cells were two distinct immune cell types that both possess adaptive properties (Miller and Sprent, 1971). Advances in molecular techniques soon turned the focus of immunology to the molecular mechanisms underlying adaptive immunity. Studies of the B cell receptor gene, encoding secreted antibody, led to the discovery of antigen receptor gene rearrangement (Hozumi and Tonegawa, 1976), crucially explaining how the diverse repertoires of B and T cell receptors are formed. Both T cells and B cells undergo somatic rearrangement of their antigen receptor genes during development; dependent on the recombination-activating gene (RAG) system (Schatz et al., 1989). This creates a pool of adaptive immune cells with uniquely rearranged receptors, each with the potential to recognise a slightly different antigen structure. For a given pathogen (that the host has not been previously exposed to), the abundance of specific B and T cells is very low. The adaptive response delay is due to activation and clonal expansion stages, needed to generate high enough numbers of specific cells. During the adaptive immune response, naive B and T cells differentiate into effector cells, taking on different roles. These include antibody production by plasma cells, cell mediated cytotoxicity by cytotoxic T cells, and activation of multiple adaptive processes by T helper (T_h) cells (Yatim and Lakkis, 2015). An important advantage of the adaptive response is that a proportion of highly specific B

and T cells are retained as memory cells, ready to initiate a recall response to a secondary pathogen challenge.

The evolutionarily older innate immune system (Boehm, 2012) serves as the first line of defence against pathogens. Innate immune cells do not undergo somatic gene rearrangement; instead they rely on germline encoded receptors that recognise common patterns in pathogen structures or other danger signals. For example, the toll like receptors (TLRs) recognise a range of bacterial and viral components: such as TLR4, which recognises bacterial lipopolysaccharide (LPS) (Poltorak et al., 1998), and TLR3, which recognises viral double stranded RNA (dsRNA) (Alexopoulou et al., 2001). The innate immune system limits the spread of pathogens before the adaptive immune system can mount a response, but also plays an important role in initiating and shaping the adaptive response. The discovery of dendritic cells (DCs) in the 1970s proved this, as DCs became central in the current model of adaptive immunity. Those early experiments demonstrated that DCs were the "critical accessory cell" needed for the T cell response to progress (Nussenzweig et al., 1980). We now know that T cells can only recognise foreign antigen when it is processed and presented within host major histocompatibility complex (MHC) molecules, which is the system used to present endogenous cytosolic proteins on the cell surface. DCs are specialised antigen presenting cells, capable of presenting both endogenous and exogenous antigens, including bacterial protein fragments, viral antigens from other infected host cells, and also tumour cell antigens. DCs undergo maturation in the tissue, activated by stimulation of innate receptors such as the TLRs, take up antigens and present these molecules to potential antigen specific T cells in the lymph nodes, as well as providing co-stimulatory signals to enhance the initiation of adaptive immunity (Guermonprez et al., 2002). Other innate immune cells can directly kill infected host cells, providing a valuable defence against intracellular pathogens before the adaptive arm fully responds, as well as providing signals to T cells. These include large granular lymphocytes named natural killer (NK) cells.

1.1.2 Immune cell classification

All of the cell types discussed above originate from the haematopoietic stem cell (HSC) compartment, the source of all circulating immune cells. HSCs give rise to two lineages: 1) myeloid, which includes erythrocytes, platelets and several types of leukocytes, and

2) lymphoid, which gives rise to lymphocytes – the B, T and NK cells. Circulating leukocytes can also be divided into polymorphonuclear and mononuclear leukocytes. Named polymorphonuclear for the segmented appearance of their nuclei, this group includes neutrophils, basophils and eosinophils; short lived cells that respond rapidly to inflammatory stimuli (also known as granulocytes) (Geering et al., 2013). Mononuclear leukocytes in the blood consist of lymphocytes and also monocytes, large leukocytes that differentiate into antigen presenting cells when recruited to the tissue. Mononuclear leukocytes can be isolated by centrifugation, and are often used for *in vitro* immunological studies, as a convenient way to study lymphocyte biology.

1.2 Natural Killer cells

1.2.1 Identification

As part of the innate immune system, natural killer (NK) cells play an important role in controlling viral infections and tumour growth. NK cells are cytotoxic lymphocytes but, unlike cytotoxic T cells, do not rely on prior sensitisation and they are not dependent upon somatically rearranged antigen receptors. Target killing without prior sensitisation was termed "natural killing" and led to the initial discovery of NK cells in 1975, within mouse splenic leukocytes (Kiessling et al., 1975). Each NK cell is equipped with a diverse set of germline encoded receptors, which allow the recognition and killing of target cells. Cells that are dangerous to the host are recognised by NK cells, through the balance of activating and inhibitory ligands on the target cell surface. Along with their cytotoxic capability, NK cells also contribute to innate immunity by producing cytokines.

Within human peripheral blood, NK cells range from 5.35–30.93 % of lymphocytes (Bisset et al., 2004). In humans, NK cells are defined as lymphocytes expressing CD56 (also known as neural cell adhesion molecule, or NCAM1) but lacking expression of CD3 (a component of the T cell receptor complex). Mouse NK cells do not express CD56, but do widely express the NK1.1 receptor. Alternatively, both species express NKp46 (also known as CD335; encoded by the NCR1 gene), which is sometimes used to identify NK cells (Morvan and Lanier, 2016).

1.2.2 Activating and inhibitory receptors

NK cell recognition and killing of target cells depends on interactions between target cell ligands and NK cell activating or inhibitory receptors. The inhibitory receptors were discovered following the proposal of the "missing self" hypothesis in 1985. MHC molecules are assembled from a set of highly polymorphic genes, and are therefore highly variable across the population, making MHC a crucial marker of "self". Tumour cell lines deficient for MHC class I were susceptible to NK cell killing *in vivo* (Ljunggren and Karre, 1985). Karre proposed that the absence of MHC class I on target cells was a key determinant for NK cell killing. Following this discovery, a number of different molecules were identified that bind to MHC class I and have an inhibitory effect on NK cells. These included the first inhibitory killer cell immunoglobulin-like receptors (KIRs), initially known as p58 family molecules (Moretta et al., 1993)), and the CD94/NKG2A heterodimer (Carretero et al., 1998). The KIRs recognise the classical, highly polymorphic MHC class I molecules, coded by HLA-A, B and C, while the CD94/NKG2A receptor recognises the non-classical HLA-E. In addition to NKG2A, there are a group of related proteins that, similarly, dimerise with CD94. These include NKG2B and NKG2C, which were also found to recognise HLA-E (Braud et al., 1998). Surprisingly, a fraction of KIRs and CD94/NKG2 family receptors function as activating receptors, so MHC class I molecules presented on target cells can induce both inhibitory and activating signals in NK cells (Della Chiesa et al., 2015).

Inhibitory receptors ensure that NK cell cytotoxicity is not unleashed upon normal healthy cells. Furthermore, this strategy maximises NK cell killing when T cell responses may be compromised. T cell activation relies on the presentation of antigen on MHC molecules, but sometimes transformed or infected cells downregulate expression of MHC. The herpesviruses in particular produce a number of viral proteins interfering with antigen presentation (VIPRs) (Yewdell and Hill, 2002). Downregulation of host MHC molecules allows viral evasion of the T cell response – but should enhance NK cell responses through the release of inhibitory receptor signalling. Small changes in target cell expression of MHC molecules can dramatically change the target's susceptibility to NK cell killing. This has been demonstrated *in vitro*, with high MHC expressing cell lines proving much less susceptible to NK cell killing than lower expressers. Interestingly, a

threshold for target cell MHC expression was identified, with cell lines expressing MHC above this threshold appearing resistant to NK cell mediated killing (Holmes et al., 2011).

NK cell activating receptors, on the other hand, stimulate NK cell cytotoxicity as well as cytokine release; generally in response to signs of stress on the target cell surface. NKG2D (CD314) is an important receptor found on NK cells and some T cell subsets, related to the CD94/NKG2 receptors, but structured differently and recognising different ligands. These include a number of cell surface molecules induced by infection, proliferation, DNA damage and other 'stress' conditions (Lanier, 2015). In particular, stressed cells can upregulate the MHC class I polypeptide-related sequence A/B (MICA/B) and the UL16 binding proteins (ULBPs). Several other NK cell activating receptors have been identified, including the natural cytotoxicity receptors (NCRs): NKp30, NKp44, and NKp46. The list of ligands for the NCRs is expanding every year as more are discovered, and includes many viral proteins as well as tumour expressed proteins. A common set of cellular ligands for the NCRs are heparin or heparan sulphate proteoglycans (Hecht et al., 2009), thought to direct NK cell recognition of tumour cells. The first viral ligands of the NCRs to be discovered were influenza virus haemagglutinin (HA) and sendai virus haemagglutinin–neuraminidase (HN), which, when expressed by infected cells, bind to NKp46 (Mandelboim et al., 2001). In addition to NKG2D and the NCRs, another important activating receptor is DNAX accessory molecule (DNAM-1). The principal ligands discovered for DNAM-1 are CD155 (poliovirus receptor, PVR) and CD122 (nectin-2) (Bottino et al., 2003). CD155 expression is upregulated in many cancers, with induction of the DNA-damage response pathway proposed as the trigger (de Andrade et al., 2014).

The NK cell receptors mentioned here, and their major known ligands, are summarised in Table 1.1. The majority of the receptors discussed here are present in both humans and mice, except for the KIRs, which are only present in humans. Mice do possess a set of receptors that bind to murine MHC class I; these are the Ly49 family receptors, which also include both inhibitory and activating types (Pegram et al., 2011).

Human or mouse?	Receptor	Known ligands	Activating/Inhibitory?
Human	Inhibitory KIRs: KIR2DL1,2,3 and 4, KIR3DL1 and 2	MHC class I: HLA-A,B and C	Inhibitory
Human	Activating KIRs: KI2DS1,2,3,4 and 5, KIR3DS1	MHC class I: HLA-A,B and C	Activating
Mouse	Inhibitory Ly49: Ly49A,C,I and P	MHC class I	Inhibitory
Mouse	Ly49H	m157 (peptide expressed on MCMV infected cells)	Activating
Both	CD94/NKG2A,B	MHC class I: HLA-E	Inhibitory
Both	CD94/NKG2C,E	MHC class I: HLA-E	Activating
Both	NKG2D	Human: MIC-A/-B, ULBP1/2/3/4 Mouse: RAE-1, MULT-1, H60	Activating
Both	NKp30	Heparan sulphate, BAT-3, B7-H6	Activating
Both	NKp44	Viral HA	Activating
Both	NKp46	Heparan sulphate, viral HA and HN	Activating
Both	DNAM-1	CD155, CD122	Activating

Table 1.1 NK cell activating and inhibitory receptors

The human and mouse NK cell receptors discussed in this thesis are summarised here, with their known interacting ligands. Adapted from (Pegram et al., 2011).

The signalling pathways downstream of the main activating and inhibitory receptors are illustrated in Figure 1.1. The structures of the NK cell activating receptors vary, but the majority contain short intracellular domains that associate with adapter proteins, responsible for the initiation of activatory signalling pathways. Most adapter proteins, including DAP12, FcR-γ and CD3-ζ, contain an immunoreceptor-based **activation** motif (ITAM) (Vivier et al., 2004). Receptor engagement induces tyrosine phosphorylation of the ITAM sequence, leading to downstream activatory signalling. NKG2D is associated with DAP10, a different adapter protein, which contains the alternative tyrosine-isoleucine-asparagine-methionine (YINM) motif rather than an ITAM motif, and so signals through slightly different pathways (Billadeau et al., 2003). DNAM-1 also does not signal through an ITAM motif; its own intracellular domain is phosphorylated instead (de Andrade et al., 2014).

NK cell inhibitory receptors typically contain long intracellular domains containing an immunoreceptor tyrosine-based **inhibition** motif (ITIM). Engagement of inhibitory receptors induces phosphorylation of the ITIM sequence, leading to recruitment of SHP-1 and SHP-2 tyrosine phosphatases. SHP-1 and 2 function to inhibit activatory signalling, by targeting activatory phosphorylated residues for dephosphorylation (Binstadt et al., 1996; Yusa and Campbell, 2003). Interactions between NK cell receptors and target cell ligands, as well as adhesion molecules, lead to the formation of an immunological synapse. If the overriding signal received by the NK cell is activatory, this triggers a series of changes within the NK cell, leading to death of the target. Importantly, co-stimulation of multiple activatory receptors is necessary for the activation of target killing, although an exception is activation through the Fcγ receptor CD16, which recognises antibody bound target cells through the antibody Fc region (Bryceson et al., 2006). Engagement of CD16 by itself is sufficient to activate NK cell killing, termed antibody dependent cellular cytotoxicity (ADCC).
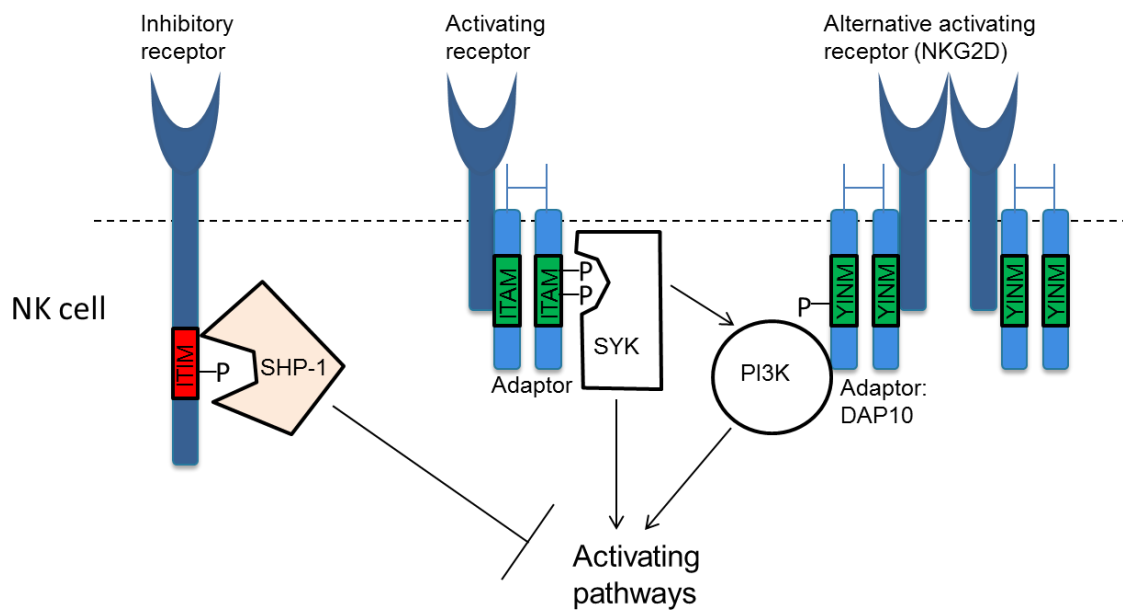
Figure 1.1 Activating and inhibitory receptor mechanisms

Signalling downstream of NK cell activating and inhibitory receptors. Activating receptors are typically associated with adapter proteins containing an ITAM motif (or alternative motif in the case of NKG2D), which can recruit downstream signalling factors, including Syk kinase and phosphoinositide 3-kinase (PI3K), to trigger activation of the NK cell. Inhibitory receptors typically contain an ITIM motif, which can recruit the phosphatase SHP-1 to oppose activatory pathways. Adapted from (Farag et al., 2002).

1.2.3 Target killing mechanisms

NK cells kill target cells through two main mechanisms: granule dependent killing and death ligand mediated killing. These processes are summarised in figure 1.2.

Granule dependent killing describes the exocytosis of cytotoxic granules from NK cells into target cells, a process shared with cytotoxic T cells. In NK cells, it is triggered following interactions between NK cell activating/inhibitory receptors and target cell ligands. NK cells form an immunological synapse with their target cells during this interaction. When the balance of signals is activatory (as described in section 1.2.2), intracellular signalling triggers mobilisation of calcium from the endoplasmic reticulum and actin cytoskeleton reorganisation, leading to granule polarisation at the immunological synapse. Finally, cytotoxic granules fuse with the NK cell plasma membrane and granule contents are exocytosed towards the target, also known as degranulation (Stinchcombe and Griffiths, 2007). During degranulation, proteins such as CD107a, which are normally present inside the cytotoxic granules, are externalised on the cell surface. This provides the basis of a useful assay for detecting degranulated NK cells (Alter et al., 2004).

NK cell cytotoxic granules contain perforin and granzyme B. Perforin release triggers pore formation in the target cell membrane, in order to deliver granzyme directly into the target cytoplasm. When perforin deficient mice were generated, their NK cells and T cells could not lyse targets *in vitro* (Kagi et al., 1994), demonstrating that cytotoxic lymphocytes are completely reliant on perforin for granule dependent killing. Cytotoxic cells themselves are relatively resistant to the effects of perforin, in comparison to other cell types (Liu et al., 1989). The granzymes are serine proteases, capable of cleaving specific intracellular proteins. There are five types of granzyme known in humans: granzyme A, B, H, K and M (Trapani, 2001). Granzyme B induces apoptosis through cleavage of the pro-apoptotic protein Bid in the target cell cytosol (Sutton et al., 2000). It is the main granzyme used in granule dependent killing by NK cells and T cells. This was demonstrated in granzyme B deficient mice; NK cells from these animals lost the ability to rapidly kill targets *in vitro*, requiring dramatically longer incubation times (Heusel et al., 1994). The fact that cytotoxic killing can still progress (although very slowly) in granzyme B deficient NK cells suggests that the other granzymes may partly contribute to granule dependent killing. Granzyme K and M have also been implicated in the processing of

cytokines and the cleavage of some target cell proteins required for viral replication (Voskoboinik et al., 2015).

Alternatively, NK cells can induce target cell apoptosis through expression of death receptor ligands. These include TNF-related apoptosis-inducing ligand (TRAIL) and FAS ligand (FasL), which engage with TRAIL receptors and Fas on target cells, respectively. Engagement of death receptors on target cells recruits caspases, initiating apoptosis (Warren and Smyth, 1999). Studies in humans and mice have shown that immature NK cells preferentially use TRAIL dependent killing (Zamai et al., 1998) and TRAIL expression is lost as NK cells mature, although cytokine stimulation can upregulate its expression (Takeda et al., 2005).
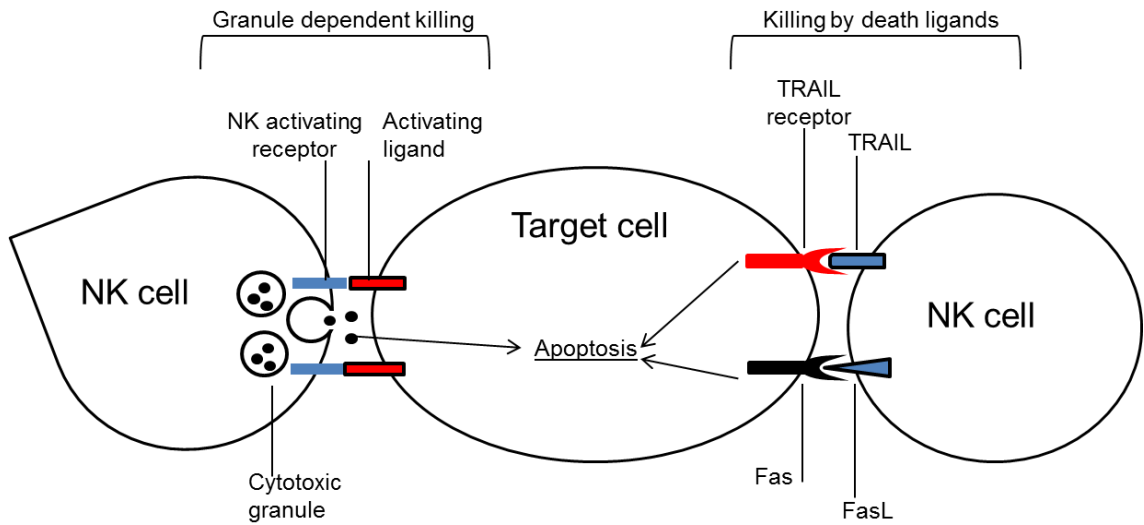
Figure 1.2 Target killing mechanisms

NK cells kill their targets through two distinct mechanisms: granule dependent or death ligand dependent killing. Granule dependent killing involves the release of cytotoxic granules from NK cells into targets to induce apoptosis, while death ligands on NK cells engage death receptors on targets to induce apoptosis directly. Adapted from (Sutlu and Alici, 2009).

1.2.4 NK cell classification and subsets

Since the discovery of NK cells, several other types of innate lymphocyte like cells, also lacking somatically rearranged antigen receptors, have been described. A new category of innate lymphoid cells (ILCs) was proposed, to include both NK cells and this new set of cell types. A common feature of this family is the production of immune modulating cytokines; NK cells are classified as group 1 ILCs based on their capacity to produce interferon γ (IFN-γ), a crucial cytokine for immunity against intracellular pathogens. However, NK cells are the only cytotoxic ILCs (Cortez and Colonna, 2016).

In humans, NK cells can be further divided into two main subtypes, which differ in their ability to produce IFN-γ. These distinct populations are categorised by their levels of cell surface CD56. CD56^{dim} NK cells express lower levels of this marker and are able to lyse target cells more effectively, whereas CD56^{bright} cells are more efficient cytokine producers (Jacobs et al., 2001) (Cooper et al., 2001). CD56^{dim} NK cells also express higher levels of CD16 (Cooper et al., 2001), the activating receptor responsible for ADCC. CD56^{bright} NK cells are abundant in the lymph nodes (Fehniger et al., 2003), where they can receive signals from antigen presenting cells (APCs), and release cytokines to signal to other immune cell types. Therefore, they can participate in crosstalk between different cell types, helping to drive the innate and adaptive immune response. In peripheral blood, CD56^{dim} cells make up the majority of the population (Cooper et al., 2001). Thought to be the effector subtype, it has been suggested that CD56^{dim} NK cells differentiate from CD56^{bright} NK cells, with maturation occurring in the periphery (Chan et al., 2007).

Mouse NK cells do not express CD56, however similar subsets do exist in mice. CD27^{high}CD11b^{dull} are immature mouse NK cells, analogous to CD56^{bright} human NK cells, while CD11b^{high} CD27^{dull} are the most mature subset, displaying stronger effector functions (Gregoire et al., 2007). One study demonstrated similarities between human CD56^{bright} NK cells and CXCR3^{+}CD27^{bright} cells in mice, and proposed this subset of CD27^{+} NK cells as the mouse equivalent (Marquardt et al., 2010). On the other hand, a recent transcriptomic study showed that human CD56^{bright} NK cells expressed a strikingly similar gene expression signature to mouse CD127^{+} innate lymphoid cells (Allan et al., 2017). Therefore, in order to specifically study CD56^{dim} and CD56^{bright} NK cells, human samples are required.

1.2.5 Tumour Killing

There is a growing interest in the immune response against tumours, with recent approvals of a number of cancer immunotherapies. NK cells, like cytotoxic T cells, are known to participate in tumour immunosurveillance, eliminating transformed cells that may form tumours. The evidence for this comes from *in vivo* models in which NK cells were selectively depleted. Treatment with specific anti-NK cell antibodies is one strategy, although selection of appropriate antibodies that do not deplete other cell types is crucial. Treatment with anti-asialo-GM1 successfully depleted NK cells but not NKT cells (which display similar markers) in mice, and as a result increased susceptibility to methylcholanthrene induced sarcomas (Smyth et al., 2001). In another approach, depletion of NK cells in a transgenic mouse model resulted in a higher number of lung metastases following tumour cell injection (Kim, S. et al., 2000). NKG2D may be particularly important for innate anti-tumour immunity, as ligands for this receptor are expressed on a number of different tumour cell lines (Pende et al., 2002) and on freshly isolated tumours (Groh et al., 1999). Furthermore, mice lacking NKG2D are more prone to spontaneous tumour growth (Guerra et al., 2008). Human studies also offer strong evidence for NK cell immunosurveillance. In an eleven year follow up study of a Japanese general population, higher natural cytotoxicity levels at baseline (tested by measuring peripheral blood cell mediated killing of K562 cells, the prototypical NK cell target line) was associated with reduced cancer risk (Imai et al., 2000).

Although activating receptor ligands may be upregulated during transformation, developed tumours can evade the immune system in many ways. For example, tumours may release immunosuppressive cytokines to dampen down the immune response, or the cancer may develop 'immune privilege' by expressing FasL, inducing apoptosis in cytotoxic lymphocytes (OConnell et al., 1996). Some cancers may even cause downregulation of activating receptors at the NK cell surface. Transforming Growth Factor β (TGF-β) is an immunosuppressive cytokine implicated in NK cell inhibition by tumours. *Ex vivo* exposure to a number of different cancer cell lines triggered the downregulation of NK cell activating receptors at the cell surface and reduced expression of cytotoxic molecules, in a TGF-β dependent manner (Wilson et al., 2011).

The combination of immune evasion strategies employed by many cancers creates an immunosuppressive tumour microenvironment, which effectively protects the tumour

from natural killing. Indeed, immune evasion is now recognised as a hallmark of cancer (Hanahan and Weinberg, 2011). Recent immunotherapy strategies aim to re-activate the cytotoxic lymphocytes of the patient, or to release these cells from the immunosuppressive block created by the tumour.

1.2.6 Anti-viral Response

The other key role of NK cells is in the control of viral infections. NK cell activity is thought to be crucial during the first few days of a viral infection, when the adaptive immune response is still developing. NK cells can recognise markers on the surface of a target cell, which are indicative of viral infection. This is co-ordinated through activating and inhibitory receptors, similar to tumour cell recognition. As discussed in section 1.2.2, the activating natural cytotoxicity receptors (NCRs) are thought to bind certain viral ligands including haemagglutinin (HA) and haemagglutinin–neuraminidase (HN), presented on infected cells. Furthermore, virally infected cells display additional signs of stress on the surface, such as downregulation of MHC class I due to viral interference with MHC presentation. The adenovirus E19 protein is one example; E19 interference with MHC class I processing was some of the first evidence for this viral immune evasion strategy (Andersson et al., 1985). Other viral proteins that interfere with MHC processing are commonly found in the herpesviruses. Human cytomegalovirus (HCMV) is a herpesvirus with a particularly large genome, encoding numerous proteins capable of downregulating MHC class I expression: US2, US3, US6 and US11 (Roder et al., 2008). MHC class I downregulation on HCMV infected cells should increase susceptibility to NK cell killing and, indeed, NK cells are crucial for defence against herpesviruses. Early studies to support this include depletion of NK cells in mice using the anti-asialo GM1 antibody, which increased susceptibility to herpes simplex virus (HSV) (Habu et al., 1984) and to murine CMV (MCMV) (Bukowski et al., 1983). In fact, the latter study found that NK cell depletion increased susceptibility to disease in a range of murine viral infections, except for lymphocytic choriomeningitis virus (LCMV). Therefore, NK cell contribution to the anti-viral immune response may vary across species of virus.

In humans, immune deficiencies observed in the clinic emphasise the importance of NK cells in the control of viral infections. In the first case reported, a patient with a specific

NK cell deficiency had a severe susceptibility to herpesvirus infections (Biron et al., 1989). Subsequent studies have identified numerous types of human NK cell deficiencies (either lacking NK cells or possessing functionally deficient NK cells) with a common feature being susceptibility to herpesviruses and papillomavirus infections, and virus driven cancers (Orange, 2013).

Cytokine release during a viral infection is a powerful activating stimulus for NK cells. Type I interferons (IFN-I) can be produced by most (if not all) cell types, especially by antigen presenting cells, as a response to viral infection. Viral detection by toll like receptors (TLRs) in the endosome or retinoic acid-inducible gene 1 (RIG-I) activation in the cytosol leads to IFN-I production, shown in Figure 1.3. The ability of IFN-I to upregulate NK cell cytotoxicity was discovered over four decades ago (Santoli et al., 1978), but the precise mechanism of gene induction and the contribution of other cytokines are not well understood. IFN-I includes IFN-α, of which there are 13 types (encoded by 13 genes) , and IFN-β (encoded by a single gene) (Honda et al., 2006). IFN-I signals through the Janus kinase and Signal transducer and activator of transcription (JAK/STAT) family of signalling pathways; the basic pathway is shown in Figure 1.4.

The IFN-I receptor, also known as the IFNαβ receptor, consists of the IFNAR1 and IFNAR2 subunits. Binding of IFN-I to either IFNAR1 or IFNAR2 recruits the second subunit and triggers the signalling cascade. JAK family kinases phosphorylate each other and phosphorylate the receptor, which induces the recruitment, phosphorylation and dimerisation of STAT1 and STAT2 molecules. The STAT heterodimer subsequently binds Interferon regulatory factor 9 (IRF9) to form the interferon stimulated gene factor 3 (ISGF3) transcription factor complex (Platanias, 2005). A consensus DNA sequence known as the interferon stimulated response element (ISRE) is able to bind ISGF3 (Platanias, 2005), providing a direct pathway from interferon binding to gene induction in the same cell. The other major type of interferon that acts during viral infection is IFN-γ, but this is a type II interferon and therefore acts through the separate IFN-II receptor, using slightly different JAK and STAT pathway components. IFN-γ predominantly activates a homodimer of STAT1, forming a transcription factor that binds to the gamma interferon activation site (GAS) consensus sequence, rather than ISRE (Schneider et al., 2014). Interferon stimulated genes often contain both ISRE and GAS sequences in their

promoter regions, but some genes are regulated by only one or the other. Consequently, IFN-I and IFN-II induce different transcriptional responses with many overlapping genes, as shown in microarray studies (Der et al., 1998).

Interferon stimulated gene (ISG) expression in virally infected cells is essential for restricting viral replication. ISG encoded proteins have a wide array of functions, including shutting down protein translation (achieved by protein kinase R (PKR)), acting directly on viral particles (such as the Myxovirus resistance (Mx) proteins) and potentiating the IFN response (components of IFN signalling such as STAT1) (Schneider et al., 2014). In addition, IFN-I acts upon immune cells to promote anti-viral responses, not least through the induction of NK cell cytotoxicity.
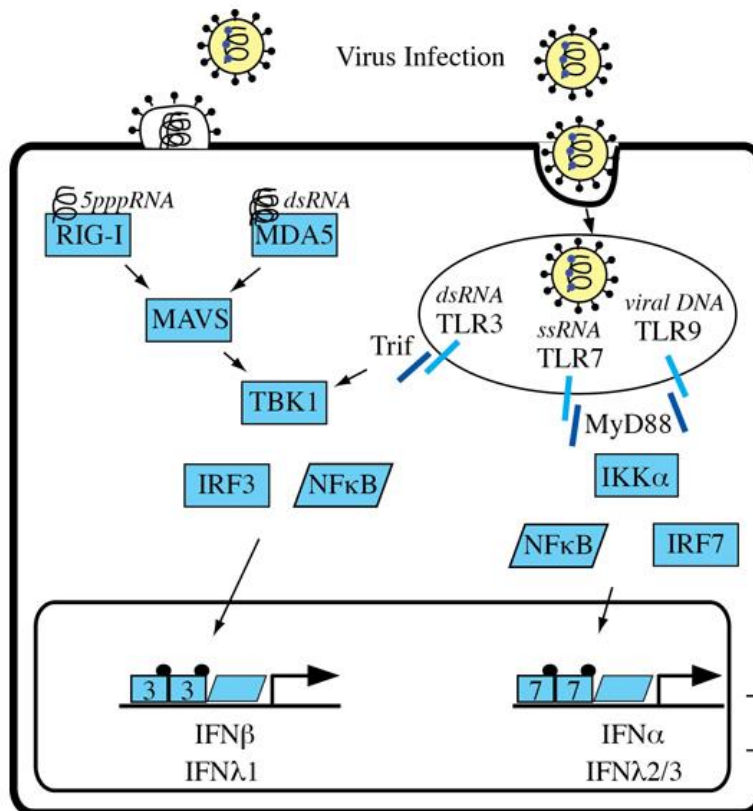
Figure 1.3 Type I Interferon (IFN-I) induction by viruses

When a virus gains entry to a host cell, its genome may be exposed to molecular sensors inside the cell. Intracellular toll like receptors (TLRs), positioned on the endosome membrane, are able to recognise the RNA or DNA of viruses which have been endocytosed into the cell. The retinoic acid-inducible gene 1 (RIG-I) like helicases, including RIG-I and melanoma differentiation-associated 5 (MDA5) are able to sense uncapped 5′-triphosphate RNA or cytoplasmic double stranded RNA (dsRNA) from replicating viruses. Sensing of viral RNA or DNA activates downstream signalling pathways, leading to the expression of IFN-I such as interferon α (IFNα) and interferon β (IFNβ). Adapted from (Heim, 2012).

Canonical JAK-STAT pathway

- Cytokine binds
- JAK molecules phosphorylate the receptor
- Receptor phosphorylates STAT proteins
- Dimerisation
- STAT dimer enters the nucleus to regulate gene expression

Type I interferon pathway

- Interferon α/β receptor
- Type I interferon binds its receptor
- TYK2 and JAK1 phosphorylate the receptor
- Receptor phosphorylates STAT1 and STAT2 proteins
- ISGF3 complex
- Dimerisation + IRF9 binding
- Transcription factor complex enters the nucleus to regulate gene expression
- ISRE

Figure 1.4 JAK/STAT signalling

The canonical Janus kinase and Signal transducer and activator of transcription (JAK/STAT) pathway, and the specific molecules involved in type I interferon signalling. JAK molecules associated with the cytokine receptor are activated to phosphorylate the receptor when bound to ligand. The receptor then phosphorylates the relevant Signal Transducer and Activator of Transcription (STAT) molecules, which are recruited through their Src homology-2 (SH2) domains. Phosphorylation induces STAT dimerisation and translocation to the nucleus, where modulation of gene expression occurs. In the case of IFN-I, the activated receptor primarily phosphorylates STAT1 and STAT2, leading to the formation of the Interferon stimulated gene factor 3 (ISGF3) transcription complex.

1.2.6.1 **Regulation by additional cytokines**

IFN-I is a crucial anti-viral cytokine, but additional cytokines also play a role in the NK cell response against viruses. Murine models of viral infection have proven to be useful tools in this field of research. Using a murine model of CMV (MCMV) infection, Nguyen *et al.,* (2002) argued that anti-viral response functions in NK cells, including target cell killing and the release of interferon γ (IFN-γ), are actually separately regulated by different cytokines (Nguyen, K.B. et al., 2002a). They showed that NK effector functions are regulated by independent JAK/STAT pathways; cytotoxicity via the IFN-I receptor/ STAT1 pathway, and IFN-γ release via the interleukin 12 (IL-12) receptor and STAT4.

Additionally, the importance of another cytokine, interleukin 15 (IL-15), was demonstrated in the regulation of NK cells during viral infection. IL-15 signals primarily through STAT5 and also through non JAK/STAT pathways including phosphoinositide 3-kinase (PI3K) signalling (Mishra et al., 2014). Experiments using neutralising antibodies showed that IL-15 was required for NK cell proliferation and survival during infection, but not involved in NK cell cytotoxicity or IFN-γ induction (Nguyen, K.B. et al., 2002a). However, this finding is not consistent with what others have observed. In another MCMV infection model, Baranek *et al.*, (2012) showed that IL-15 was in fact necessary for activation of NK cell cytotoxicity. In their IL-15 neutralisation model, there was a reduction in the number of NK cells positive for granzyme B, a serine protease required for cytotoxic activity (Baranek et al., 2012). They also showed that many NK cell genes upregulated during viral infection did not contain interferon response elements, but did contain response elements for IL-15 activated transcription factors, suggesting a more important role for IL-15 in the activation of NK cells. Despite differences, the studies of Nguyen et al (2002) and Baranek et al (2012) do agree that IL-15 is upregulated in an IFN dependent manner during viral infection.

In another contrasting viral infection model, the direct action of IFN-I on NK cells was sufficient for NK cell activation in response to vaccinia virus *in vivo* (Martinez et al., 2008). It is unclear whether the differences in reported mechanisms are due to the type of virus, or can be explained by the experimental model used. It could be the case that different viruses trigger varying combinations of cytokines in the host, due to differences in viral structures. For example, DNA viruses and RNA viruses are detected via different mechanisms (figure 1.3). Figure 1.5 summarises the main cytokines thought to be

involved in virus induced NK cell activation. However, the inconsistencies in the literature indicate that a better understanding of this topic is much needed.
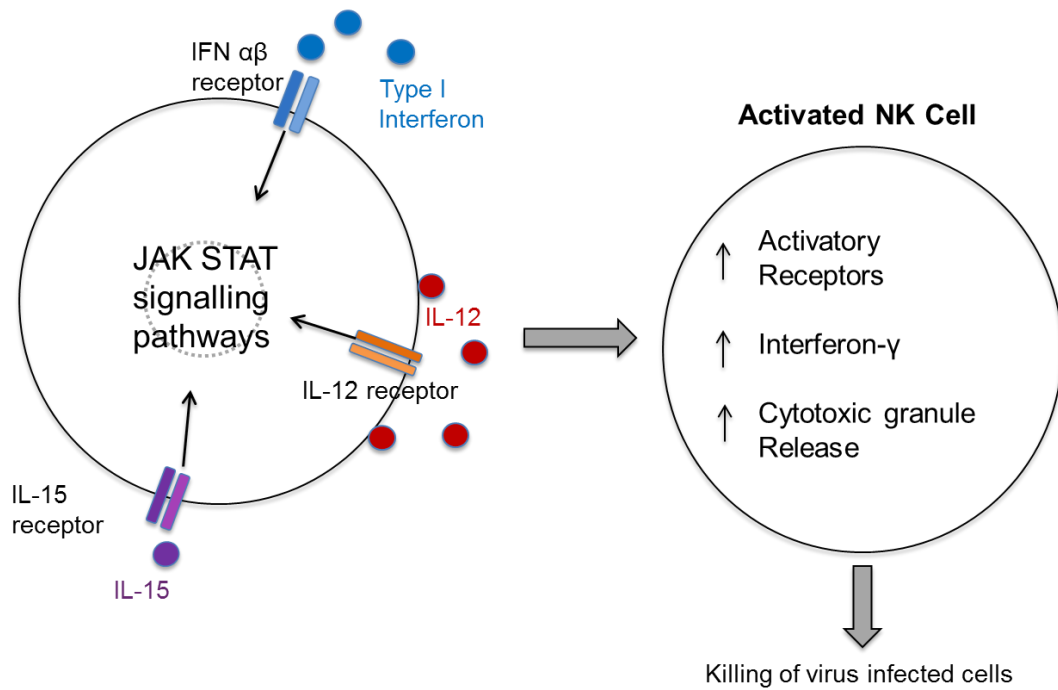
Figure 1.5 Cytokines involved in NK cell activation

The cytokines interleukin 12 (IL-12), interleukin 15 (IL-15) and type I interferon (IFN-I) are able to activate NK cell effector functions. Exactly how they function during a viral infection is not well understood.

1.2.7 Migration

NK cells are widely distributed throughout the body, in the blood, lymphoid tissues and other organs. Mouse studies have demonstrated the presence of NK cells in a wide range of tissues, with the highest proportions found in the lungs, liver and peripheral blood (Gregoire et al., 2007). Therefore NK cells are well adapted for immune surveillance. However, during an acute viral infection, rapid recruitment of NK cells to the affected area may be necessary. One mechanism for NK cell recruitment is the release of chemokines from infected tissues, triggering chemotaxis of NK cells.

In the MCMV model, macrophage inflammatory protein 1 alpha (MIP-1alpha, also known as CCL3) is critical for recruitment of NK cells to infected liver (Salazar-Mather et al., 1998), as is monocyte chemoattractant protein-1 (MCP-1/ CCL2), interacting with the chemokine receptor CCR2 (Hokeness et al., 2005). Another cytokine receptor, CCR1, has also been implicated in NK cell recruitment to the inflamed liver, in a model of hepatitis (Gregoire et al., 2007). Recruitment of NK cells to lymph nodes has also been demonstrated in mice, following injection of mature dendritic cells (simulating inflammatory events). This was dependent on expression of the chemokine receptor CXCR3 (Martin-Fontecha et al., 2004). Chemotaxis mechanisms are also likely responsible for NK cell recruitment to tumour sites. In mice, NK cells can migrate towards implanted tumours, in a CX3CR1 dependent manner (Gregoire et al., 2007).

Much less is known about the migration of human NK cells. Studies comparing the CD56^{dim} and CD56^{bright} NK subsets have revealed differences in migratory receptor expression. Expression of CD62L (L-selectin) on leukocytes is required for binding and rolling on endothelial cells, a process crucial for recruitment into lymph nodes (Arbones et al., 1994), and this molecule is expressed selectively on the CD56^{bright} subset (Frey et al., 1998). Furthermore, CD56^{bright} NK cells express much higher levels of CCR7 than the CD56^{dim} subset (Campbell et al., 2001; Berahovich et al., 2006); CCR7 is a chemokine receptor usually expressed on lymphocytes homing to the lymph nodes. This is also a key difference between human and mouse NK cells, which do not express CCR7 (Gregoire et al., 2007). The selective expression of key lymph node homing receptors on CD56^{bright} NK cells explains why it is the dominant NK cell subset in human lymph nodes. Figure 1.6 summarises the important functional differences between the two human NK cell subsets.

Finally, another important system controlling lymph node trafficking is the gradient of sphingosine-1-phosphate (S1P) between lymph node and blood. S1P concentrations are much higher in the blood, so lymphocyte expression of the receptors for S1P are crucial for lymph node egress (Matloubian et al., 2004; Walzer et al., 2007). Changes in expression of S1P receptors may therefore impact on NK cell migration.
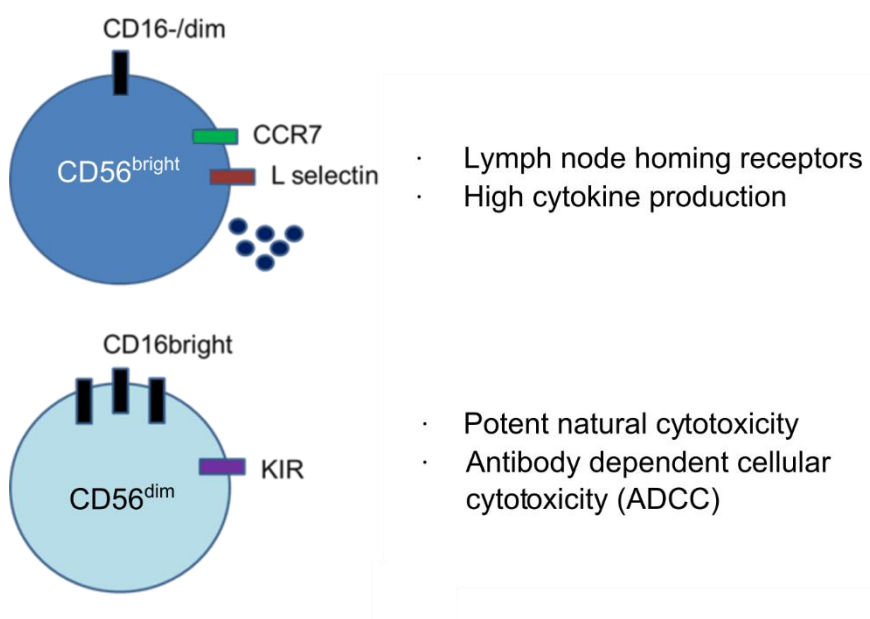
Figure 1.6 Functional differences between CD56^{dim} and CD56^{bright} NK cells

Although CD56^{bright} NK cells are less efficient killers, this subset displays high expression of lymph node homing receptors and strong capability for cytokine production. CD56^{dim} NK cells are more efficient natural killers, and express high levels of CD16, for ADCC.

1.2.8 Proliferation

Research into NK cell proliferation began by defining the signals required for NK cell division *in vitro*. These studies agreed that interleukin 2 (IL-2) was the most potent inducer of NK cell proliferation (Robertson et al., 1993; Ythier et al., 1985), and that mitogenic signals delivered by IL-2 could be enhanced by co-culture with target cell lines such as K562, the prototypical NK-susceptible cell line (Ythier et al., 1985; Baume et al., 1992). However, mice deficient in IL-2 have a normal complement of NK cells (Kundig et al., 1993) and this suggested that a distinct cytokine regulated NK cell development and proliferation *in vivo*.

Later, IL-15 was identified as an inducer of NK cell proliferation (Carson et al., 1994). The receptors for IL-2 and IL-15 share 2 out of 3 subunits: common γ chain (also shared with a number of other cytokine receptors), as well as the β subunit. As expected, IL-2 and IL-15 consequently share downstream signalling pathways, including STAT5 activation and phosphoinositide 3-kinase (PI3K) signalling, which promote survival and proliferation (Waldmann, 2015). A third subunit, the α chain, is unique to each cytokine. IL-2Rα (CD25) is expressed on activated T cells, and on the CD56^bright NK cell subset. When IL-2Rα is associated with the γ and β subunits, the high affinity IL-2 receptor is formed, allowing CD56^bright NK cells to respond to picomolar concentrations of IL-2 (Cooper et al., 2001). IL-15Rα is thought to function differently; it binds to IL-15 and presents the cytokine on the surface of monocytes or dendritic cells, where NK cells can interact through IL-15Rβγ, in a process termed IL-15 *trans* presentation (Burkett et al., 2004). *In vivo*, IL-15 promotes homeostatic proliferation of NK cells (Burkett et al., 2004), as well as NK cell differentiation from HSCs in a humanised mouse model (Huntington et al., 2009).

In some cases, expansion of NK cells has been reported during infection. In the mouse MCMV model, there is a characteristic expansion of NK cells which follows two phases of proliferation: the first is dependent on cytokines, while the later phase is dependent on a specific interaction between the MCMV glycoprotein m157 (expressed on the surface of infected cells) and the mouse NK cell activatory receptor Ly49H (Dokun et al., 2001). In this model, Ly49H+ NK cells expand and persist in infected mice, providing a "memory pool" of NK cells. Following this discovery, it was initially unclear whether "memory" NK cells were unique to MCMV infection. Interestingly, evidence of NK cell memory like

behaviour has been observed in human HCMV infection, with expansion of CD94/NKG2C+ NK cells detected in response to co-culture with HCMV infected fibroblasts (Guma et al., 2006) and expansion of this subset observed in CMV(+) donors (Lopez-Verges et al., 2011).

In humans, controlled studies of NK cell proliferation during infection are generally not possible, but clinical case studies offer some insight. In the case of hantavirus, infected patients experience NK cell expansion in the blood, which has been linked to expression of IL-15 and IL-15Rα on infected endothelial cells, with the IL-15 trans presented to NK cells (Bjorkstrom et al., 2011; Braun et al., 2014).

Vaccination studies are also valuable sources of human *in vivo* data. In individuals vaccinated with heat-inactivated rabies virus, *ex vivo* re-stimulation of their PBMC with rabies virus induced high levels of NK cell proliferation. The proliferative response was not observed in pre-vaccination PBMC, suggesting that NK cell proliferation may occur during the recall response – the authors suggest that NK cells proliferate in response to effector T cell derived IL-2 (Horowitz et al., 2010). Overall, there have been a number of diverse mechanisms proposed for infection induced NK cell proliferation, which might be determined by the type of virus or infection model. However, the mechanisms controlling NK cell proliferation are not well defined.

1.2.9 Markers of NK cell activation

When examining NK cell responses to various stimuli, the use of an activation marker, detectable by flow cytometry, can be a convenient and quick way to assay NK cell activation. CD69 is a transmembrane protein, used widely as a lymphocyte activation marker ever since it was linked to early activation of T cells (Ziegler et al., 1994). NK cells upregulate CD69 when exposed to activating cytokines *in vitro*, and high CD69 expression predicts increased NK cell cytotoxicity (Clausen et al., 2003). CD69 is also highly expressed on tissue resident memory T cells (Cibrian and Sanchez-Madrid, 2017). Furthermore, CD69 expression by B cells and T cells is known to inactivate the S1P receptor, thereby preventing lymph node egress (Shiow et al., 2006), implying that CD69 may function as a regulator of lymphocyte trafficking.

1.3 Oncolytic Viruses

1.3.1 Replication in cancer cells

Oncolytic viruses (OVs) are viruses which preferentially replicate in cancer cells compared to healthy human cells. A link between viral infection and tumour regression was observed more than 100 years ago, but initial trials of pathogenic viruses were often risky for the patients (Kelly and Russell, 2007). Recent developments, both in the identification of new viruses and engineering of existing ones, have reduced those risks and enhanced the efficacy of OVs.

Many cancer cell types are more susceptible to viral infection than non-transformed cells. Several mechanisms have been proposed to explain this. Firstly, selective entry of OVs into tumour cells can occur due to upregulated expression of viral entry receptors; for example oncolytic Coxsackie virus preferentially infects cells with high intracellular adhesion molecule 1 (ICAM) expression (Au et al., 2007). Secondly, cancer cells have high metabolic activity and hence larger pools of nucleotides and amino acids, which may enhance viral replication. Common cancer mutations can also enhance susceptibility to OVs, for example constitutive Ras activation increases replication of reovirus (Strong et al., 1998). A recent study demonstrated that phosphatase and tensin homolog (PTEN) depletion inhibited host cell interferon production in response to viral infection (Li et al., 2016). PTEN is a frequently mutated tumour suppressor, so this finding may explain why so many cancers are vulnerable to viral infection. It is now generally accepted that the spectrum of genetic and biochemical changes observed in cancer cells makes them attractive targets for viral infection, not least because they frequently suppress interferon responses and the resultant cell intrinsic mechanisms of preventing viral infection (Chen et al., 2009).

Additionally, many OVs are genetically engineered to increase selectivity for cancer cells over healthy cells. DNA viruses such as adenovirus are ideal for genetic manipulation strategies. One of the first was an adenovirus with a mutated E1B region, which was unable to produce the viral E1B 55K protein. In the wild type adenovirus, this protein binds to and inactivates host cell p53, allowing viral replication. The mutated adenovirus (which was named ONYX-015 later in clinical development) showed selectivity for cancer cells with deficient p53 (Bischoff et al., 1996). Alternatively, oncolytic adenoviruses have

been engineered to express "tumour directing antigens"; peptides expressed within viral surface proteins that are specific for receptors overexpressed in cancers. For example, the epithelial integrin αvβ6 is often overexpressed in carcinoma, so an adenovirus expressing an αvβ6-selective peptide in its outer structure was engineered. The retargeted virus showed enhanced uptake into carcinoma tumours *in vitro* and *in vivo* (Coughlan et al., 2009).

An initial focus of OV research was on the mechanism of direct tumour cell lysis. Host tumour cells can be killed through lytic viral replication, or even toxicity from viral proteins (Kuruppu and Tanabe, 2005), and numerous *in vitro* studies demonstrated virus induced killing of cancer cell lines but not non-transformed cells. In early studies, successful delivery of OVs and subsequent tumour regression was shown in immune deficient mice engrafted with human tumours (known as xenograft models) (Fueyo et al., 2000; Walker et al., 1999). These earlier studies generally did not consider the contribution of the immune system, and used *nude* mice lacking T cells. Even in these models, the response of NK cells and other immune cells cannot be ruled out as a contributing mechanism to tumour regression, other than direct lytic viral replication.

Initially the immune response was seen as a barrier to effective therapy, as a specific anti-viral immune response can trigger clearance of the virus before it reaches the tumour. This is especially problematic for systemic delivery of OVs. Strategies to shield oncolytic viruses from this initial anti-viral response have been encouraging. In the case of oncolytic measles virus (MV), loading of virus onto bone marrow-derived mesenchymal stromal cells (BM-MSCs) *ex vivo* enabled the successful delivery of MV to acute lymphoblastic leukemia (ALL) targets in a xenograft mouse model (Castleton et al., 2014). Enhanced delivery of virus was observed despite the presence of injected anti-MV antibodies.

During a clinical trial of reovirus, intravenous delivery of the virus to tumour tissue was demonstrated despite the presence of neutralising antibodies from previous natural exposure, and virus was detected within blood immune cells, suggesting cellular carriage of the virus (Adair et al., 2012). These approaches increase the chance of the OV reaching the tumour to replicate there. Once viral replication is taking place, ideally the patient immune response can be directed against the tumour rather than solely against

the virus. More recently, OV research has changed focus towards the immune response, as increasing numbers of studies support the use of OVs as immunotherapies.

1.3.2 Immune activation

Given that many viruses are efficient activators of NK cells and other immune cells during an infection, it is not surprising that OVs stimulate immune responses. Interest in the immunotherapeutic potential of OVs increased when several preclinical studies highlighted the beneficial role of the host immune system during OV therapy. In one study, treatment with vesicular stomatitis virus enhanced the survival of tumour bearing mice, and actually required both NK cells and CD8 T cells for this effect (Diaz et al., 2007).

Specific anti-tumour immunity was also observed following intratumoural oncolytic herpes simplex virus (HSV) treatment in a neuroblastoma model (Li, H. et al., 2007) and in a mouse breast tumour model (Li, H.T. et al., 2007), which was enhanced by multiple doses of virus. Intratumoural OV injection even resulted in growth inhibition of secondary implanted tumours, which were not exposed to virus. This secondary effect was only observed in immune competent mice, and not in *nude* mice (which lack T cells), so the adaptive immune response was crucial (Li, H.T. et al., 2007).

In a mouse model of melanoma metastases, priming of anti-tumour immunity was demonstrated after intravenous delivery of another OV, reovirus (Prestwich et al., 2008). In particular, dendritic cell (DC) maturation was demonstrated following OV infection of cancer cell lines; this is important as activated mature DCs are thought to cross present tumour antigens to prime the adaptive immune response. Many of these studies used whole splenocytes from treated mice, in order to study cytotoxic T cells. However, NK cells are also likely to play an important role; in fact cytotoxic killing measured within whole splenocytes would probably include killing mediated by NK cells.

In 2015 a milestone was reached, as the first OV was approved for treatment by the US Food and Drug Administration (FDA) in the United States. Named talimogene laherparepvec (T-VEC), it is a modified herpes simplex virus type 1 (HSV-1) expressing granulocyte–macrophage colony stimulating factor (GM-CSF). The inclusion of the GM-

CSF gene, encoding a cytokine that promotes immune cell infiltration, demonstrates the importance of immune stimulation in the context of OV therapy.

1.4 Reovirus

Mammalian orthoreovirus (referred to as reovirus) is a non-enveloped, double stranded RNA (dsRNA) virus in the *Reoviridae* family, which infects mammals, including humans. In fact, most of us have been exposed to this virus during childhood (as evidenced by the widespread occurrence of neutralising antibodies). The reovirus structure is illustrated in Figure 1.7. Its genome is composed of 10 separate dsRNA segments, termed either large (L), medium (M), or small (S), according to size of the strands. The proteins encoded on these segments are labelled either lambda (λ), mu (μ) or sigma (σ) respectively (Danthi et al., 2013). Reovirus proteins form two concentric shells, the outer capsid and core. The outer capsid contains the attachment protein σ1, which binds junctional adhesion molecule-A (JAM-A) on host cell membranes (Barton et al., 2001). Other reovirus proteins facilitate internalisation of the virus by endocytosis and penetration of the endosome membrane to release disassembled virus into the cytoplasm, and the core contains RNA dependent RNA polymerase (protein λ3), for replication of the viral genome.
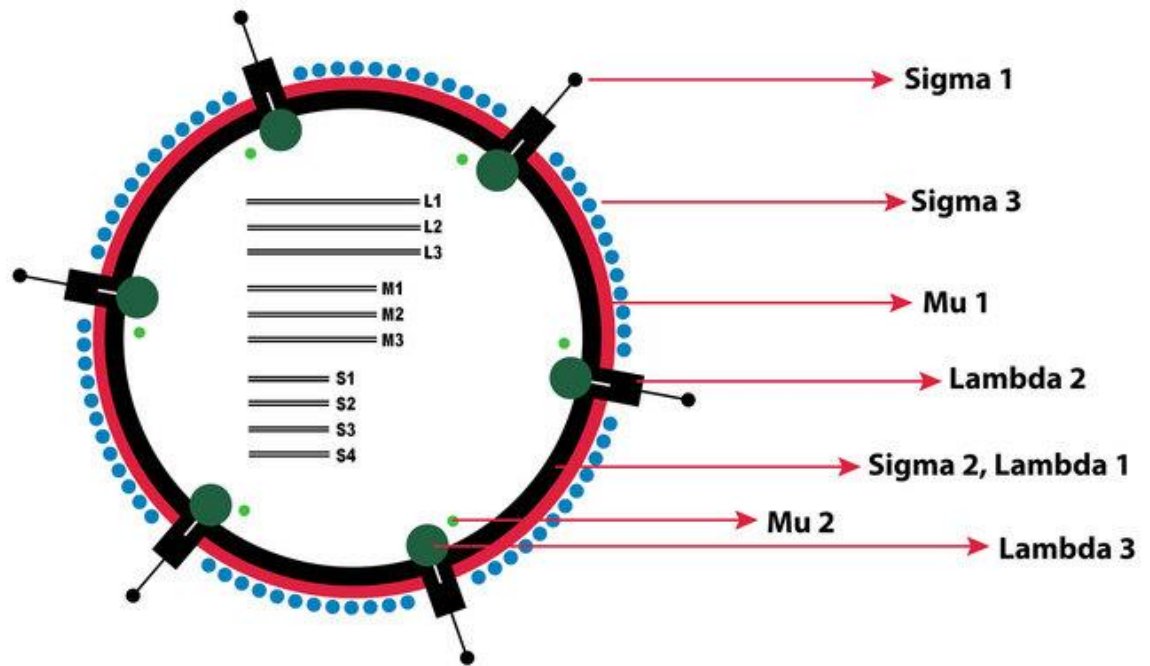
Figure 1.7 Reovirus structure

Diagram showing the structure of mammalian reovirus. The dsRNA genome is segmented, with 3 large (L) strands, 3 medium (M) strands and 4 small (S) strands. Key reovirus proteins are shown, making up two concentric shells, the outer capsid and core. Figure reproduced from (Sahin et al., 2013).

1.4.1 Cancer cell selectivity

Reovirus is not a significant human pathogen. In 1977, Hashiro et al. discovered that reovirus could replicate in a number of transformed mammalian cell lines, but not in normal human cells (Hashiro et al., 1977). Since this important discovery, reovirus specificity for cancer cells has been exploited for the development of OV therapy. The type 3 Dearing strain of reovirus was selected to develop as a therapeutic (Reolysin). Unlike many oncolytic viruses, which are genetically engineered to selectively replicate in cancer cells, reovirus is naturally oncolytic. This is a great advantage in terms of cost and safety.

What is the basis for the cancer cell selectivity of reovirus? There is strong evidence that host cell activation of the Ras signalling pathway enhances the production of reovirus (Strong et al., 1998), specifically constitutive activation of RalGEF and p38 (Norman et al., 2004), downstream of Ras. In those studies, cell lines were artificially transformed with constitutively active forms of Ras pathway genes, which led to increased reovirus protein production. Based on this data, many speculated that Ras transformation in human cancers was the reason for the oncolytic properties of reovirus. In more recent studies, others have demonstrated that Ras pathway activation in cancer cell lines does not correlate with reovirus induced killing (Twigger et al., 2012). It is likely that reovirus oncolysis is not solely dependent on Ras transformation, and may be explained by a number of contributing mechanisms. One study showed that cell cycle phase influenced the selectivity of reovirus, as host cells induced to accumulate in S phase were more sensitive to reovirus mediated killing (Heinemann et al., 2010). Therefore, rapidly cycling cancer cells may be more vulnerable to reovirus infection. Other mechanisms may include the more general downregulation of anti-viral defence machinery observed in many cancers, as discussed in section 1.3.1.

1.4.2 Clinical trials

To date, there have been a number of phase I and phase II clinical trials of reovirus, recruiting patients with many different types of solid tumours. In these trials, reovirus was well tolerated, and maximum tolerated doses were not reached in most cases (Gong et al., 2016). The most common adverse effects were flu like toxicities, which is not

surprising given the high doses of replicating virus. Phase I trials have tested both intratumoural and intravenous delivery of reovirus, with most phase II trials continuing with intravenous delivery (which is more amenable to the clinic than intratumoral injection).

Currently, there has been one phase III trial of reovirus, to test the efficacy of intravenous reovirus for the treatment of advanced head and neck cancer. This was a randomised, double-arm, double-blinded trial of reovirus in combination with the chemotherapy agents paclitaxel and carboplatin. Oncolytics Biotech, the developer of Reolysin, reported a higher median progression-free survival in the reovirus test group compared with the placebo group, in preliminary data from 2013 (Gong et al., 2016).

1.4.3 NK cell activation

A number of studies have demonstrated reovirus induced activation of NK cells, both *in vitro* and *in vivo*. In cell culture, the virus can activate DCs through soluble factors. 'Reo activated' DCs can activate NK cells *in vitro*, as might be the case in patient lymph nodes (Errington et al., 2008). Further studies have shown that NK cells can be activated directly by the conditioned media from reovirus infected tumour cells (Steele et al., 2011) and also by monocytes in peripheral blood when exposed to reovirus (Parrish et al., 2015). This suggests that NK cells may be activated both systemically and at the local tumour site in patients. A recent study showed that reovirus was effective as a combined anti-tumour and anti-viral therapy, against HCV and liver cancer (Samson et al., 2016). Interestingly, UV inactivated virus was able to inhibit tumour growth and activate NK cells just as well as replication competent virus, indicating that direct lysis of tumour cells was probably not important in this model - instead recognition of virus by the immune system was sufficient (for example by detection of the dsRNA genome). The activation of NK cells has also been studied in patients, receiving intravenous infusions of reovirus during a clinical trial. Following viral treatment, a number of interferon induced genes and activatory markers were upregulated on peripheral blood NK cells from these patients (El-Sherbiny et al., 2015). Blocking IFN-I *in vitro* completely inhibited reovirus induced cytotoxic granule release in peripheral blood NK cells (Parrish et al., 2015). The evidence suggests that, at least in peripheral blood, NK response to reovirus is dependent on the release of IFN-I, as is the case in natural viral infections. In order to improve on this

treatment, it will be important to understand the molecular mechanisms of OV induced immune activation in more detail.

1.5 Aims of the PhD project

Reovirus is an oncolytic virus (OV) which shows evidence of anti-tumour immunity induction in several *in vitro* and *in vivo* studies, particularly with the involvement of NK cells. Reovirus therapy is likely to activate NK cells by the release of cytokines, triggering activation of a number of signalling pathways that lead to upregulation of NK cell effector functions.

The broad aim of this project was to increase our understanding of NK cell activation in the context of viral infection, as there is conflicting evidence in the literature concerning the role of different cytokines and signalling pathways. The work focuses specifically on reovirus, as there is a need to better understand the molecular mechanisms that drive the induction of anti-tumour immunity seen in pre-clinical trials with this OV.

I have used an *in vitro* model of reovirus treatment, to study the response of human NK cells, and in particular the two major subsets, CD56^{dim} and CD56^{bright} NK cells. The main aims were:

- To define the reovirus induced mechanism of NK cell activation through IFN-I, and the signalling events leading to activation. In particular, to test the hypothesis that reovirus triggers NK cell activation directly through the IFN-I receptor.
- To determine the wider effects of reovirus treatment on human NK cells, by performing a gene expression screen. Studies to date have focussed largely on granule dependent cytotoxicity mechanisms. I hypothesised that other NK cell functions will be enhanced by viral therapy, such as proliferation and migration, which are altered during some viral infections.
- To further investigate NK cell pathways highlighted by the gene expression screen, and to determine the consequences of pathway activation on NK cell function.

A better knowledge of the cytokines and pathways involved should lead to improvements in OV therapy, for example it may inform the choice to combine OV treatment with other immunotherapies.

Chapter 2. Materials and Methods

2.1 Cells

2.1.1 Isolation of peripheral blood mononuclear cells (PBMC)

Apheresis cones containing platelet depleted peripheral blood from healthy donors were obtained from NHS Blood and Transplant (Leeds) and separated by density gradient centrifugation on the day of donation. Briefly, donor blood was diluted with 50 ml of phosphate buffered saline (PBS), giving a final volume of 60 ml. Each 30 ml of eluate was carefully layered onto 15 ml of room temperature Lymphoprep (Axis-Shield) and centrifuged at 800 x g for 20 minutes, with no brake. Post-centrifugation the PBMC collect in a layer at the interface of the Lymphoprep and plasma as shown in Figure 2.1. This layer was collected using a 5 ml pastette and washed with PBS before centrifugation at 200 x g for 15 minutes (brake on). The supernatant was discarded and the pelleted PBMC were pooled and washed again in 20 ml PBS before centrifugation at 300 x g for 10 minutes. The supernatant was discarded and the pellet was resuspended in Roswell Park Memorial Institute medium (RPMI) 1640 (Sigma) + 10 % foetal calf serum (FCS) (Sigma) at a concentration of 2×10^6 cells/ml and cultured at 37 °C with 5 % CO_2.
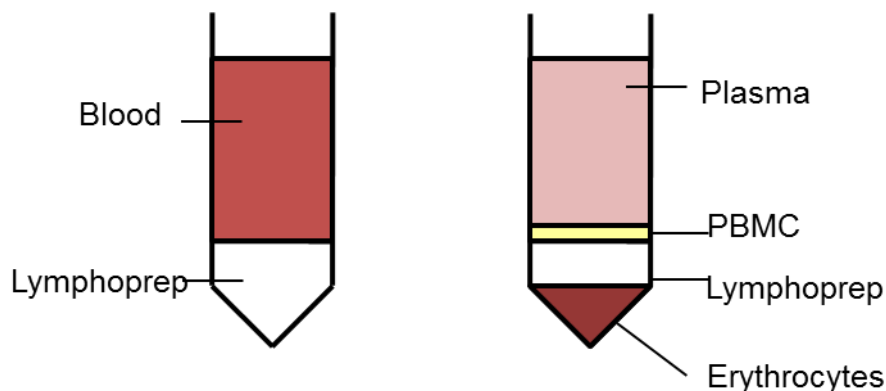
Figure 2.1 Isolation of PBMC by density gradient centrifugation

Left – blood layered over Lymphoprep pre-centrifugation. Right – Post centrifugation, PBMC collect in the interface of the plasma and Lymphoprep layers.

2.1.1.1 **Isolation of PBMC from patients with systemic lupus erythematosus (SLE)**

Ethical approval to collect blood samples after informed consent was obtained from the ethics committee at the Leeds Teaching Hospitals NHS Trust (REC number 10/H1306/88). Blood was collected from consenting patients, and from consenting healthy donors, into EDTA treated tubes, to be processed the same day. PBMC were isolated as in section 2.1.1, except blood was diluted 1 in 2 with PBS in the first stage.

2.1.2 Isolation of NK cells from PBMC

NK cells were purified from whole PBMC, either on the day of donation or after culturing for the specified number of hours/days. NK cell isolation was performed by untouched, negative selection using a bead-based human NK cell isolation kit (Miltenyi), according to the manufacturer's instructions. PBMC (isolated as in 2.1.1) were centrifuged at 300 x g for 10 minutes at 4 °C and resuspended in MACS buffer (PBS with 0.5 % bovine serum albumin (BSA) and 2 mM EDTA) and biotin antibody cocktail (Miltenyi). 'Non NK' cells were labelled with the biotin conjugated antibodies. After incubating for 5 minutes at 4 °C, MACS buffer and anti-biotin magnetic beads (Miltenyi) were added to the cell suspension. After a further incubation of 10 minutes at 4 °C, the cell suspension was passed through an LS magnetic column in a strong magnetic field (Miltenyi). The column was flushed through with 9 ml of cold MACS buffer, to elute the non labelled cells. Eluted NK cells were cultured in Dulbecco's Modified Eagle Medium (DMEM) (Sigma), supplemented with 10 % human AB serum (Gemini Bio-Products) at 37 °C, 5 % CO_2, unless otherwise specified.

2.1.3 Cell lines

The NK sensitive leukaemia cell line, K562, was cultured in RPMI 1640 medium (Sigma), supplemented with 10 % FCS, at 37 °C, 5 % CO_2. Cells were subcultured according to ATCC guidelines.

2.2 Treatment of primary cells

2.2.1 Reovirus treatment

Commercial reovirus (Reolysin®) was provided by Oncolytics Inc. (Canada). Viral titre of reovirus stocks were determined by routine plaque assays performed by members of Prof Alan Melcher's group. After culturing overnight, PBMC were seeded into cell culture plates (Corning) at 2×10^6 cells per ml (NK cells at 1×10^6 cells per ml) and reovirus was added at a multiplicity of infection (MOI) of 1 (unless otherwise stated). Plates were returned to standard cell culture conditions, as described in section 2.1.

2.2.2 Cytokine treatment

PBMC or NK cells were cultured overnight before seeding into plates (as above). Cytokines from Table 2.2 were added to the plate at the specified concentrations, then cells were returned to standard cell culture conditions (section 2.1). In chapter 3, human purified IFN-α from Sigma was used, however this product was discontinued so recombinant IFN-α from Miltenyi was used in chapter 5. IL-12 from R&D Systems was used in chapter 3, but IL-12 from Peprotech was used in chapter 5.

Cytokine	Source
Human Interferon α (IFN-α)	Sigma, purified from human leukocytes
Human Interferon α2	Miltenyi, recombinant
Human Interleukin 12 (IL-12)	R&D systems, recombinant
Human Interleukin 12	Peprotech, recombinant
Human Interleukin 15 (IL-15)	Miltenyi, recombinant

Table 2.1 Details of cytokines

2.2.3 Polyinosinic:polycytidylic acid (Poly(I:C)) treatment

PBMC were seeded into a 12 well cell culture plate (Corning) at 2×10^6 cells per ml and transfected with 1 µg Poly(I:C) (high molecular weight, Invivogen) according to instructions in the Effectene transfection kit (Qiagen). Briefly, 1 µg Poly(I:C) was diluted with DNA-condensation buffer and incubated with Enhancer solution. Effectene transfection reagent was added to the Poly(I:C)–Enhancer solution to allow complexes

to form. Finally, growth medium (RPMI 1640 + 10% FCS) was mixed with the complexes and the mixture was added, drop wise, to cells in the plate. Mock treated cells were treated in exactly the same way, except PBS rather than Poly(I:C) was added.

2.2.4 Type I interferon neutralisation

To neutralise type I interferons during culture of PBMC or NK cells, a cocktail of antibodies, including a monoclonal mouse antibody and sheep serum polyclonal antibodies, was added at the start of the culture. As a control, mouse isotype control antibody plus heat inactivated sheep serum were used:

Antibody	Source	Stock concentration	Dilution in culture
Anti-human interferon α/β receptor chain 2 (mouse IgG2a). Clone MMHAR-2.	PBL Assay Science	0.5 mg/ml	2.5 % v/v
Anti-human interferon α, sheep serum polyclonal.	PBL Assay Science	0.48 mg/ml (estimated)	1.5 % v/v
Anti-human interferon β, sheep serum polyclonal.	PBL Assay Science	0.53 mg/ml (estimated)	1.5 % v/v
Mouse IgG2a.	BioLegend	0.5 mg/ml	2.5 % v/v
Heat inactivated sheep serum	Sigma		3 % v/v

Table 2.2 Antibodies and controls for type I interferon neutralisation experiments

2.2.5 IL-15 neutralisation

For IL-15 neutralisation, an antibody against human IL-15 (R&D systems, clone 34593, mouse IgG1) was added at the start of the culture, at 1 µg/ml. As a control, 1 µg/ml of mouse IgG1 antibody (R&D systems, clone 11711) was used.

2.3 Flow cytometry

For all flow cytometry experiments, staining buffer (PBS + 2 % FCS + 0.09 % sodium azide) was used for washing and staining steps. Cells were centrifuged at 300 x g for 5 minutes, unless otherwise stated. For staining of NK cells within PBMC, antibodies against CD56 and CD3 were routinely added (for gating of CD3- CD56+ NK cells). To assess background staining levels for markers of interest, cells were stained with isotype matched control antibodies. Where % positive values are reported, a gate was set whereby 2 % of isotype control stained cells were positive. For multicolour experiments, single stain controls (using PBMC) were included, for compensation calculations. For a list of antibodies used in this thesis, see table 2.3.

2.3.1 Surface staining

Cells were collected into 5 ml polystyrene tubes (Falcon) and centrifuged, then washed with 2 ml of staining buffer. Samples were resuspended at 1×10^6 cells/100µl staining buffer, in a mixture of antibodies specific to the experiment and incubated for 15 minutes at room temperature, protected from light. Cells were washed once more in staining buffer and resuspended in staining buffer. For virus containing samples, cells were fixed in Cytofix fixation buffer (BD Biosciences) on ice for 15 minutes, before the final wash and resuspension. Samples were analysed by flow cytometry, either on an LSRII flow cytometer (BD Biosciences) or a Cytoflex cytometer (Beckman Coulter).

2.3.2 Viability staining

Cells were collected into 5 ml polystyrene tubes (Falcon), centrifuged and washed with PBS, then resuspended at 1×10^6 cells/100 µl, in PBS + 0.5 % v/v zombie NIR dye (BioLegend). Samples were incubated for 10 minutes at room temperature, protected from light, then cells were washed with staining buffer and finally surface stained (section 2.3.1).

2.3.3 Fluorescence activated cell sorting of NK cells into CD56^{dim} and CD56^{bright} subsets

In this case, cells were centrifuged for 10 minutes for wash steps, rather than 5 minutes. NK cells were first magnetically isolated from cultured PBMC (section 2.1.2). Then, NK

cells were collected into 5 ml polypropylene tubes (Falcon) and resuspended at 1 x 10^7 cells/ml, in staining buffer plus antibodies against CD3, CD56 and CD16. Samples were incubated at room temperature for 15 minutes, protected from light, then washed and resuspended in RPMI + 10 % FCS (at the same density). Stained NK cells were sorted into CD56^{dim} CD16+ and CD56^{bright} CD16- subsets using a BD Influx cell sorter (BD Biosciences). NK cells were collected into tubes containing RNAprotect reagent (Qiagen) for stabilisation of RNA, then stored at -20 °C until RNA extraction.

2.3.4 CD107a degranulation assay

PBMC were co-cultured with K562 cells in a 96 well, round bottomed cell culture plate (Corning), at a 10:1 effector:target ratio (1:1 NK:target assuming NK cells are 10 % of PBMC). After 1 hour of culture, GolgiStop (containing monensin, BD Biosciences) was added to each well at 1 in 1000, to prevent the internalisation of CD107a after degranulation. After a further 5 hours, cells were collected into 5ml polystyrene tubes (Falcon), centrifuged and washed with staining buffer. Samples were resuspended in staining buffer plus antibodies against CD3, CD56 and CD107a (or matched isotype control), and incubated at room temperature for 15 minutes. Cells were fixed in Cytofix fixation buffer (BD Biosciences) on ice for 15 minutes, then washed and resuspended in staining buffer. Staining was analysed on an LSRII flow cytometer (BD Biosciences).

2.3.5 Intracellular phosphorylated protein staining

After incubation with reovirus or cytokine for the specified time, cells were fixed in Cytofix fixation buffer (BD Biosciences). Briefly, Cytofix buffer was warmed to 37 °C and treated cells were harvested into 15 ml falcon tubes. An equal volume of Cytofix buffer was added to the cells, which were then incubated at 37 °C for 10 minutes. Fixed cells were centrifuged at 600 x g for 5 minutes and resuspended in 1 ml staining buffer. For time-course experiments, fixed cells were stored at 4 °C and all cells within an experiment were stained at the same time. On the day of staining, cells were centrifuged at 600 x g for 5 minutes, and the remaining centrifugation steps were all at 600 x g. Samples were vortexed to disrupt the pellet and resuspended in 1 ml of ice cold Permeabilisation Buffer III (BD Biosciences, contains methanol), then permeabilised on ice for 30 minutes. This was followed by washing with staining buffer three times.

Cells were stained at 1 x 10^6 cells per 100 µl stain buffer with the appropriate antibodies, against phosphorylated proteins or isotype controls, for 1 hour at room temperature, protected from light. Antibodies against CD3 and CD56 were added together with phosphoprotein antibodies. Finally, cells were washed in stain buffer twice more, then resuspended in staining buffer. Samples were analysed on an LSRII flow cytometer (BD Biosciences) or a Cytoflex cytometer (Beckman Coulter).

2.3.6 Intracellular staining for Ki67 and PCNA

Cells were fixed, permeabilised and stained as in section, 2.3.5, except cells were stained for 30 minutes. Antibodies against CD3 and CD56 were added together with Ki67 or PCNA antibodies.

2.3.7 Intracellular staining for Granzyme B (saponin method)

Cells were collected into 5 ml polystyrene tubes (Falcon) and surface stained, as in section 2.3.1. Following this, samples were washed with 2 ml staining buffer and fixed in Cytofix fixation buffer (BD Biosciences) for 15 minutes on ice. Samples were washed again in staining buffer, then resuspended in saponin buffer (staining buffer + 0.1 % saponin) at 1 x 10^6 cells per 100 µl. Samples were incubated for 15 minutes at room temperature, then resuspended in saponin buffer + anti Granzyme B (or a matched isotype control), at 1 x 10^6 cells per 100 µl. Samples were stained for 30 minutes at room temperature, then washed in 2 ml saponin buffer. Finally, cells were resuspended in 0.5 % paraformaldehyde in staining buffer, and analysed on a Cytoflex flow cytometer (Beckman Coulter).

2.3.8 Carboxyfluorescein Diacetate, Succinimidyl Ester (CFDA-SE) labelling assay

Firstly, PBS, FCS and RPMI 1640 (Sigma) + 10% FCS were pre-warmed in a 37 °C water bath. After culturing overnight, PBMC were centrifuged for 10 minutes then resuspended in warm PBS + 2 µM CFDA-SE (Invitrogen) at 10^7 cells/ml. Cells were incubated for 10 minutes at 37 °C, then the labelling reaction was quenched with an equal volume of warm FCS. Cells were washed twice with warm RPMI 1640 + 10 % FCS, centrifuging for 10 minutes each time. Finally, PBMC were resuspended in RMPI

+ 10 % FCS, at 2×10^6 cells/ml and cultured with or without virus/cytokine for the specified time.

After culturing, cells were collected into 5 ml polystyrene tubes (Falcon), then stained with viability dye (section 2.3.2) followed by surface staining with antibodies against CD56, CD3 and CD16 (section 2.3.1). Finally, cells were fixed in Cytofix fixation buffer (BD Biosciences) on ice for 15 minutes, then washed and resuspended in staining buffer. Staining was analysed on an LSRII flow cytometer (BD Biosciences), on the lowest speed setting.

2.3.9 Propidium iodide staining for cell cycle analysis

Cells were collected into 15 ml falcon tubes and centrifuged for 10 minutes, then washed once in PBS. Next, cells were resuspended in ice cold 70 % ethanol, at 1×10^6 cells/ml, while vortexing to avoid cell clumping. Samples were fixed on ice for 30 minutes, then stored at -20 °C until staining.

Fixed cells were transferred into FACS tubes and washed with 2ml stain buffer, centrifuging at 600 x g. Next, each sample (between $0.5 - 1 \times 10^6$ cells) was resuspended in 50 µl of 100 µg/ml RNase A (Qiagen). Next, DNA staining solution was prepared by diluting propidium iodide (PI) (Life Technologies) to a working concentration of 16.6 µg/ml in staining buffer. DNA staining solution was added directly to cells resuspended in RNase A, so the final concentration of cells was $1 \times 10^6/650$ µl. Samples were incubated at room temperature for 10 minutes, then analysed on an LSRII flow cytometer (BD Biosciences), on the lowest speed setting.

2.3.10   List of antibodies

Table 2.3 details all antibodies used in flow cytometry experiments, including antibody clone number, isotype and experimental concentration.

Target	Conjugate	Clone	Isotype	Manufacturer	Experimental concentration (per 100 µl)
CD56	PE-Vio770	REA196	Human IgG1	Miltenyi	1 µl / 8.25 ng
CD56	APC	AF12-7H3	IgG1	Miltenyi	2 µl / 16.5 ng
CD3	FITC	UCHT1	IgG1	BD Biosciences	5 µl / 62.5 ng
CD3	BV421	UCHT1	IgG1	BD Biosciences	2 µl / 100 ng
CD69	BV421	FN50	IgG1	BioLegend	2 µl / 50 ng
CD69	FITC	FN50	IgG1	BioLegend	5 µl / 500 ng
CD69	PE	FN50	IgG1	BioLegend	2 µl / 20 ng
CD317 (Tetherin)	PE	REA202	Human IgG1	Miltenyi	5 µl / 550 ng
pY701 STAT1	APC	REA345	Human IgG1	Miltenyi	10 µl / 20 ng
pY693 STAT4	PE	38/p-Stat4	IgG2b	BD Biosciences	6 µl / 24 ng
pY694 STAT5	PerCP-Cy5.5	47/Stat5(pY694)	IgG1	BD Biosciences	10 µl / 15 ng
Granzyme B	PE	GB11	IgG1	Thermo Fisher Scientific	5 µl / 500 ng (approx.)
CD253 (TRAIL)	APC	RIK-2.1	IgG1	Miltenyi	10 µl / 550 ng
CD16	BV421	3G8	IgG1	BioLegend	2 µl
CD16	BUV395	3G8	IgG1	BD Biosciences	5 µl / 1 µg
CCR7 (antibody 1)	-	3D12	Rat IgG2a	BD Biosciences	0.5 µl / 250 ng
Rat IgG	Alexa Fluor 488		Chicken IgY	Thermo Fisher Scientific	0.5 µl / 1 µg
CCR7 (antibody 2)	VioBlue	REA546	Human IgG1	Miltenyi	10 µl / 1.65 µg
PCNA	PE	PC10	IgG2a	BD Biosciences	20 µl / 125 ng
Ki67	PE	REA183	Human IgG1	Miltenyi	10 µl / 220 ng

pY694 STAT5	BV421	47/Stat5(pY694)	IgG1	BD Biosciences	3 µl / 150 ng
pS2448 mTOR	PE	O21-404	IgG1	BD Biosciences	5 µl / 16 ng
pS473 Akt	Alexa Fluor 488	M89-61	IgG1	BD Biosciences	15 µl / 45 ng
Controls					
	BV421	MOPC-21	IgG1	BioLegend	
	FITC	MOPC-21	IgG1	BD Biosciences	
	PE	REA293	Human IgG1	Miltenyi	
	APC	REA293	Human IgG1	Miltenyi	
	PE	27-35	IgG2b	BD Biosciences	
	PerCP-Cy5.5	MOPC-21	IgG1	BD Biosciences	
	PE	MOPC-31C	IgG1	BD Biosciences	
	VioBlue	REA293	Human IgG1	Miltenyi	
	PE	MOPC-173	IgG2a	BD Biosciences	
	BV421	X40	IgG1	BD Biosciences	
	Akt	MOPC-21	IgG1	BD Biosciences	

Table 2.3 List of flow cytometry antibodies

All antibodies are mouse monoclonal, unless otherwise specified.

2.4 Enzyme-linked immunosorbent assay (ELISA)

The sandwich ELISA assay was carried out in 96 well protein binding plates (Thermo Fisher Scientific, Nunc MaxiSorp) and washing buffer (PBS + 0.05 % Tween) was used for wash steps.

2.4.1 ELISA for interferon α

Firstly, a mixture of coating antibodies against IFN-α (Mabtech, MT1/3/5) was diluted in PBS, to a final concentration of 4 µg/ml, and added to the plate at 100 µl per well. The plate was coated overnight at 4 °C. Next, the plate was washed 3 times with washing buffer. To block the plate, 200 µl of PBS + 10 % FCS was added to each well and the plate was incubated for 2 hours at room temperature. After washing 3 more times, PBMC supernatant samples were added to the plate. At the same time, recombinant IFN-α2 (Miltenyi) of known increasing concentration was added to the plate, to generate a standard curve. IFN-α was diluted in RPMI 1640 (Sigma) + 10 % FCS, starting at 2500 pg/ml, with 6 sequential 1 in 2 dilutions. A blank sample, with only RPMI + 10 % FCS, was also added. All samples were added in triplicate, at 100 µl per well. The plate loaded with samples was incubated overnight at 4 °C, then washed 6 times. A mixture of biotinylated detection antibodies against IFN-α (Mabtech, MT2/4/6) was diluted in PBS + 10% FCS to a final concentration of 1 µg/ml, and added to the plate at 100 µl per well. The plate was incubated for 2 hours at room temperature, then washed another 6 times. Avidin conjugated alkaline phosphatase (Sigma, ExtrAvidin) was diluted 1 in 5000, in washing buffer, and added to the plate at 100 µl per well. After incubating at room temperature for 1 hour, the plate was washed 3 times with distilled water. Finally, p-Nitrophenyl phosphate substrate was prepared according to manufacturer instructions (Sigma, SigmaFast tablets) and added to the plate at 100 µl per well. The plate was incubated at room temperature for 10 to 30 minutes to develop, protected from light, then absorbance was read at 405 nm on a Multiskan EX plate reader (Thermo Fisher). A standard curve was fitted using Excel. The limit of detection (LoD) was calculated as follows (LoB = Limit of blank):

LoD = LoB + 1.645(Standard deviation of low concentration sample)

LoB = meanblank + 1.645(SDblank)

Low concentration sample = bottom of standard curve.

2.4.2 ELISA for interferon β

ELISA was carried out as in section 2.4.1, except for the following changes:

The plate was initially coated with an antibody against IFN-β (Peprotech, 500-P32B, rabbit polyclonal), diluted 1 in 1000 in coating buffer (100 mM NaHCO$_3$). A biotinylated antibody against IFN-β (Peprotech, 500-P32BBT, rabbit polyclonal), diluted 1 in 1000 in PBS + 10 % FCS, was used as the detection antibody.

2.5 Sodium dodecyl sulphate polyacrylamide gel electrophoresis (SDS-PAGE) and Western Blotting

2.5.1 Preparation of cell lysates for SDS-PAGE

Cells were collected into Eppendorf tubes, centrifuged at 300 x g for 5 minutes, then washed with 1 ml ice cold PBS. Next, cells were lysed with ice cold RIPA buffer (150mM NaCl, 10mM Tris pH7.2, 0.1% SDS, 0.1% Triton-X, 1% deoxycholic acid, 5mM EDTA) with added cOmplete™ Mini EDTA-free protease inhibitor cocktail and PhosStop phosphatase inhibitors (both Roche), at 1 x 10^6 cells/50µl, for 20 minutes on ice. Samples were sonicated in 2 x 2 second pulses, in order to shear DNA. At this point, samples could be stored at -80 °C until the next step. Protein sample buffer (5x) (250 mM Tris pH 6.8, 50 % glycerol, 10 % sodium dodecyl sulphate (SDS), 0.1 % bromophenol blue, 1 % β-mercaptoethanol) was added to each sample at 1 part to 4 parts lysate, and samples were boiled at 95 °C for 10 minutes, to denature and reduce protein.

2.5.2 SDS-PAGE

A 10% Tris Glycine resolving gel (10 % acrylamide, 380 mM Tris pH 8.8, 0.1 % SDS, 0.1 % APS , 0.1 % TEMED) with 4 % stacking gel (4 % acrylamide, 120 mM Tris pH 6.8, 0.1 % SDS, 0.1 % APS, 0.1 % TEMED) was prepared and immersed in 1x SDS-PAGE buffer (25 mM Tris, 192 mM glycine, 0.1 % SDS) in a miniPROTEAN Tetra Cell gel electrophoresis tank (Bio-Rad). Protein samples were loaded into the gel, along with 10 µl of SeeBlue Plus 2 pre-stained protein standard (Invitrogen) in the first well. A potential difference of 150 V was applied across the gel for 1 hour.

2.5.3 Western Blot

A 6 x 8 cm^2 piece of Hybond-P polyvinylidene fluoride (PVDF) membrane (GE Healthcare Life Sciences) was activated in methanol for 20 seconds, then immersed in 1 x Towbin buffer (25 mM Tris, 192 mM glycine, 20 % methanol). Two filters (BioRad) were also

immersed in 1 x Towbin buffer. The SDS-PAGE gel was then placed on top of the membrane, between the two filters, in a semi dry transfer machine (Bio-Rad). A potential difference of 15 V was applied for 1 hour.

For probing of the PVDF membrane, antibody details are specified in Table 2.4. The PVDF membrane with transferred protein was blocked in 1 x Tris Buffered Saline with 0.1% Tween (TBST) and 5% skimmed milk, for 1 hour at room temperature, with continuous agitaton. The skimmed milk solution was removed and replaced with primary antibody at the specified dilution (see Table 2.4), and incubated overnight at 4 °C, with continuous agitation. The primary antibody solution was removed and the membrane was washed in TBST for 5 minutes, a total of 3 times. Secondary antibody was added at the specified dilution and the blot was incubated for 1 hour at room temperature, with continuous agitation. The membrane was washed another 3 times in TBST before enhanced chemiluminescence (ECL) solution 1 (0.4 mM p-coumaric acid, 2.5 mM Luminol, 0.1 M Tris pH 8.5) and ECL solution 2 (0.02 % hydrogen peroxide, 0.1 M Tris pH 8.5) were added at a 1:1 ratio, and mixed by pipetting over the membrane. The blot was transferred to a light proof cassette and developed using a Konica SRX-101A Tabletop X-ray Film Processor (Konica, UK). The expression of β-actin was used to assess the equal loading of protein samples.

Target	Clone	Manufacturer	Dilution	Buffer
MCM4	Rabbit polyclonal	Abcam	1 in 5000/ 200 ng/ml	2.5 % BSA in TBST
Cyclin B	Mouse IgG1, clone 18	BD Biosciences	1 in 1000/ 250 ng/ml	2 % BSA in TBST
CDK2	Mouse IgG2a, clone 55	BD Biosciences	1 in 1000/ 250 ng/ml	2 % BSA in TBST
β actin	IgG2a, clone AC-74	Sigma	1 in 10,000	2 % BSA in TBST
Rabbit IgG	Goat polyclonal, HRP conjugated	Sigma	1 in 5000	2 % BSA in TBST
Mouse Ig	Rat IgG, clone eB144, HRP conjugated	Rockland	1 in 10,000	2 % BSA in TBST
Mouse IgG	Sheep polyclonal, HRP conjugated	Sigma	1 in 5000	2 % BSA in TBST

Table 2.4 List of Western Blotting antibodies

2.6 Transcriptome microarray

2.6.1 Sample preparation

PBMC cultured with or without reovirus at an MOI of 1 were magnetically labelled to isolate PB-NK cells (section 2.1.2). Helen Close provided purified NK cell samples, cultured with or without 100 international units/ml of IL-15 (Miltenyi). After the last wash step, NK cells were resuspended in RNAprotect Cell Reagent (Qiagen), to stabilise RNA, and tubes were vortexed to resuspend the pellet completely. Cells in RNAprotect were stored at -20 °C until samples from 5 separate donors were collected. Samples were sent to an external service provider (Hologic, Manchester, UK). Staff at Hologic isolated RNA from the samples with the RNeasy mini kit (Qiagen), according to manufacturer instructions. Contaminating DNA was removed by on column DNase

digestion and RNA integrity was checked using an Agilent 2100 Bioanalyzer (Agilent Technologies).

2.6.2 Microarray

Hologic also carried out all microarray steps: First, total RNA was amplified, then sense strand cDNA was synthesised and labelled using the GeneChip™ WT PLUS Reagent Kit, according to manufacturer instructions (Applied Biosystems, Thermo Fisher Scientific). Labelled cDNA was hybridised to a GeneChip® Human Transcriptome Array 2.0 (Applied Biosystems, Thermo Fisher Scientific), according to manufacturer instructions.

2.6.3 Differentially expressed genes

Raw intensity files for each microarray chip were received from Hologic. Raw data (CEL files) for all conditions were processed with the Expression Console software (Affymetrix) which performed background correction, normalisation and summarisation steps, using the Signal Space Transformation-Robust Multi-Chip Analysis (SST-RMA) algorithm. All chip intensity data passed quality control steps. Then, normalised signal values were analysed with the Transcriptome Analysis Console (TAC, Affymetrix) software, to identify statistically significant differences between conditions. Following manufacturer guidelines, TAC software was used to run paired ANOVA tests and false discovery rate (FDR) prediction. Differentially expressed genes were defined as at least 1.5 fold up/downregulated and FDR p value < 0.05 (unless otherwise stated).

2.6.4 Pathway enrichment analysis

Pathway enrichment analysis was performed with MetaCore GeneGo (Thomson Reuters).

2.7 Real time PCR

2.7.1 Sample preparation

Cells were resuspended and stored in RNAprotect cell reagent (Qiagen), as in section 2.6.1. For time-course experiments, samples were stored until all time-points could be processed together. Then, RNA was extracted with the RNeasy mini kit (Qiagen),

according to manufacturer instructions (following specific instructions for RNAprotect stored cells). Contaminating DNA was removed by on column DNase digestion, with the RNase-Free DNase Set (Qiagen). RNA was eluted from the column in nuclease free water.

RNA concentration was measured using a Nanodrop spectrophotometer (Thermo Fisher Scientific). Next, complementary DNA (cDNA) was synthesised from the extracted RNA. In a 13 µl reaction volume, random primers (New England Biolabs) to a final concentration of 4.6 µM and dNTP mix (New England Biolabs) to a final concentration of 800 nM were combined with 30-100 ng RNA. This was incubated at 65 °C for 5 minutes and cooled on ice for 1 minute. To a final volume of 20 µl, the following components were added: 1x First strand buffer (Invitrogen), 5 nM DTT, 40 units RNase OUT (Invitrogen) and 200 units of Superscript III reverse transcriptase (Invitrogen). This mixture was incubated at 25 °C for 5 minutes, followed by incubation at 50 °C for 1 hour and inactivation at 15 °C for 15 minutes. cDNA samples were stored at -20 °C.

2.7.2 Taqman method

In a MicroAmp fast optical 96 well reaction plate (Applied Biosystems), 1x Taqman gene expression master mix (Applied Biosystems) was combined with 10ng cDNA, 1x Taqman gene expression assay probe (see section 2.7.5) and nuclease free water to a final volume of 20 µl.

Amplification was carried out in a 7500 Real Time PCR machine (Applied Biosystems) or a QuantStudio 5 machine (Applied Biosystems), using the following thermal cycling conditions: 50 °C for 2 minutes, 95 °C for 10 minutes, followed by 40 cycles of 95 °C for 15 seconds/ 60 °C for 1 minute. Reactions were performed in triplicate and all replicate values were within 0.5 cycles. Cycle threshold (Ct) values were calculated using Applied Biosystems software.

2.7.3 SYBR Green method

For targets with standard primers already available, the SYBR Green method was used instead. Reactions were prepared in plates as in section 2.7.2, except for the following changes:

- PowerUp™ SYBR™ Green Master Mix (Applied Biosystems) was used instead of Taqman gene expression master mix.
- Primers (section 2.7.5) were used instead of Taqman gene expression assay probes. Primers were included at a final reaction volume of 500 nM.
- Identical cycling conditions to section 2.7.3 were used, plus melt curve analysis was included to test for specific product amplification.

2.7.4 Analysis

Fold change gene expression over resting was calculated by the ΔCt method (below). ABL1 was used as the housekeeping gene.

$$\Delta Ct = Target\ Ct\ mean - Housekeeping\ Ct\ mean$$

$$\Delta\Delta Ct = \Delta Ct\ control - \Delta Ct\ treatment$$

$$Fold\ change\ expression\ over\ resting = 2^{\Delta\Delta Ct}$$

2.7.5 Primers

	Target	Probe/Sequence	
Taqman probes (Taqman method)	ABL1	Applied Biosystems Hs01104728_m1	
	CCR7	Applied Biosystems Hs01013469_m1	
	S1PR1	Applied Biosystems Hs01922614_s1	
	MCM4	Applied Biosystems Hs00907398_m1	
Primers (SYBR Green method)	CDK2	F	ATGGATGCCTCTGCTCTCACTG
		R	CCCGATGAGAATGGCAGAAAGC
	CCNA2	F	CTCTACACAGTCACGGGACAAAG
		R	CTGTGGTGCTTTGAGGTAGGTC
	CCNB1	F	GACCTGTGTCAGGCTTTCTCTG
		R	GGTATTTTGGTCTGACTGCTTGC

Table 2.5 List of probes and primers for Real Time PCR

2.8 Statistics

Statistical tests were performed using Graphpad Prism (Graphpad Software).

Chapter 3. Interferon dependent activation of NK cells during reovirus treatment

3.1 Introduction

Oncolytic virus therapy has the potential to enhance the patient's innate immune response against tumour cells. Evidence of human NK cell activation was observed during a clinical trial of intravenous reovirus (EUDRACT number 2007/000258-29) (El-Sherbiny et al., 2015), and recent studies have demonstrated enhanced NK cell killing of targets following *in vitro* treatment of PBMC (Parrish et al., 2015) or liver mononuclear cells (Samson et al., 2016) with reovirus. However, the precise mechanism of NK cell activation is not well understood. Type I interferons (IFN-I), released during viral infection, are important for NK cell responses *in vivo*, but studies disagree on the mechanistic details, in particular, whether IFNs act directly on NK cells or indirectly through a secondary cytokine. In this chapter, I have attempted to answer this question using a simple *in vitro* model of reovirus therapy.

3.2 Results

3.2.1 Reovirus treatment activates NK Cells within PBMC

Blood from healthy donors was used as a source of immune cells, from which peripheral blood mononuclear cells (PBMC) were isolated by density gradient separation (section 2.1.1). Human NK cells are defined as CD56+CD3- lymphocytes, and antibody staining and flow cytometry can be used to identify NK cells within PBMC, where NK cells represent approximately 10% of lymphocytes (PBMC; Figure 3.1a). Furthermore, this staining can be used to assess the purity of NK cells enriched via immunomagnetic selection from PBMC, with purity exceeding 95% routinely obtained (Purified NK; Figure 3.1a).

Human NK cell activation can be assessed via expression of the lymphocyte activation marker CD69, via flow cytometry. In the clinical study referred to above (EUDRACT

number 2007/000258-29), CD69 expression by NK cells peaked approximately 48 hrs post-intravenous delivery at a multiplicity of infection estimated at approximately 1 (El-Sherbiny et al., 2015). This time point was therefore chosen for the *in vitro* model used here, together with MOIs of 1 and 10. The effect of reovirus on NK cells was analysed in two ways. First, PBMC were treated with reovirus and the activation of NK cells within PBMC was analysed. Secondly, NK cells were purified from PBMC and treated directly with reovirus. Figure 3a (bottom) shows that reovirus treatment induced CD69 expression on ~90 % of NK cells within PBMC, compared to ~10 % in untreated cells (figure 3.ab). CD69 expression was also induced by reovirus on purified NK cells, although the response was lower in magnitude and showed more donor variability. Most importantly, use of PBMC (containing multiple blood cell types) for *in vitro* studies more closely mimics the intravenous delivery of reovirus into patients. Therefore, PBMC based assays were used for the majority of experiments in this thesis.

Several studies have shown that reovirus treatment enhances the anti tumour response of NK cells *in vitro* by enhancing granule dependent killing. *(Parrish et al., 2015; Samson et al., 2016; Errington et al., 2008; Steele et al., 2011; El-Sherbiny et al., 2015).* To confirm this, PBMC were treated with reovirus and exposed to the NK sensitive leukaemia cell line, K562). Display of CD107a (a marker of degranulation) on the surface of NK within PBMC, was analysed using flow cytometry. NK cells from reovirus treated PBMC exhibited greater levels of degranulation than their untreated counterparts (Figure 3.1b). These results confirm that reovirus treatment of PBMC initiates a pathway that induces the anti-tumour activity of NK cells. Subsequent experiments were aimed at determining the nature of this activation step.
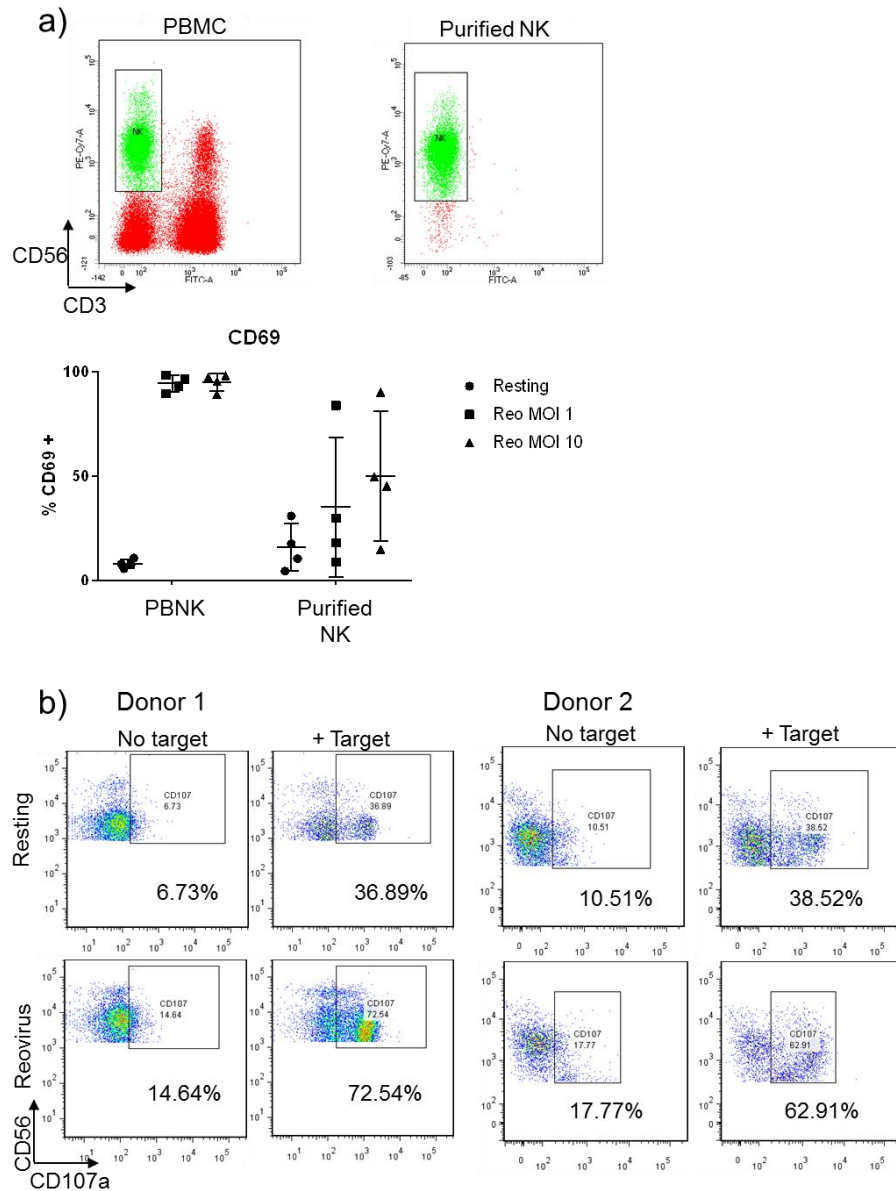
Figure 3.1 Effect of reovirus on CD69 expression and NK degranulation

a) Top: NK cells were identified as a CD3-CD56+ population within the whole PBMC population (left panel). The purity of isolated NK cells was confirmed using the same antibody panel (right panel). Bottom: Flow cytometric data to show the mean percentage of NK cells expressing CD69, either within PBMC (PBNK) or isolated from PBMC (purified NK), 48 hours post reovirus treatment (MOI of 1 or 10) or resting (unstimulated cells). Four donors were analysed, error bars represent the standard deviation for each condition. b) PBMC were cultured without (untreated) or with reovirus at an MOI of 1 for 48 hours, followed by co-culture with K562 target cells. Degranulation of PBMC-NK cells was examined by measuring expression of surface CD107a, by flow cytometry. CD107a display was analysed on unstimulated cells (Resting), or cells treated with reovirus in the presence or absence of K562 target cells. The experiment was repeated with 2 separate donors.

3.2.2 PBMC derived IFN-I activates NK cells

One clear candidate for the activation of NK cells by reovirus is IFN-I. Previous studies showed that IFN-I was necessary for the upregulation of CD69 and degranulation induced by reovirus (El-Sherbiny et al., 2015; Parrish et al., 2015). However, these studies did not address whether IFNs induced NK cell activation directly, or indirectly through other cell types. One possible indirect mechanism could be the IFN dependent induction of monokines such as IL-12 and/or IL-15.

I first tested whether soluble factors, released into the media during culture of PBMC with reovirus, were sufficient to activate purified NK cells. Conditioned media was collected from both untreated and reovirus treated PBMC, and filtered (using Viresolve®) to remove reovirus. The remaining media was predicted to contain extracellular factors but lack cells or virus (Figure 3.2).

Conditioned media was collected at various time points, after the addition of reovirus to PBMC, in order to determine an optimum time point for NK cell activation. Purified NK cells upregulated surface CD69 when cultured in conditioned media collected at 24 or 48 hours, but not that collected 4 hours post reovirus treatment (Figure 3.3a, top panel). Expression of surface tetherin (CD317), an IFN inducible protein (Neil et al., 2008), was also measured. Expression of tetherin by NK cells was similarly upregulated by reovirus conditioned media, more so by that collected 24 and 48 hours post reovirus treatment than that collected at 4 hours (Figure 3.3a, bottom panel).

Conditioned media that was collected at 24 hours post reovirus treatment was selected to take forward for further experiments, as it induced the highest levels of CD69 and tetherin on the surface of purified NK cells. Virus free, conditioned media from this time point reproducibly upregulated CD69 and tetherin expression on purified NK cells from multiple donors and the differences were statistically significant (Figure 3.3b). Together, these data suggest that molecules released by reovirus treated PBMC, most likely cytokines (with IFN-I being a favoured candidate), are directly responsible for the activation of NK cells in this setting.

Figure 3.2 Schematic diagram of experimental pipelines
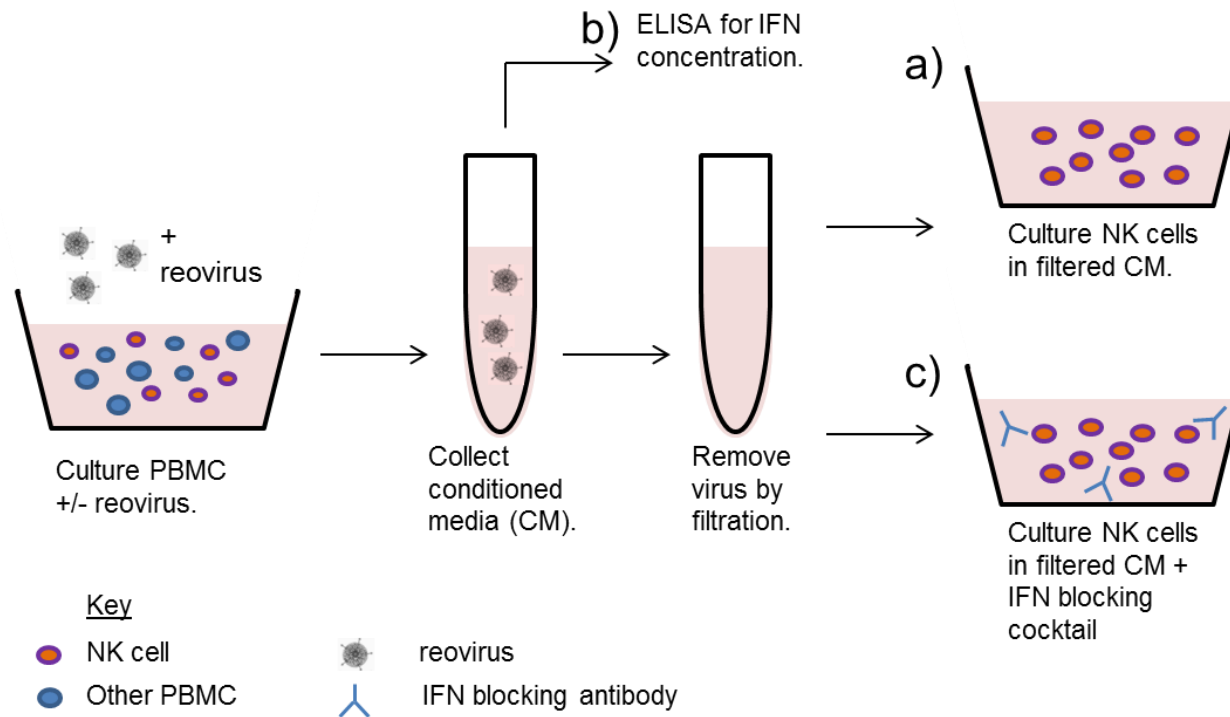
Conditioned media (CM) was collected from PBMC, cultured with or without reovirus at an MOI of 1, by centrifugation, then virus particles were removed using a Viresolve filter. a) Purified NK cells (from a separate donor) were cultured in the filtered CM. b) IFN-I concentration in CM was analysed by ELISA. c) Purified NK were cultured in filtered CM, plus IFN-I blocking cocktail.
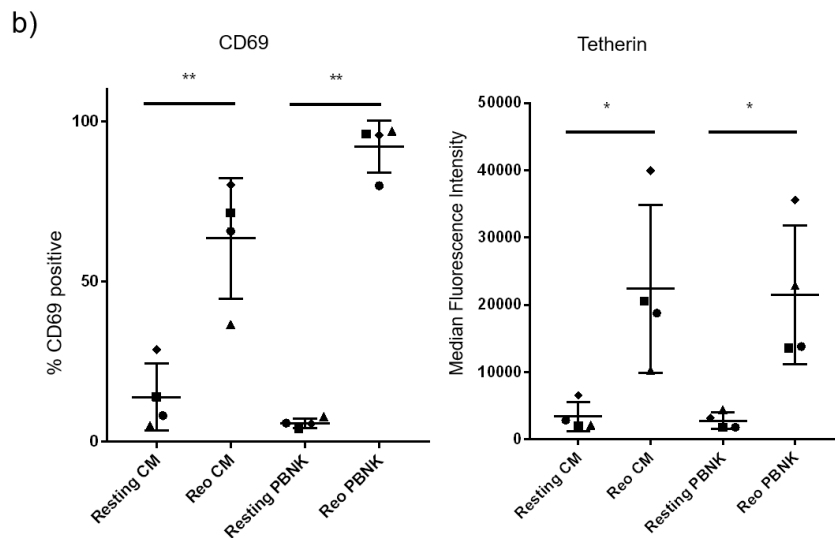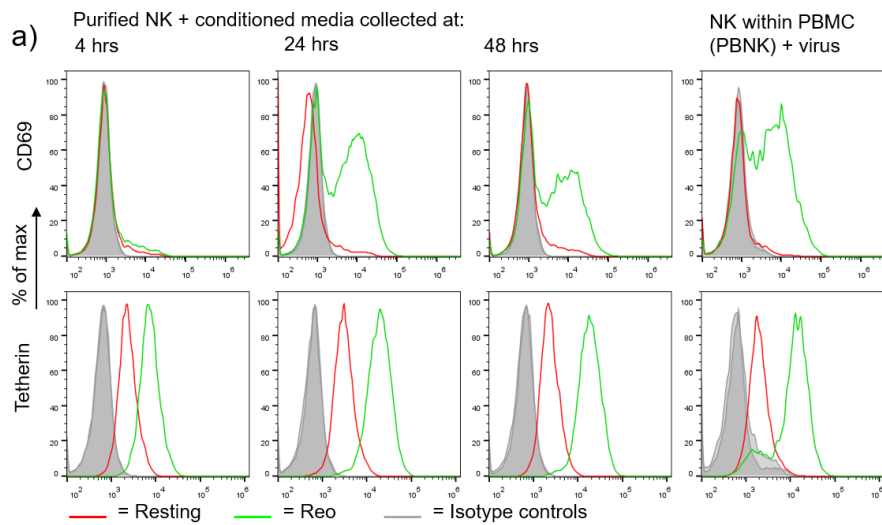
Figure 3.3 Effect of conditioned media on NK cell surface CD69 and tetherin

a) PBMC were cultured for 4, 24 or 48 hours either without virus (resting) or with reovirus at an MOI of 1 (reo). Conditioned media (CM) was collected as in Figure 3.2 and purified NK cells were cultured in the collected media, for 48 hours. CD69 and Tetherin expression on the surface of purified NK was measured by flow cytometry. Whole PBMC from the same donor were cultured with or without reovirus at an MOI of 1 for 48 hours, and NK cells within PBMC were analysed alongside. This experiment was performed once. **b)** CM collected at 24 hours was tested further for potential to activate purified NK cells. On the left are purified NK cells cultured in CM, and on the right are NK cells within PBMC (PBNK). Plotted are the percentage of NK cells positive for CD69, and Tetherin median fluorescence intensities. Graphs show mean and standard deviation for 4 separate donor PBMC. The effect of treatment on MFI was tested by one way repeated measures ANOVA, followed by Tukey's multiple comparisons test to determine significant differences between treatments. * $p<0.05$ ** $p<0.01$.

The induction of IFN-α and IFN-β by reovirus was analysed, by measuring the concentrations of these cytokines in conditioned media using ELISA (as in figure 3.2). Conditioned media from reovirus treated PBMC and untreated PBMC was compared. The concentration of IFN-α in conditioned media was much higher at 24 hours of reovirus treatment than at 8 hours, and was still detectable at high levels at 72 hours. (Figure 3.4a). The 48 hour time-point was chosen for further analysis. In reovirus conditioned media from 48 hours, both IFN-α and IFNβ were detected (Figure 3.4b and c), with higher concentrations of IFN-α. PBMC transfected with the dsRNA analogue poly(I:C), also released detectable levels of IFN-α and IFN-β, as expected. However, PBMC secreted higher concentrations of IFN-I when exposed to reovirus, than when transfected with poly(I:C), at the doses used in this study.

Conditioned media collected from reovirus treated PBMC contained both IFN-α and IFN-β, but was likely to contain many other cytokines. This could include IL-12 or IL-15, also known to activate NK cells. The importance of IFN-I in the reovirus induced cytokine milieu was investigated, using an optimised antibody cocktail to specifically block IFN-α and β. The cocktail contains antibodies against the IFN-I receptor, IFN-α and IFN-β. Culture of purified NK cells in conditioned media from untreated or reovirus treated PBMC was repeated, with or without inclusion of the IFN-I antibody cocktail (as in Figure 3.2), and expression of CD69 and tetherin was analysed by flow cytometry.

I analysed whether IFN-I had a direct role in NK cell activation by reovirus. Blocking IFN-I within the conditioned media inhibited the upregulation of surface CD69 and tetherin on purified NK cells (Figure 3.5a), while a control blocking cocktail, consisting of isotype matched antibody and sheep serum, did not block upregulation of these molecules. These data confirmed that IFN-I, induced by reovirus-stimulated PBMC, acts directly on NK cells to upregulate activation markers in the absence of any other cell type. Furthermore, purified IFN-α was able to upregulate CD69 and tetherin on isolated NK cells, in a dose-dependent manner (Figure 3.5b). These results confirm that reovirus-induced activation of NK cells is IFN-I dependent and that IFN-I is sufficient to induce NK cell activation, as characterised by CD69 and tetherin expression.
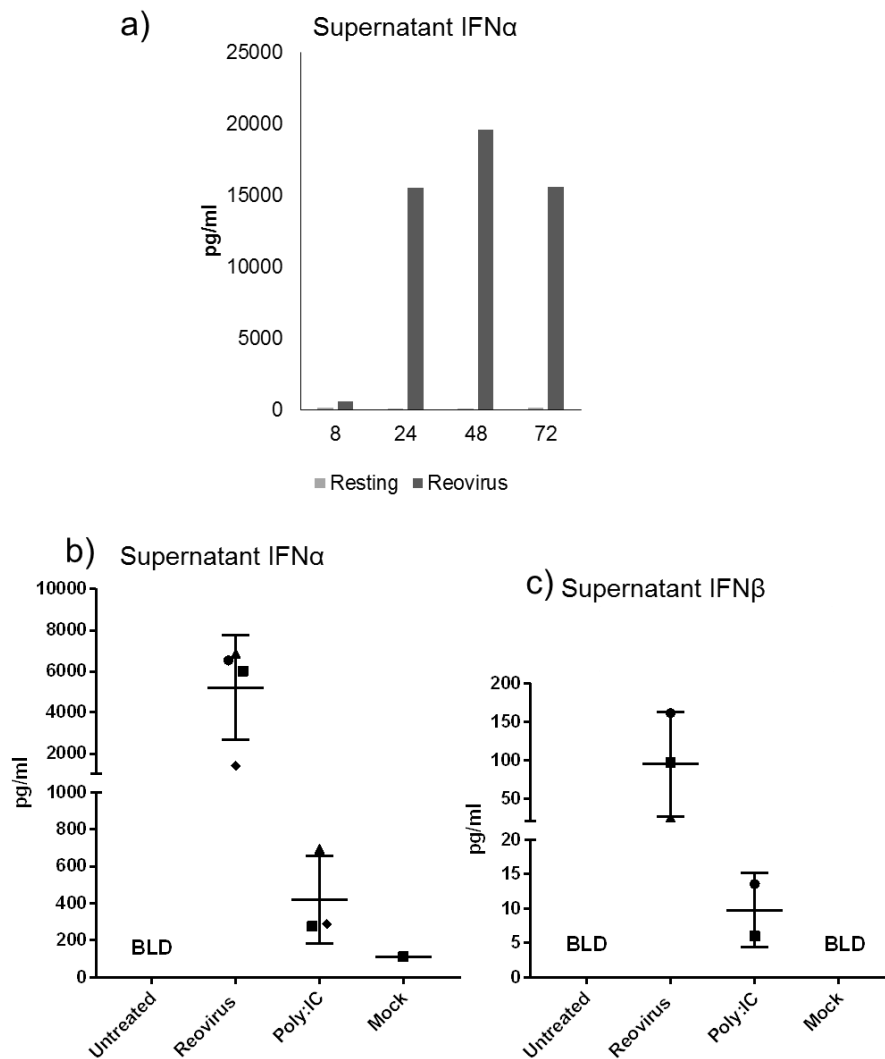
Figure 3.4 IFN-I concentrations in conditioned media from reovirus treated PBMC

a) PBMC were cultured with or without reovirus at an MOI of 1. At the time points shown above, media was collected and IFN-α concentration was measured by ELISA. **b)** PBMC were cultured alone, or with reovirus at an MOI of 1, poly(I:C) effectene transfection or mock transfection, for 48 hours. Media was collected and IFN-α and **c)** IFNβ concentrations were measured by ELISA. N = minimum of 3, BLD = below limit of detection.
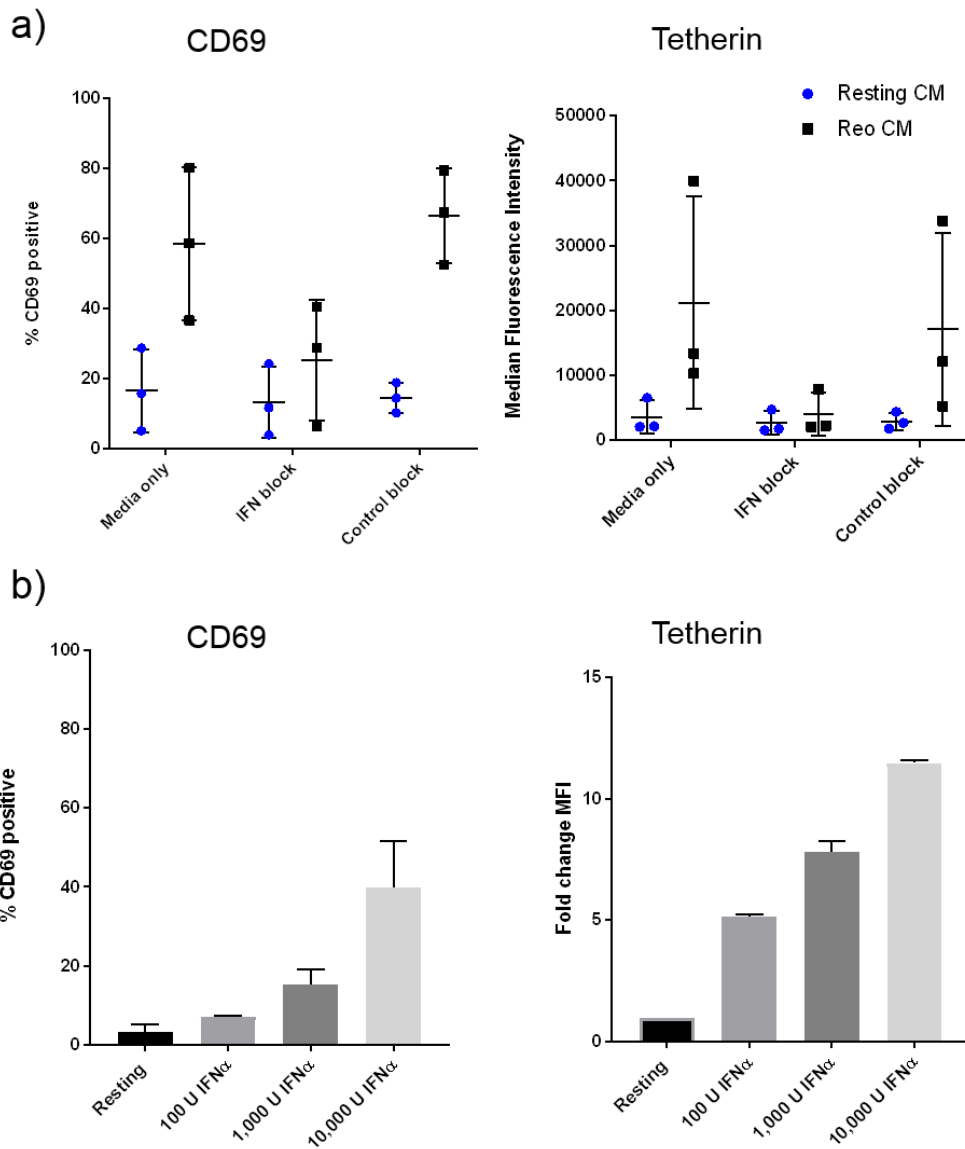
Figure 3.5 Inhibition of NK cell activation by IFN blocking antibodies

NK cell CD69 and tetherin expression after culturing in conditioned media with IFN-I block, or purified IFN. **a)** Purified NK cells were cultured in CM collected at 24 hours, as in Figure 3.3. Additionally, CM was either left untreated or treated with an IFN-blocking antibody cocktail or a control blocking cocktail. NK cells were cultured in CM and blocking antibodies for 48 hours, then NK cell surface expression of CD69 and tetherin was measured by flow cytometry. N=3 donors. **b)** A titration of purified IFN-α induces a dose-dependent upregulation of CD69 and tetherin on the surface of NK cells. Purified NK cells were cultured with IFN-α for 48 hours. N=2. Graphs in a) and b) show the mean and standard deviation for each condition.

3.2.3 Cytokines activate different JAK/STAT signalling pathways in NK Cells

The results described in Section 3.2.2 suggest that reovirus induces IFN-I production, which acts directly on NK cells to induce activation. Type I interferons typically induce the phosphorylation of STAT1 and STAT2 (Platanias, 2005), while other cytokines activate different JAK/STAT signalling pathways (Thierfelder et al., 1996; Tagaya et al., 1996). Flow cytometric analysis of phosphorylated proteins is a convenient method that enables the analysis of JAK/STAT signalling within a mixed population of cells. The phosphorylation of three different signalling proteins, namely STAT1, STAT4 and STAT5, was analysed after treatment of PBMC with several different cytokines, including IFN-α. The aim was to validate the assay, by comparing results with that reported in the literature, and to establish NK cell STAT phosphorylation profiles for relevant cytokines. Comparing the STAT phosphorylation profile of reovirus activated NK cells to the profiles generated for each cytokine might then indicate which cytokines are responsible for reovirus-induced NK cell activation.

PBMC were treated individually with three different cytokines for 1 hour and STAT phosphorylation in the NK cell population was analysed by permeabilisation, antibody staining and flow cytometry. The cytokines IFN-α, IL-12 and IL-15 were chosen as each have been implicated in viral activation of NK cells (section 1.1.7). Different patterns of STAT phosphorylation were induced in NK cells by IFN-α, IL-12 and IL-15 (Figure 3.6). Flow cytometry allowed the further subdivision of NK cells into CD56^{dim} and CD56^{bright} subsets, based on CD56 staining intensity. The phosphorylation of STAT molecules was quantified in both NK cell subsets (Figure 3.7). Only IFN-α significantly increased the levels of STAT1 phosphorylation, and both NK cell subsets responded similarly. In contrast, STAT4 phosphorylation differed across subsets. In CD56^{dim} NK cells, STAT4 phosphorylation was significantly increased by all treatments, including IL-15. Although STAT4 is thought to be primarily activated downstream of IL-12, in the CD56^{dim} subset the highest upregulation was observed with IFN-α stimulation. In CD56^{bright} NK cells, IL-12 treatment induced the highest levels of STAT4 phosphorylation. Finally, IL-15 treatment increased STAT5 phosphorylation, which was statistically significant only in the CD56^{bright} subset.. These results match the typical JAK/STAT pathways reported for

each cytokine (Section 1.2.6 and 1.2.8), and show that STAT phosphorylation profiles vary across NK cell subsets.

Next, I analysed the duration of NK cell STAT activation following stimulation with the three cytokines. IFN-α treatment induced a transient increase in STAT1 and STAT4 phosphorylation, which decreased to baseline levels at 8 hours post treatment (Figure 3.8). In contrast, IL-12-induced STAT4 phosphorylation gradually increased and was detectable both 8 and 24 hours post cytokine treatment. Thus, whilst IFN-α and IL-12 activate overlapping pathways, the duration of STAT phosphorylation differs depending on the cytokine. The duration of STAT5 phosphorylation was variable across donors, but the mean staining intensity was similar at all three time-points.
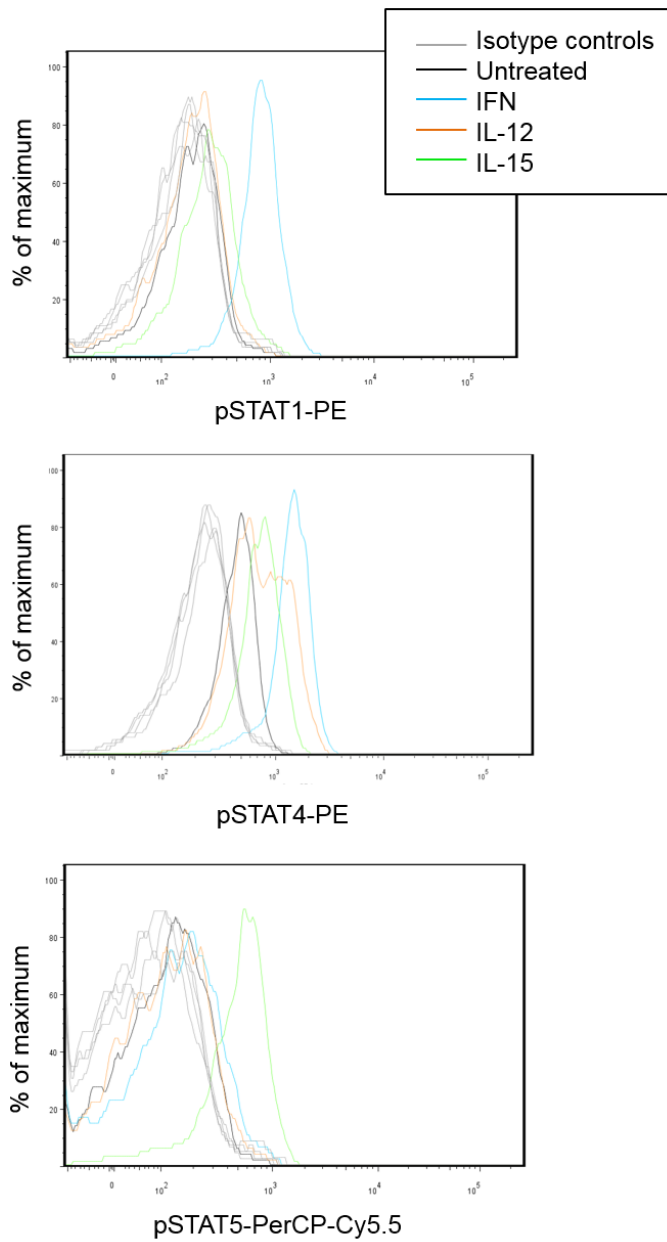
Figure 3.6 Intracellular phosphoprotein staining to detect activation of JAK STAT pathways
PBMC were treated with 100 IU/ml IFNα, 10 ng/ml IL-12 or 50 IU/ml IL-15 for 1 hour. NK cells within PBMC were evaluated for levels of phosphorylated STAT1, STAT4 and STAT5 by intracellular flow cytometry. Histograms show isotype control or phosphorylated protein staining in total NK cells, representative of 3 donors.
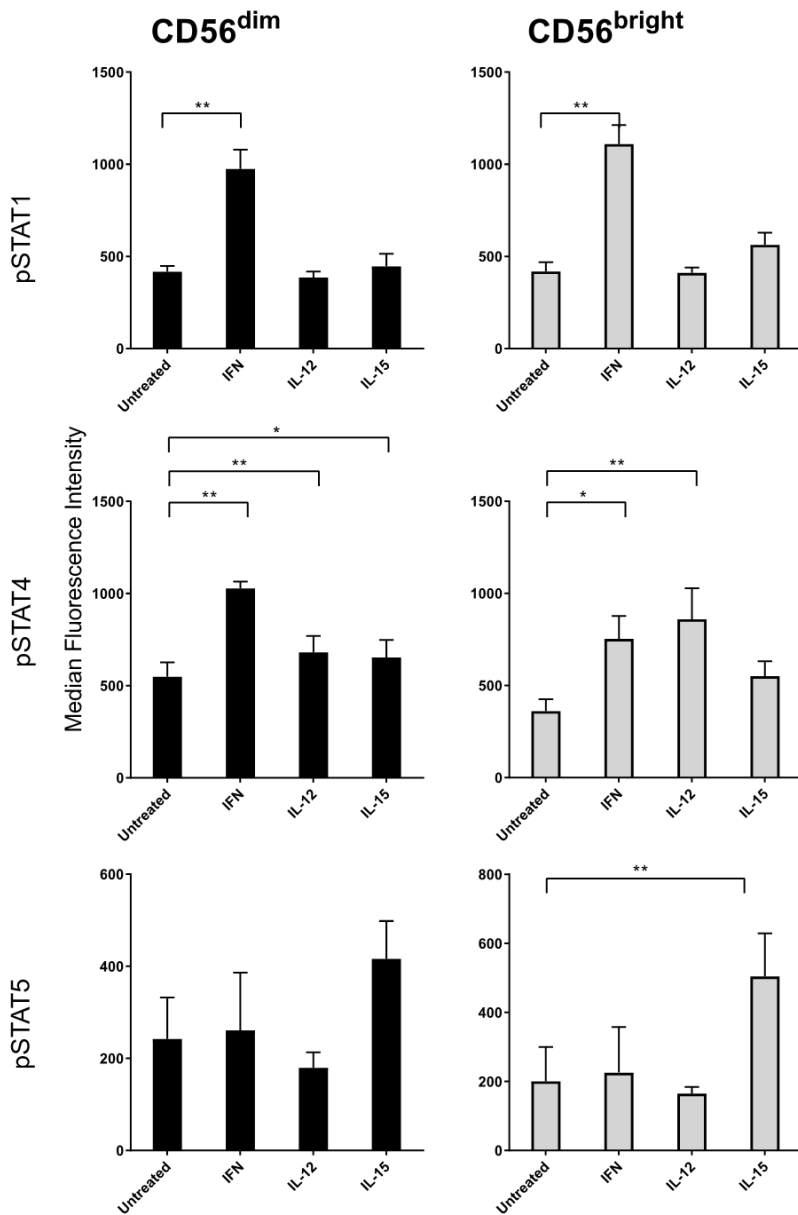
Figure 3.7 Cytokine induced STAT phosphorylation in CD56^{dim} and CD56^{bright} NK cells

PBMC were treated with 100 IU/ml IFNα, 10 ng/ml IL-12 or 50 IU/ml IL-15 for 1 hour. CD56^{dim} and CD56^{bright} NK cells within PBMC were evaluated for levels of phosphorylated STAT1, STAT4 and STAT5 by intracellular flow cytometry. Graphs show median fluorescence intensities, with mean MFI and standard deviation from three separate donors. The effect of treatment on MFI was tested by one way repeated measures ANOVA, followed by Dunnet's multiple comparison test to determine which cytokine treatments were significantly different from untreated. * p < 0.05 ** p < 0.01
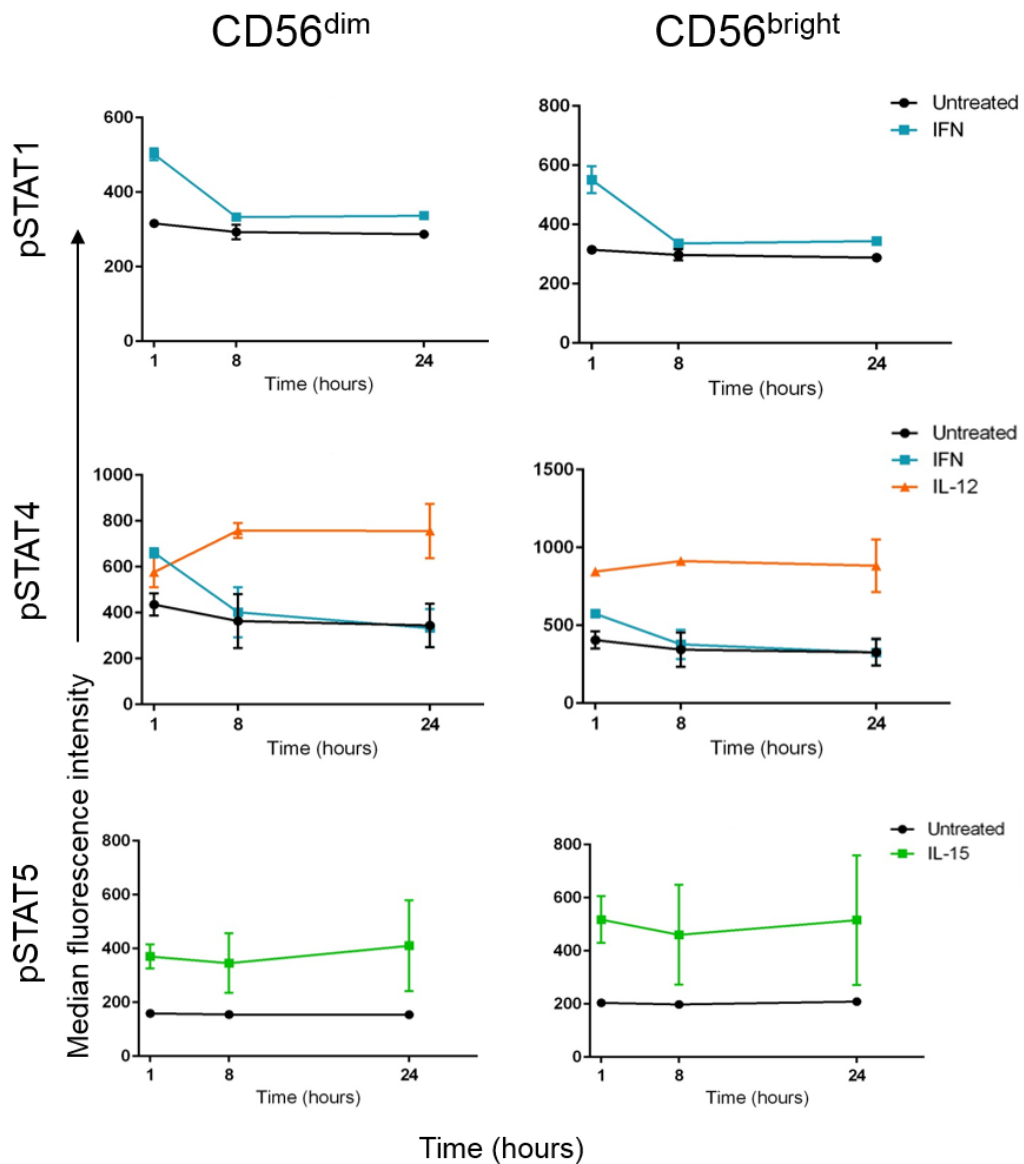
Figure 3.8 STAT phosphorylation kinetics in cytokine treated CD56^{dim} and CD56^{bright} NK cells

PBMC were treated with 100 IU/ml IFNα, 10 ng/ml IL-12 or 50 IU/ml IL-15 for 1 hour, 8 hours or 24 hours. CD56^{dim} and CD56^{bright} NK cells within PBMC were evaluated for levels of phosphorylated STAT1, STAT4 and STAT5 by intracellular flow cytometry. Graphs show median fluorescence intensities, with mean MFI and standard deviation from two separate donors.

3.2.4 Reovirus-induced JAK/STAT signalling in NK Cells resembles IFN-I signalling.

Reovirus treatment is likely to trigger the production of multiple cytokines over time, which may lead to the activation of several different JAK/STAT pathways. NK cell STAT phosphorylation was measured at several time points during culture of PBMC with or without reovirus (Figure 3.9). In order to ensure enough time for virus-induced cytokines to be produced in the culture medium, the earliest time point at which the cells were assessed was 8 hours post cytokine treatment.

Reovirus treatment induced a statistically significant increase in phosphorylated STAT1 and phosphorylated STAT4, at 8 hours post treatment, when compared to untreated cells (Figure 3.9). Levels of phosphorylated STAT1 remained significantly higher in reovirus treated cells at 24 hours and 48 hours, when compared to untreated cells, and the mean staining intensity remained similar at all three time points. In contrast, levels of phosphorylated STAT4 decreased after 8 hours. STAT1 and STAT4 activation profiles were similar in both CD56^{dim} and CD56^{bright} NK cells. Phosphorylated STAT5 levels appeared similar between resting and reovirus treated cells; there was a very small but significant increase in phosphorylated STAT5 staining after 8 hours, but only in CD56^{bright} NK cells. The upregulation of STAT1 and STAT4 phosphorylation following reovirus treatment is similar to the profile of STAT activation induced by IFN-I (shown in Figure 3.7 and 3.8), except reovirus treatment led to more sustained levels of STAT1 phosphorylation.
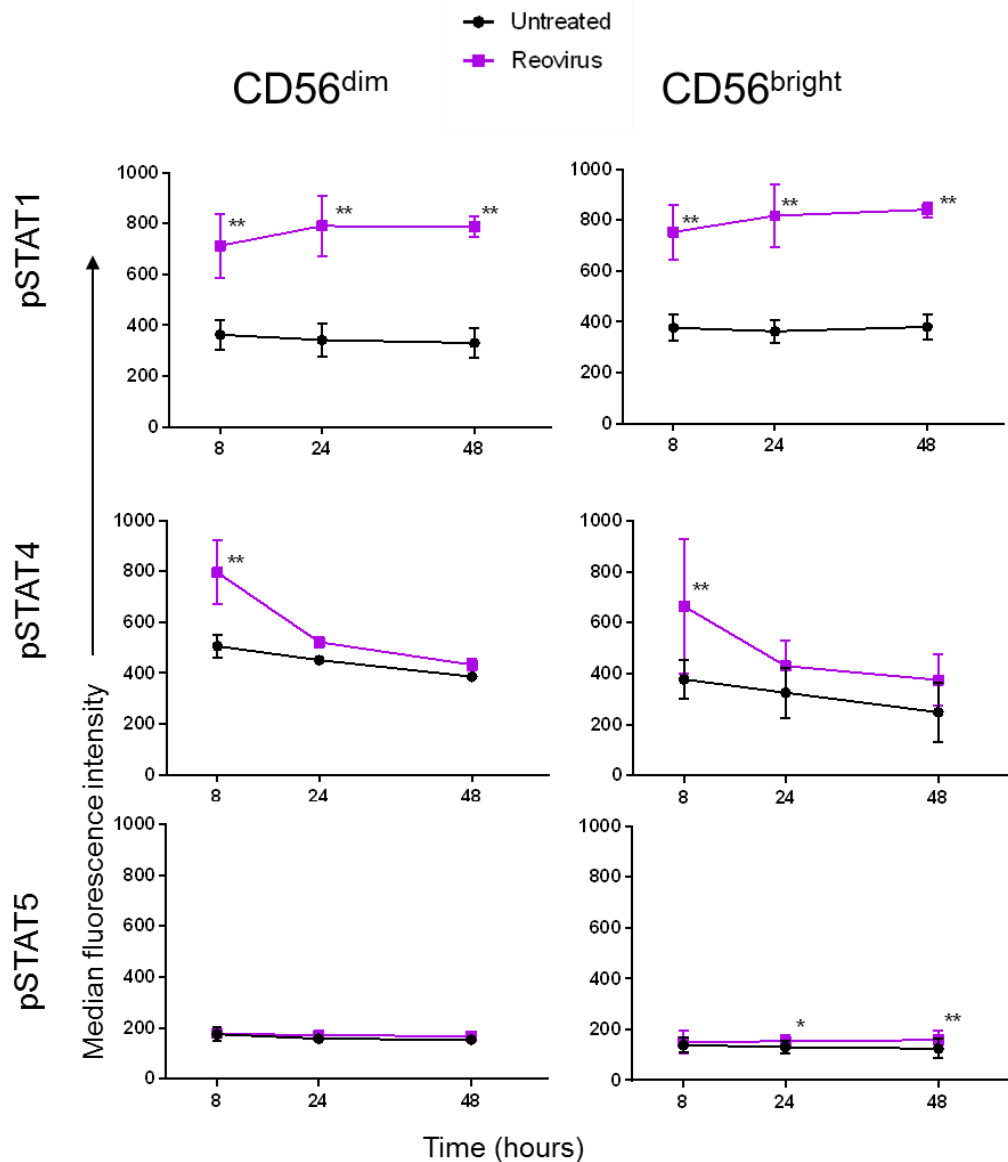
Figure 3.9 Reovirus induced STAT phosphorylation in CD56^{dim} and CD56^{bright} NK cells

PBMC were cultured without virus (untreated) or with reovirus at an MOI of 1, for 8, 24 and 48 hours. At these time points, CD56^{dim} and CD56^{bright} NK cells within PBMC were evaluated for levels of phosphorylated STAT1, STAT4 and STAT5 by intracellular flow cytometry. Graphs show median fluorescence intensities (MFI), with mean MFI and standard deviation from three separate donors;. The effect of time and treatment on MFI was tested by two way repeated measures ANOVA, followed by Sidak multiple comparisons test to determine at which time-points there were significant differences between untreated and reovirus treated cells. * $p < 0.05$ ** $p < 0.01$

Next, a more extensive set of time points were tested, with the aim to define when the peak of STAT1 and STAT4 phosphorylation occurred. PBMC were treated with either reovirus or a high concentration of IFN-α (Figure 3.10a). The results show that reovirus induced a peak of STAT4 phosphorylation approximately 6 hours post-treatment, before returning to baseline levels. Following IFN-α stimulation, peak phosphorylation of STAT4 was detected very rapidly and decayed with similar kinetics to the reovirus induced STAT4 phosphorylation. The delay between IFN-α induced and reovirus induced STAT4 phosphorylation was probably due to the time taken for reovirus exposed PBMC to produce sufficient levels of IFN, in agreement with the kinetics of IFN-α production shown in Figure 3.3. Similarly, STAT1 phosphorylation in NK cells from reovirus treated PBMC also resembled a delayed IFN response, except that there was a striking upregulation of phosphorylated STAT1 between 12 and 24 hours (Figure 3.8a top left). Phosphorylated STAT5 staining was similar between untreated and reovirus treated cells at all time points, with no evidence of induction. Furthermore, IFN treatment did not upregulate STAT5 phosphorylation (Figure 3.8a bottom graph). These results suggest that reovirus induced NK cell activation in PBMC stems from the virus-induced production of IFN-I which acts directly on the NK cells and triggers STAT1 and STAT4 signalling cascades.

The production of IFN-I in response to viral infection occurs as a result of the interaction between host cell pattern recognition receptors (PRRs) and pathogen associated molecular patterns (PAMPs) present in viruses. An important PAMP in reovirus infection is dsRNA (Goubau et al., 2014) and this PAMP can be mimicked using the synthetic dsRNA analogue, poly(I:C). A comparison of reovirus treatment and poly(I:C) transfection of PBMC showed that poly(I:C) induced a similar pattern of STAT phosphorylation to that observed with the virus (Figure 3.10b), suggesting that similar cytokines are produced following poly(I:C) treatment. Interestingly, the simple addition of poly(I:C) to the culture medium (as opposed to transfection) did not induce these responses, suggesting that intracellular detection of poly(I:C) via PRRs such as RIG-I and MDA5 was more important than engagement of TLR3 in endosomes (data not shown).
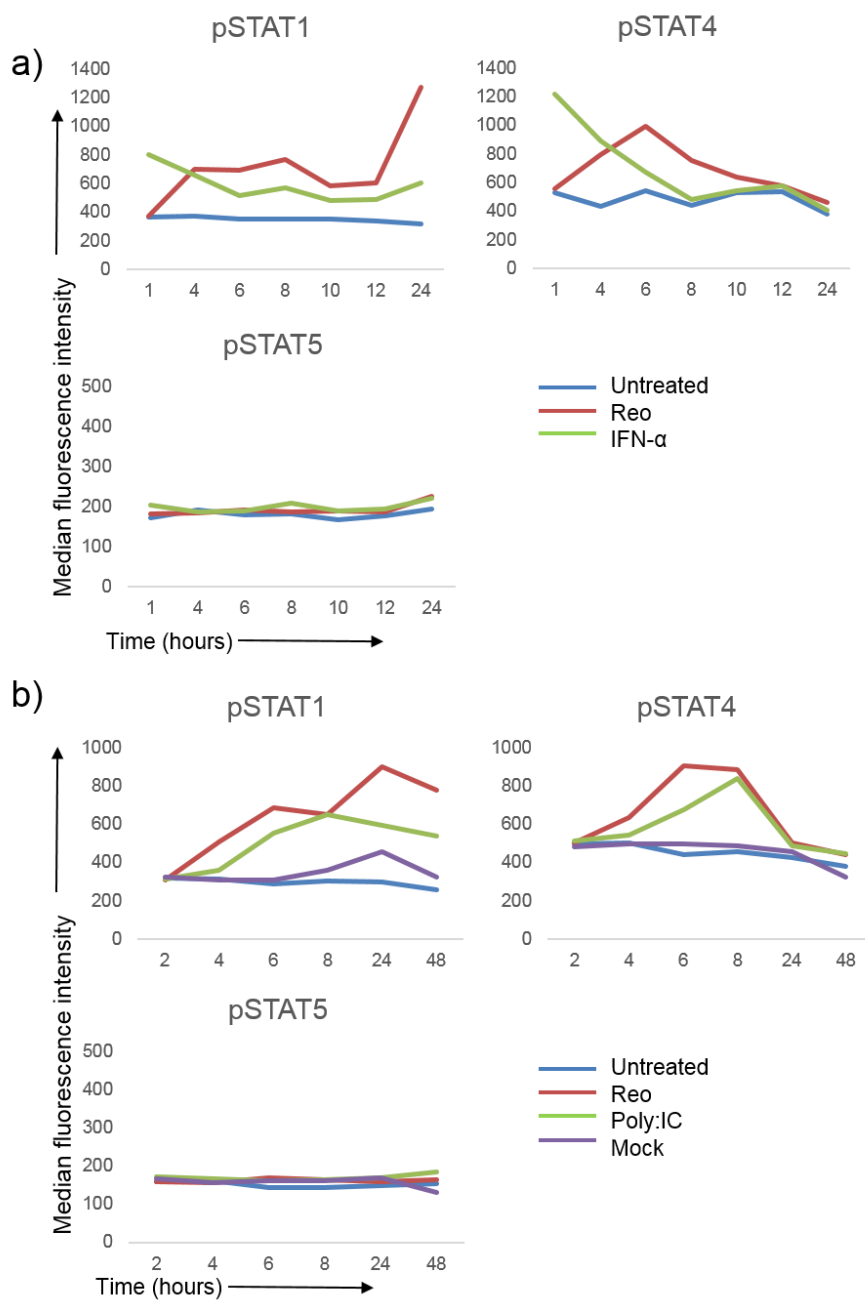
Figure 3.10 STAT phosphorylation during reovirus, IFN-α or poly(I:C) treatment

PBMC were cultured without virus (untreated), with reovirus at an MOI of 1 or with 1000U/ml IFNα in **(a)**, or with 1 µg/ml poly(I:C) via effectene transfection or mock transfection in **(b)**. At the time points above, NK cells within PBMC were evaluated for levels of phosphorylated STAT1, STAT4 and STAT5 by intracellular flow cytometry. Results shown in a) are from one experiment. Results in b) are representative of two experiments from 2 separate donor PBMC.

3.3 Discussion

The experiments presented in this chapter had two key aims. First, to establish and characterise a simple *in vitro* model which mimics the responses of human NK cells to intravenous reovirus therapy, and second, to use this system to explore the pathway of NK cell activation. The results suggest a model in which reovirus detection by PBMC (probably by recognition of dsRNA via RIG-I) leads to the production of IFN-I. This IFN-I acts directly on NK cells, via STAT1 and STAT4 signalling pathways, to induce NK cell activation. The possibility that IFN-I induces IL-15 and that IL-15 then acts on the NK cells has not been formally disproven (e.g. using an anti-IL-15 blocking antibody), but the absence of STAT5 activation (a major signal downstream of IL-15) suggests that its role is, at most, secondary to IFN-I.

A link between IFN-I and NK cell activation has been in the literature for four decades, after Gidlund et. al showed that interferon injection into mice enhanced NK cell cytotoxicity (Gidlund et al., 1978). However, the mechanistic link between IFN-I and NK cell activation is not well defined. A clinical trial of oncolytic reovirus demonstrated that NK cells were activated 24-48hrs post-treatment and this overlapped with a IFN-I response (El-Sherbiny et al., 2015), implicating reovirus induced IFN-I in NK cell activation *in vivo*. *In vitro* studies have shown that blocking IFN-I reduces NK cell activation in response to reovirus (El-Sherbiny et al., 2015; Parrish et al., 2015) and the results shown here confirm these findings. Expanding on these studies, I demonstrated that IFN-I released by PBMC acts directly on NK cells to induce an activated phenotype (figure 3.5). Work by Parrish *et al.*, showed that treatment of PBMC with reovirus activates NK cells in a monocyte dependent manner and that these monocytes produced IFN-I (Parrish et al., 2015). Host cells produce IFN-I following detection of RNA viruses, usually via TLR or RLR activation. Although most mammalian cells probably produce some level of IFN in response to viral infection, there are cell types particularly specialised for this role. Plasmacytoid DC are rare cells capable of producing high levels of IFN-I, and are believed to play a key role in initiating many antiviral responses (Izaguirre et al., 2003). However, monocytes are highly abundant, presumably compensating for the reduced IFN-I production per cell, indeed one study demonstrated that monocytes produce most of the PBMC derived IFN-α in response to transfected

poly(I:C) (Hansmann et al., 2008). In my experiments, reovirus treatment of purified NK cells did not upregulate CD69 to the same extent as treatment of whole PBMC (Figure 3.1b), probably due to the removal of monocytes by the NK cell isolation column. There was however, a small percentage of CD69+ cells in the purified NK cell population exposed to reovirus. This suggests that a proportion of NK cells are able to respond directly to reovirus. This might occur by NK cell detection of reovirus (e.g. via RIG-I) and autocrine IFN-I production. Alternatively, a recent paper showed that the NK cell receptor NKp46 recognises the reovirus σ1 protein (Bar-On et al., 2017), allowing direct activation of NK cells by reovirus. However, optimal responses were obtained using PBMC, presumably reflecting the role of monocytes in IFN-I production. Use of PBMC in these experiments is convenient. However, PBMC do not contain the full complement of blood cells, lacking neutrophils, red blood cells and platelets (which do not survive in culture). Whilst these cell types are not typically described as IFN producing cells, their absence does reflect a limitation of the *in vitro* model.

Experiments performed here indicate that IFN-I is necessary and sufficient for NK cell activation. However, this does not exclude a role for other cytokines. It is possible that IFN-I acts on NK cells to induce autocrine production of activating cytokines, such as NK cell *cis*-presentation of IL-15 in response to IFN-β (Zanoni et al., 2013). Furthermore, I have only tested how type I IFN blocking affects the expression of CD69 and tetherin. Others have shown that IFN-I blockade reduces NK cell degranulation and tumour cell killing in response to reovirus (El-Sherbiny et al., 2015; Parrish et al., 2015). However, other functions such as IFN-γ production may be under the control of other cytokines, and this has not been explored in the context of oncolytic reovirus. In an MCMV model, NK cytotoxicity was dependent on type I IFN while NK IFN-γ production was dependent on IL-12 (Nguyen, K.B. et al., 2002a). On the other hand, overlapping pathways can trigger the same function in NK cells; both IL-12 and type I IFN are able to trigger IFN-γ production through activation of STAT4 (Nguyen, K.B. et al., 2002b; Mack et al., 2011).

Activation of transcription factors such as STAT4 can tell us a lot about how NK cells respond in certain conditions. Therefore, as part of this study, the activation of different STAT factors was investigated. Initial experiments tested the action of purified cytokines on PBMC and confirmed the findings of previous studies, showing that IFN-α, IL-12 and

IL-15 induced different patterns of STAT phosphorylation in NK cells (Figures 3.6 and 3.7). After 1 hour of stimulation, IFN-α induced STAT1 and STAT4 phosphorylation, but no STAT5 phosphorylation. STAT1 and STAT2, together with IRF9, form the ISGF3 complex, the canonical transcription factor of the IFN-I signalling pathway (Platanias, 2005). More recently, STAT4 has been implicated in the response to IFN-I (Nguyen, K.B. et al., 2002b), particularly in NK cells (Mack et al., 2011). The cytokine IL-12 is reported to signal predominantly through STAT4 (Thierfelder et al., 1996), which I observed in CD56^{bright}, but not CD56^{dim} NK cells (Figure 3.7). It appears that CD56^{bright} NK cells may be more sensitive to IL-12 than CD56^{dim} cells, possibly due to a higher density of IL-12 receptor on the surface of the CD56^{bright} sub type. The CD56^{bright} NK cell subset produces higher levels of IFN-γ than CD56^{dim} NK cells, in response to IL-12 (Trotta et al., 2005), however not much is known on a molecular level about what makes CD56^{bright} NK cells better cytokine producers. It has been reported that a higher level of constitutive SHP-1 expression in CD56^{dim} cells inhibits IFN-γ production, possibly through inhibition of NF-κB, and that this explains the lower level of IFN-γ produced by CD56^{dim} cells in response to IL-12 and IL-18 (Trotta et al., 2005). However, there may be a number of mechanisms by which CD56^{bright} NK cells respond with higher levels of IFN-γ than CD56^{dim} cells. Here I have shown that greater phosphorylation of STAT4 in response to IL-12 might be one such mechanism.

IL-15 signals through a number of different pathways, including JAK/STAT signalling. The JAK molecules involved are JAK1 and JAK3, activation of which leads to the downstream phosphorylation of STAT3 and STAT5 (Tagaya et al., 1996). In agreement with this, IL-15 induced the phosphorylation of STAT5 in this study (figures 3.6 and 3.7). These experiments also revealed the activation of both STAT1 and STAT4 during IL-15 stimulation. Although this isn't the canonical JAK/STAT pathway downstream of IL-15, activation of STAT1 and STAT4 has been reported in NK-92 cells (Strengell et al., 2003). Much of the published research on STAT mediated signalling pathways is based on western blotting data, but the results in this study show that intracellular phosphoprotein staining and flow cytometry is a reliable alternative technique to analyse signalling pathways within primary human NK cells. Furthermore, this technique allows the analysis of multiple different cell subsets within a mixed population, which is an important advantage over western blotting (which would require laborious and costly cell isolation).

Interestingly, the duration of STAT phosphorylation, observed during time course experiments, differed with each cytokine. IFN-α induced transient phosphorylation of STAT1 and STAT4, which was evident at 1 hour post-treatment, but decreased at 8 hours (Figure 3.8). In contrast, IL-12 induced a sustained phosphorylation of STAT4, which actually increased between 1 and 8 hours post-treatment. The differential duration of STAT4 phosphorylation induced by IFN-α and IL-12 has been demonstrated before, in an NK cell line (Matikainen et al., 2001) and in T helper cells (Athie-Morales et al., 2004). I have shown that the same events occur in primary NK cells within PBMC.

There are a number of possible explanations for the differential timing of STAT4 activation by these cytokines. Firstly, STAT activation may depend on the concentration of cytokine remaining in the culture medium at the time point measured. After 8 hours of treatment, the concentration of IFN-α may have dropped below the threshold needed to activate STAT signalling, whilst the concentration of IL-12 might remain stable in culture. This could be due to quicker degradation of IFN-α, possibly because more cell types in the PBMC population are taking up IFN-α than IL-12. Alternatively, the concentration of IL-12 may remain higher than IFN-α due to a positive feedback loop which replenishes IL-12 in the medium. Positive feedback loops are common in innate immunity, when it is important to amplify a response as quickly as possible, in order to respond to infection. However, both IFN-I and IL-12 are reported to induce positive feedback loops, enhancing their own production (Ma et al., 1996) (Sato, M. et al., 1998).

A refractory period following IFN-I stimulation of cells in culture has been reported previously (Larner et al., 1986; Sarasin-Filipowicz et al., 2009). During IFN-α treatment *in vitro* and *in vivo*, downregulation of IFNα/β receptor (IFNAR) at the surface of peripheral blood lymphocytes has been reported (Lau et al., 1986). It has been suggested that inhibition of signalling may occur through internalisation of the IFNAR (Athie-Morales et al., 2004). Alternatively, differential expression of the inhibitory suppressor of cytokine signalling (SOCS) proteins may explain the transient STAT phosphorylation following IFN-α treatment, compared with the sustained response following IL-12 treatment. This could be confirmed by comparing the levels of different SOCS proteins following these two treatments, by western blotting or flow cytometry. It

is possible that SOCS proteins are recruited preferentially to the IFNAR over other cytokine receptors, as it has now been shown that SOCS1 is able to interact directly with the IFNAR, independently of JAK1 (Fenner et al., 2006).

Treatment of PBMC with reovirus induced a similar pattern of STAT phosphorylation to IFN-I treatment (Figures 3.9 and 3.10). However reovirus induced a sustained level of STAT1 phosphorylation. In fact, in the longer time course, there was an increase in STAT1 activation observed at 24 hours. This is in contrast with the transient activation of STAT1 observed after stimulation with purified IFN-α (Figure 3.8 and 3.10). Firstly, it is possible that viral treatment triggers a much higher concentration of IFN-α or IFN-β in the culture medium, which is sufficient to sustain STAT1 mediated signalling. Alternatively, virus present in the media could lead to constant production of type I IFN, leading to sustained STAT1 activation. To the best of our knowledge, reovirus does not replicate within blood cells which may allow for it to persist and continually stimulate IFN-I. However, recovery of replication competent reovirus from the PBMC of patients receiving intravenous viral therapy suggests that PBMC can act as 'cellular carriers' for reovirus (Adair et al., 2012). Replicating reovirus was recovered from blood samples taken on the day of reovirus infusion, but not at later time-points some weeks after treatment. Considering the evidence for cellular carriage of reovirus, it would be interesting to compare the STAT phosphorylation time course during treatment with live virus and treatment with virus free conditioned media. Secondly, perhaps other cytokines produced during reovirus exposure may enhance the IFN-I signalling pathway, or multiple subtypes of type I interferons were present, either of which could induce a different effect to that induced by purified IFN-α. Reovirus also induced phosphorylation of STAT4, which peaked at approximately 6 to 8 hours and decreased at 24 and 48 hours. The kinetics of STAT4 phosphorylation during reovirus treatment appeared to closer represent the transient phosphorylation induced by IFN-α rather than the sustained phosphorylation induced by IL-12 .

Interestingly, reovirus did not increase levels of STAT5 phosphorylation above the levels observed for untreated cells at the time points analysed, apart from a small shift seen in the CD56^{bright} subset (Figure 3.9). This shift was very small relative to the change induced by purified IL-15, suggesting that IL-15 is probably not involved in the response to

reovirus. This is surprising as recent research has shown that IL-15 is required for the activation of NK cells by dsRNA (Mortier et al., 2008) and that IL-15 signalling through STAT5 and mTOR was essential for the homeostasis and the activation of NK cells during viral infection (Marais et al., 2014). There are several possible explanations for the lack of STAT5 phosphorylation seen during reovirus treatment. Firstly, the assay used in my study may not be sensitive enough. The soluble IL-15 shown to induce STAT5 activation in Figure 3.7 is likely much higher than physiological IL-15 levels. It is difficult to know how sensitive the assay should be, because soluble IL-15 is not often present in infection models at detectable levels. Instead, it is now thought that *trans* presentation of IL-15 on the cell surface membrane of monocytes or macrophages is more important than soluble IL-15 release (Dubois et al., 2002) (Burkett et al., 2004). Another possible technical issue is that STAT5 phosphorylation may be transient and, as a result, the peak of phosphorylation may have been missed.

Alternatively, IL-15 may not actually play an important role in the periphery during infection with reovirus. Analysis of NK cells from patients taking part in a reovirus clinical trial showed high levels of type I interferon induced genes, but did not bear the hallmarks of IL-15 stimulation. Specifically, NK activation receptors, such as DNAM-1 and NKG2D, were not upregulated in the peripheral blood of patients, whereas *in vitro* stimulation with IL-15 increased the expression of all the NK cell activatory receptors tested (El-Sherbiny et al., 2015). Perhaps reovirus therapy stimulates NK cells similarly to vaccinia virus, which requires intrinsic STAT1 signalling in NK cells (Fortin et al., 2013). Most of the studies demonstrating virus induced IL-15 signalling in NK cells are based on samples taken from mouse spleens, rather than peripheral blood. IL-15 may be more important in primed activated cells reaching lymph nodes during reovirus therapy. At these sites, there are dendritic cells (DCs) present, known to *trans* present IL-15 (Lucas et al., 2007). Future work could include studying STAT phosphorylation in DC/NK and tumour/NK co-cultures.

The evidence presented in this chapter supports a mechanism of optimal NK activation that a) requires other cell types present in PBMC and b) requires type I interferons acting directly on NK cells, inducing the activation of STAT1 and STAT4. Activation of type I interferon signalling, as well as additional undefined pathways, will induce important

transcriptional changes in peripheral blood NK cells. In the next chapter, gene expression analysis was performed in order to further define activation mechanisms, and to predict the functional changes induced by reovirus in NK cells.

Chapter 4. Gene expression profiling of reovirus treated NK cells

4.1 Introduction

In chapter 3, I showed that the direct actions of type I interferons are required to activate NK cells in response to reovirus. This NK cell activation was marked by CD69 upregulation; CD69 is widely used as a marker of human peripheral NK cell activation (Clausen et al., 2003), and was induced by reovirus *in vivo* in the clinical trial (El-Sherbiny et al., 2015). An activated NK cell phenotype suggests that reovirus treated NK cells might respond to target cells more efficiently. This is supported by a number of *in vitro* studies, demonstrating increased killing of cancer cells by reovirus treated NK cells within PBMC. However, NK cell responses to viruses likely involve much more than just increased degranulation and release of cytotoxic molecules. Additional NK cell functions such as cytokine production, NK cell migration and proliferation are also affected by viruses, but have not been studied in the context of oncolytic virus therapy. To determine the spectrum of NK cell activity regulated by reovirus, I performed gene expression profiling (using microarray analysis) on NK cells treated with reovirus within PBMC. In this chapter, the main findings from this microarray analysis are discussed.

4.2 Results

4.2.1 Gene expression profiling strategy

For transcriptome profiling, healthy donor PBMC were treated with reovirus *in vitro*, using the model described in chapter 3; Figure 4.1 illustrates the sample collection process. Briefly, PBMC (isolated from 5 healthy donors) were cultured with or without reovirus. After 48 hours treatment, NK cells were isolated from the PBMC using magnetic immunoselection (Section 2.1.2) and a small fraction (approximately 1×10^5 cells) were stained with antibodies for surface markers and analysed by flow cytometry. This was to check that the NK cells were pure, and that reovirus treated samples had acquired an

activated phenotype (as determined by upregulation of CD69); all 5 donor PBMC upregulated NK cell CD69 in response to reovirus (figure 4.2). Surface staining with antibodies against CD56, CD3 and CD19 confirmed that there was no detectable contamination from T cells (CD3+) or B cells (CD19+).
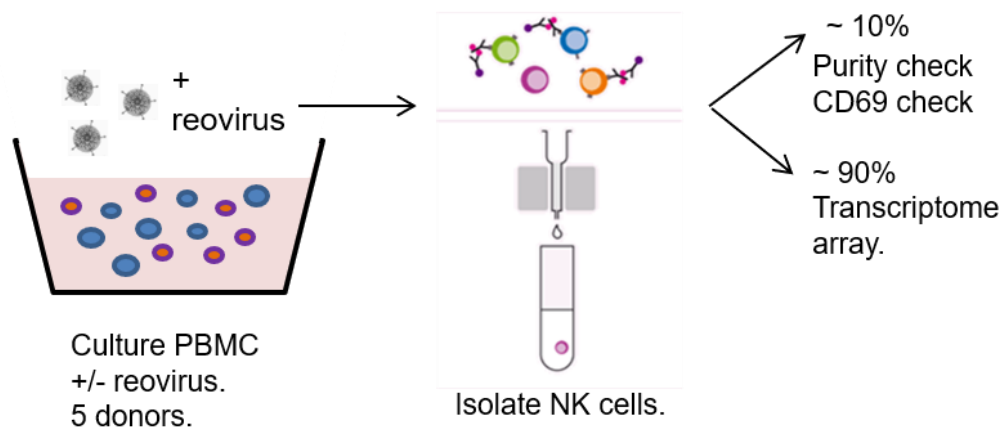
Figure 4.1 Sample collection for transcriptome array

Schematic showing NK cell collection for the gene expression study. PBMC from healthy donors were cultured for 48 hours, either untreated or with reovirus at an MOI of 1, then NK cells were isolated by magnetic labelling.
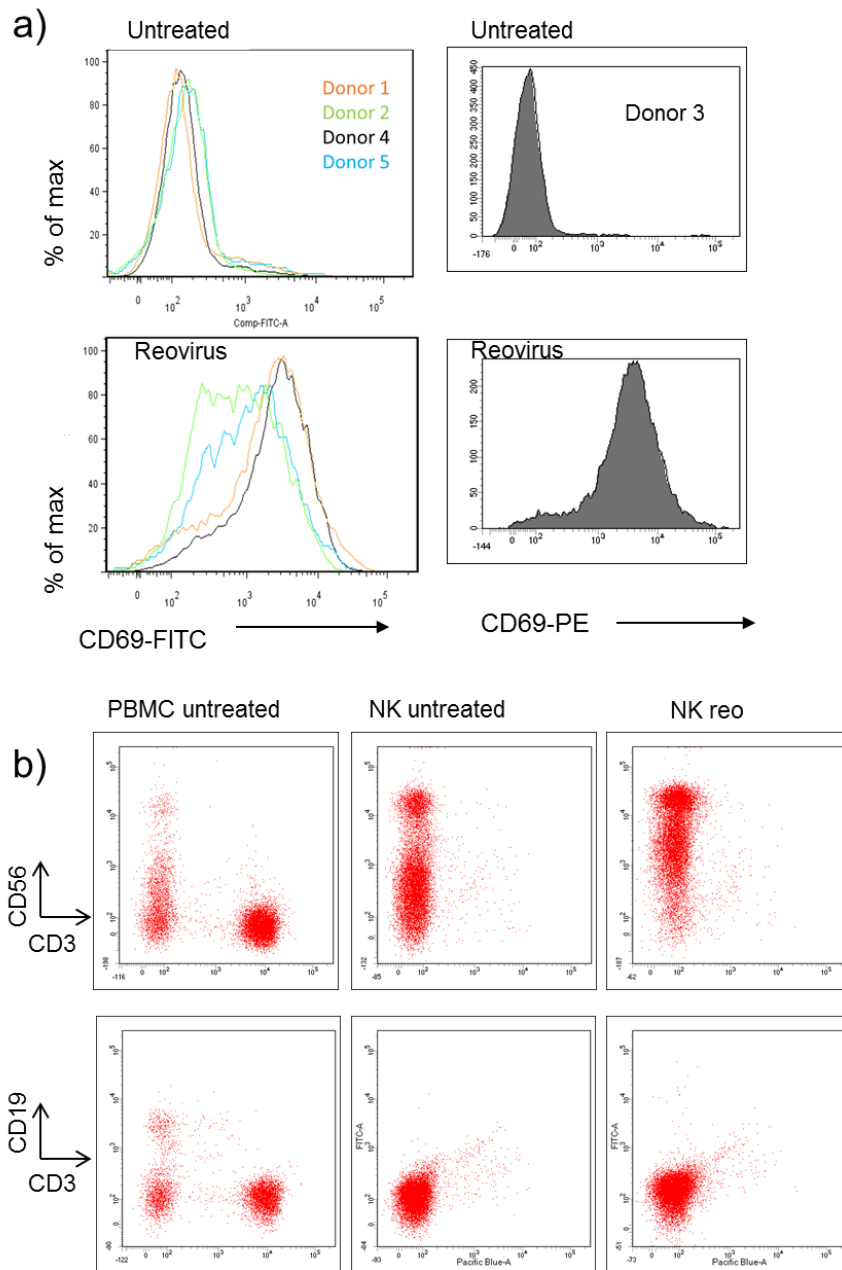
Figure 4.2 Phenotype and purity of NK cell samples

a) CD69 expression on the surface of NK cells, measured by flow cytometry. Shown are NK cells from 5 separate donors, collected for the gene expression study, after 48 hours culture of PBMC with or without reovirus at an MOI of 1. **b)** Purity of the NK cell isolation process was tested by flow cytometry analysis of NK cell, T cell and B cell markers: CD56, CD3 and CD19. PBMC were cultured for 48 hours with or without reovirus at an MOI of 1, and PBMC (before NK cell isolation) and NK cell samples (after isolation) were surface stained and analysed by flow cytometry.

The bulk of the isolated NK cell samples were sent to an external service provider who performed the necessary processing steps, from isolation of mRNA to measurement of probe intensities on an Affymetrix Human Transcriptome Array (HTA) 2.0 microarray chip. (Section 2.6). The raw intensity files were received and primary analysis was carried out using Affymetrix software. Each microarray chip was quality checked by testing the internal controls, and intensities were processed into normalised signal values. Finally, signal values for each probe were analysed with the Affymetrix transcriptome analysis console, comparing the 5 untreated samples to the 5 reovirus treated samples using a paired statistical test (Section 2.6). This generated a list of fold change expression values (reovirus treated/ untreated for each donor) with false discovery rate p values.

In order to predict which NK cell pathways or functions might be regulated by reovirus treatment, pathway enrichment analysis was carried out using the online software, Metacore. Metacore contains a database of gene and protein names, with manually curated links between names, based on protein interactions. The database also classifies networks of gene names according to function or disease, called functional ontologies. Enrichment analysis consists of mapping gene names from an experiment (for example a list of significantly upregulated genes) onto gene name IDs in Metacore's built-in functional ontologies, and calculating the statistical relevance of the matches. Firstly, data from the microarray was filtered, to produce a list of differentially expressed transcripts that were upregulated more than 1.5 fold, false discovery rate (FDR) p value < 0.05. This list of gene names, with fold change values, was submitted for enrichment analysis, mapping to Metacore's database of process networks. The top 20 enriched process networks are shown in figure 4.3, with associated p values for the match, given by the Metacore enrichment calculation. The top process identified was *Interferon signalling*, supporting the conclusions from chapter 3, that direct interferon signalling is necessary for NK activation during reovirus treatment. Another top process was *Antigen presentation*, which is explained by an upregulation of MHC transcripts. The pathway *NK cell cytotoxicity* was also identified as an important process, flagging up several associated transcripts which may play a role in enhancing tumour cell killing. Considering the results from the previous chapter, it was not surprising that both interferon and NK

cytotoxicity pathways were identified from the gene expression profiling analysis. However, what was unexpected was that cell cycle processes were also amongst the top enrichment results, including *S phase*, *Mitosis, Core, G1-S* and *G1-M* (Figure 4.3).

Process networks

-log(pValue)

1. Inflammation_Interferon signaling
2. Immune response_Antigen presentation
3. Cell cycle_S phase
4. Inflammation_NK cell cytotoxicity
5. Immune response_Innate immune response to RNA viral infection
6. Cell cycle_Mitosis
7. Cell cycle_Core
8. Cell cycle_G1-S
9. Cell cycle_G2-M
10. Inflammation_Inflammasome
11. Proteolysis_Ubiquitin-proteasomal proteolysis
12. Proteolysis_Proteolysis in cell cycle and apoptosis
13. Apoptosis_Apoptotic nucleus
14. DNA damage_DBS repair
15. Apoptosis_Anti-Apoptosis mediated by external signals via MAPK and JAK/STAT
16. Cytoskeleton_Spindle microtubules
17. Protein folding_Folding in normal condition
18. Immune response_Phagosome in antigen presentation
19. Apoptosis_Anti-apoptosis mediated by external signals via NF-kB
20. Inflammation_IFN-gamma signaling

Figure 4.3 Functional enrichment analysis of transcripts upregulated by reovirus

Microarray results were filtered to give a list of gene names upregulated more than 1.5 fold in reovirus treated PBMC-NK cells, compared to untreated cells, FDR p value <0.05. The filtered list of gene names, with fold change values, was submitted to Metacore, which identified the most enriched process networks within the data. Shown are the top 20 ranked process networks and associated p values.

Metacore also contains a database of openly available microarray data from previous studies, called the microarray repository. It consists of only Affymetrix microarray data that has passed all quality control checks. It is a useful tool to compare a new dataset against, to check for similarities in gene expression signatures. I used this online tool to compare the reovirus NK cell dataset against the microarray repository. The similarity search was based on gene names, comparing all gene IDs in the reovirus dataset with gene IDs in the repository, provided that expression of those genes exceeded a specified threshold. In this case, the threshold was set at > 1.5 fold upregulated, p value < 0.05. For my reovirus dataset, this meant transcripts had to be 1.5 fold upregulated in the reovirus treated samples compared to untreated samples. For microarray repository datasets, this meant expression was 1.5 fold upregulated in any given case group compared to a given control group sample. Metacore calculated a gene overlap between the reovirus dataset and each microarray repository dataset. The top 10 most similar datasets from the repository are shown in Figure 4.4. The top result was *Normal blood, interferon alpha stimulated*. This came from a study where healthy donor blood was stimulated *in vitro* with IFN-α (Lauwerys et al., 2013). In addition, 6 out of 10 of the top most similar results are from interferon stimulated cells or tissue, suggesting that reovirus must induce a strong interferon response signature in NK cells. Several of the most similar datasets were from *in vitro* stimulated immune cells, but there were also matches from *in vivo* experiments. For example, *Mononuclear Leukocytes from Symptomatic Influenza A Virus Challenge*, a dataset from a clinical study in which healthy volunteers were given influenza virus and PBMC gene expression was tested (Zaas et al., 2013). Thus, the gene expression signatures observed in this model of oncolytic virus therapy show similarities to both interferon and virus induced gene signatures seen previously in peripheral blood *in vivo*. This further highlights the importance of interferon in the stimulation of NK cells by reovirus and shows that the *in vitro* stimulation of PBMC with reovirus used here is a useful model of intravenous reovirus delivery, as used in oncolytic virus therapy.

Case Group	Control Group	Species	Gene Overlap	p-Value
Normal Blood, Interferon alpha Stimulated (4 hrs)	Normal Blood	Homo sapiens	348/1259	0
Normal Monocytes, 1.5 Hours IFNA2 Stimulated	Normal Monocytes without Any Incubation	Homo sapiens	288/1068	2.28E-287
Normal Skin, Interferon gamma-1b Treated	Normal Skin, Untreated	Homo sapiens	239/768	1.97E-252
Psoriasis, Normal Adjascent Skin (Non-Lesional), Interferon gamma-1b Treated	Psoriasis, Normal Adjacent Skin (Non-Lesional), Untreated	Homo sapiens	270/1192	1.79E-245
Normal Blood, Interferon alpha Stimulated (4 hrs)	Normal Blood, Interferon alpha-2b Stimulated (4 hrs)	Homo sapiens	164/261	4.53E-236
Mononuclear Leukocytes from Symptomatic Influenza A Virus, H1N1 subtype Infection, 69.5 Hours after Challenge	Normal Mononuclear Leukocytes before Influenza A Virus, H1N1 subtype Challenge	Homo sapiens	187/411	4.70E-233
Mononuclear Leukocytes from Symptomatic Influenza A Virus, H1N1 subtype Infection, 77 Hours after Challenge	Normal Mononuclear Leukocytes before Influenza A Virus, H1N1 subtype Challenge	Homo sapiens	182/459	8.85E-213
Anaplastic Thyroid Carcinoma	Nodular Goiter	Homo sapiens	328/2756	1.98E-208
Normal Blood, Interferon alpha-2b Stimulated (4 hrs)	Normal Blood	Homo sapiens	218/865	1.67E-206
Mononuclear Leukocytes from Symptomatic Influenza A Virus, H3N2 subtype Infection, 77 Hours after Challenge	Normal Mononuclear Leukocytes before Influenza A Virus, H3N2 subtype Challenge	Homo sapiens	179/477	6.97E-204

Figure 4.4 Comparison of reovirus upregulated transcripts with Metacore microarray repository.

Transcripts upregulated by reovirus in PBMC-NK cells were compared against the Metacore microarray repository, using similarity search by genes. Reovirus microarray results were filtered to give a list of gene names upregulated more than 1.5 fold in reovirus treated PBMC-NK cells, compared to untreated cells, FDR p value <0.05. The same filter was applied to microarray repository data, so only transcripts upregulated more than 1.5 fold in the case group compared to the control group were included, p value < 0.05. Above is the result of the similarity search by genes, with the most similar dataset at the top.

4.2.2 Comparative analysis of reovirus induced and IL-15 induced gene expression

Comparisons with the microarray repository revealed a strong interferon response signature in peripheral blood NK cells treated with reovirus. However, it is not known whether other cytokines play a role in this setting. Gene expression data comparing purified untreated NK cells with purified IL-15 stimulated NK cells was available in our group (Helen Close, unpublished data). This data was generated using an identical microarray (Affymetrix Human Transcriptome Array 2.0), providing a good opportunity to compare transcripts upregulated by reovirus with transcripts upregulated by IL-15. Both lists were filtered to give a list of gene names upregulated more than 2 fold relative to each untreated control, FDR p value <0.05, before taking further for analysis. IL-15 treatment triggered the differential expression of thousands of genes, so a stricter filter was applied this time. The lists were compared using a Venn diagram generator, http://bioinformatics.psb.ugent.be/webtools/Venn/. The resulting Venn diagram is shown in figure 4.5a; 182 transcripts were upregulated (2 fold, FDR p value <0.05) by both reovirus and IL-15. However, the majority of transcripts regulated were unique to either reovirus or IL-15 treatment, demonstrating that these two methods of activating NK cells likely occur by distinct mechanisms, with potentially different functional outcomes. The comparison generated three lists of transcripts: 1) Upregulated by reovirus only 2) Upregulated by both and 3) Upregulated by IL-15 only. Figure 4.5b shows the results of functional enrichment analysis (using Metacore, as described earlier) of the three lists. The list of genes upregulated by reovirus only was enriched for *Interferon signalling* and *Innate immune response to RNA viral infection*, while the IL-15 only list was enriched for multiple cell cycle processes. In the list of genes upregulated by both IL-15 and reovirus, there was also enrichment for cell cycle processes. Therefore, reovirus treatment upregulates a small proportion of genes upregulated by IL-15, involved in cell cycle processes. However overall, reovirus and IL-15 have distinct effects on NK cell gene expression.
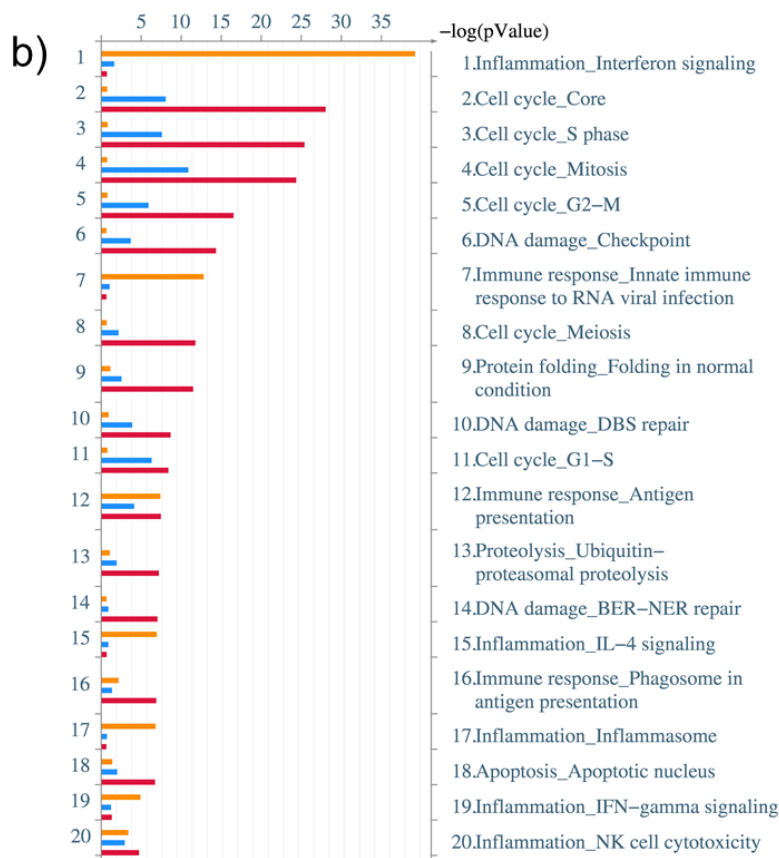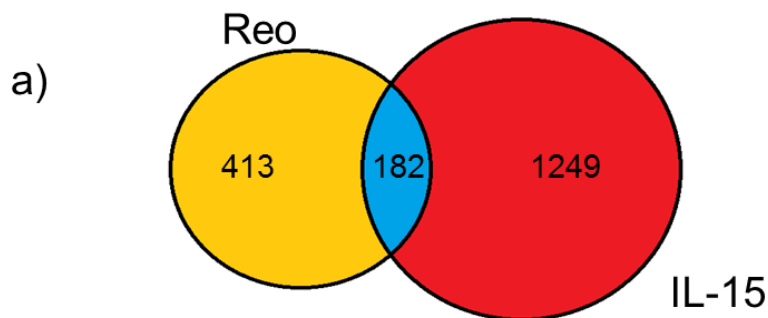
Figure 4.5 Comparison of reovirus upregulated transcripts with IL-15 upregulated transcripts

a) Transcripts upregulated by reovirus in PBMC-NK cells were compared with transcripts upregulated by IL-15 in pure NK cells (microarray data generated by Helen Close). Both lists were filtered to give a list of gene names upregulated more than 2 fold relative to each untreated control, FDR p value <0.05, before Venn diagram analysis. **b)** Metacore enrichment analysis was performed on gene name lists taken from the Venn diagram analysis. Top 20 ranked process networks are shown. Yellow = Reovirus only. Blue = Both. Red = IL-15 only.

4.2.3 Reovirus treatment upregulates NK cell cytotoxicity pathways

Functional enrichment revealed NK cytotoxicity as a potentially important process upregulated by reovirus (figure 4.3). NK cells can kill target cells through a granule dependent mechanism, or through alternative mechanisms such as death receptor pathways. Transcripts of GZMB and PRF1 (encoding the cytotoxic granule components granzyme B and perforin respectively) were upregulated by reovirus treatment (figure 4.6a). However, transcripts encoding the death receptor ligands TRAIL and FASL were upregulated to a greater extent, especially TRAIL which was increased 19 fold in reovirus treated cells. In IL-15 treated NK cells, the pattern of cytotoxicity gene expression was different, with GZMB the most upregulated transcript and the death receptor ligands less highly expressed. It is likely that NK cell TRAIL and FASL expression is sensitive to interferon signalling, which would explain the differences observed.

To validate the findings from transcriptome profiling, protein expression of NK cytotoxicity components was measured by flow cytometry. Granzyme B expression was measured by intracellular flow cytometry while TRAIL expression was measured on the cell surface. The results confirmed that granzyme B is more highly upregulated by IL-15 treatment, while TRAIL expression is much higher with reovirus treatment (Figure 4.6b).

a)

Gene		Reo fold change	FDR p-value (Reo)	IL-15 fold change	FDR p value (IL-15)
TNFSF10	TRAIL	19.27	0.004067	4.36	0.005315
FASLG	Fas ligand	3.86	0.016898	1.79	0.10785
GZMB	Granzyme B	3.26	0.019915	4.5	0.00445
PRF1	Perforin 1	2.01	0.029435	1.78	0.01147

b)
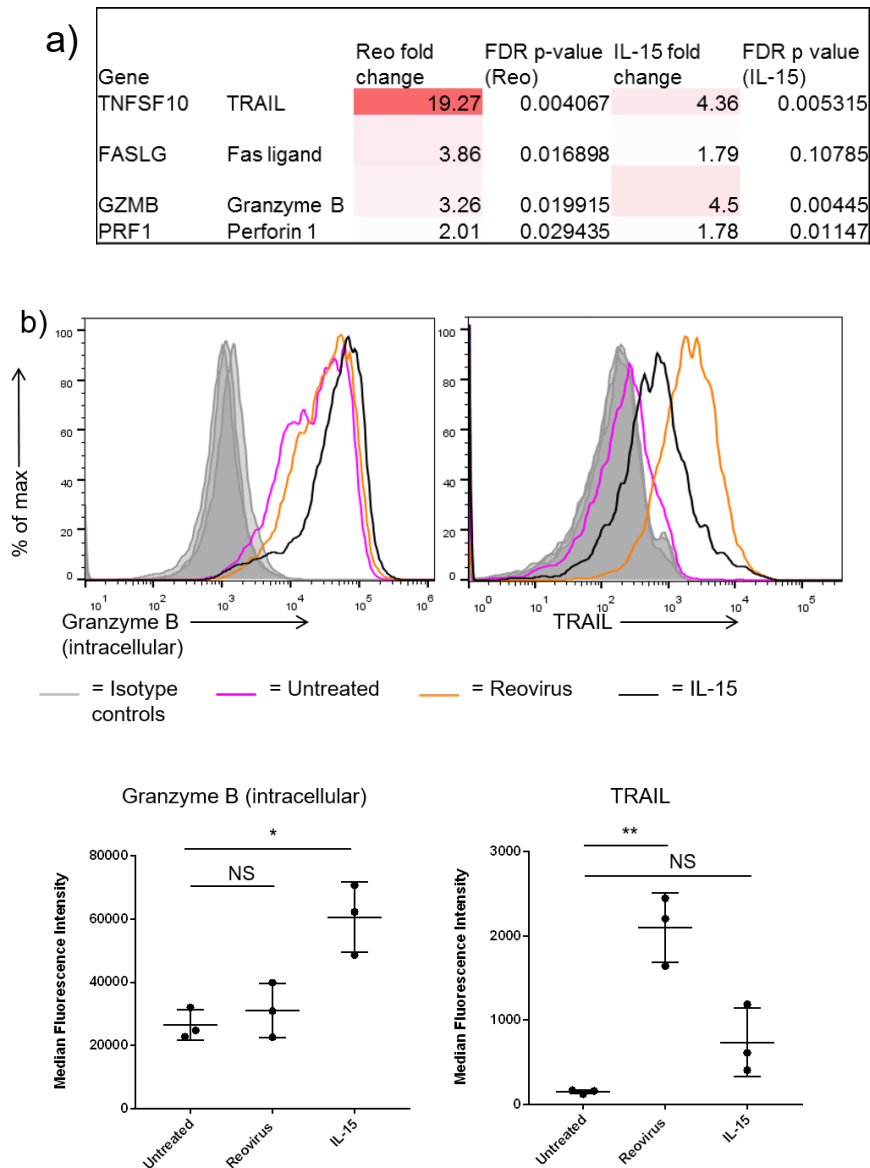
Figure 4.6 NK cell cytotoxicity associated gene expression and validation

a) NK cytotoxicity associated transcripts and fold change expression in reovirus treated PBMC-NK cells relative to untreated PBMC-NK cells (Reo), and in IL-15 treated NK cells relative to untreated NK cells (IL-15) (data from Helen Close). Data from microarray. **b)** Protein level expression of intracellular granzyme B and surface level TRAIL on NK cells within PBMC, analysed by flow cytometry. Representative histograms (top) and median fluorescence intensities from 3 separate donors (bottom). Differences in mean MFI, between untreated, reovirus treated and Il-15 treated samples, were tested by a repeated measures one way ANOVA, with Tukey's multiple comparison test. * $p < 0.05$. ** $p < 0.01$.

4.2.4 Reovirus treatment regulates lymph node homing pathways

Migration of human NK cells, especially during oncolytic virus treatment, is not well studied. Unpublished data from our group (Yasser El-Sherbiny) showed that peripheral blood NK cell population frequencies changed over time in patients receiving intravenous reovirus treatment in a clinical trial (EUDRACT number 2007/000258-29). This data is summarised in figure 4.7. 10 colorectal patients received multiple intravenous infusions of reovirus, and blood was collected at 1 time-point before virus treatment, and 6 time-points after the first infusion. The proportion of CD56^{bright} NK cells within total peripheral blood NK cells decreased at the 48 hour time-point and increased again at later time-points. The loss of CD56^{bright} NK cells coincided with a peak in NK cell CD69 expression at 48 hours, which itself in coincident with a peak in the interferon response (El-Sherbiny et al., 2015). Migration out of the blood, into lymph nodes, is one possible explanation for the disappearance of the CD56^{bright} NK cells observed at this time-point. Therefore, I interrogated the transcriptome profiling results from the *in vitro* treated NK cells, to investigate and test this hypothesis. Several receptors are involved in lymphocyte homing to lymph nodes. The adhesion molecule, L selectin (also known as CD62L), is encoded by the SELL gene and is essential for the attachment of lymphocytes to high endothelial venules (HEV) of lymph nodes (Arbones et al., 1994). Migration to lymph nodes is mediated by chemokines and the chemokine receptors CCR7 and CXCR4 recognise the lymph node chemokines, CCL19/21 and CXCL12, and have been implicated in lymph node homing of T and B cells (Baekkevold et al., 2001; Okada et al., 2002). In addition, entry into lymph nodes is antagonised by the sphingosine-1-phosphate receptor (S1PR1) which promotes egress of lymphocytes from lymph nodes (Matloubian et al., 2004). Relative transcript expression for genes encoding these receptors in reovirus treated NK cells are shown in Figure 4.8a; CXCR4 and SELL transcript levels were not significantly changed by reovirus treatment, but S1PR1 mRNA was significantly downregulated. CCR7 mRNA was upregulated by 5.62 fold on average, although FDR p value was > 0.05 due to donor variability.

Upregulation of CCR7 and downregulation of S1PR1 mRNA was confirmed by quantitative reverse transcription PCR (qRT-PCR) and additional time-points were also assessed (Figure 4.8b). The ΔΔCt (ddCt) method was used to quantify mRNA transcripts

by real time PCR. For this analysis method, the cycle threshold (Ct) values are normalised to a housekeeping gene and expressed relative to the untreated control (section 2.7.4). In this study, ABL1 was selected as the housekeeping gene, as previous experiments in our group have demonstrated stable expression in NK cells. A change of one Ct indicates a doubling in transcripts, so ddCt is equal to log2 fold change. CCR7 mRNA was upregulated in reovirus treated cells at 24, 48 and 72 hours. S1PR mRNA levels was downregulated at all time-points in reovirus treated cells, with the lowest expression at the earliest time-point tested, and appearing to increase towards untreated levels at later time-points. Upregulation of CCR7 could enhance lymph node homing of NK cells, while downregulation of S1PR1 might prevent egress, keeping NK cells in lymph nodes for longer.
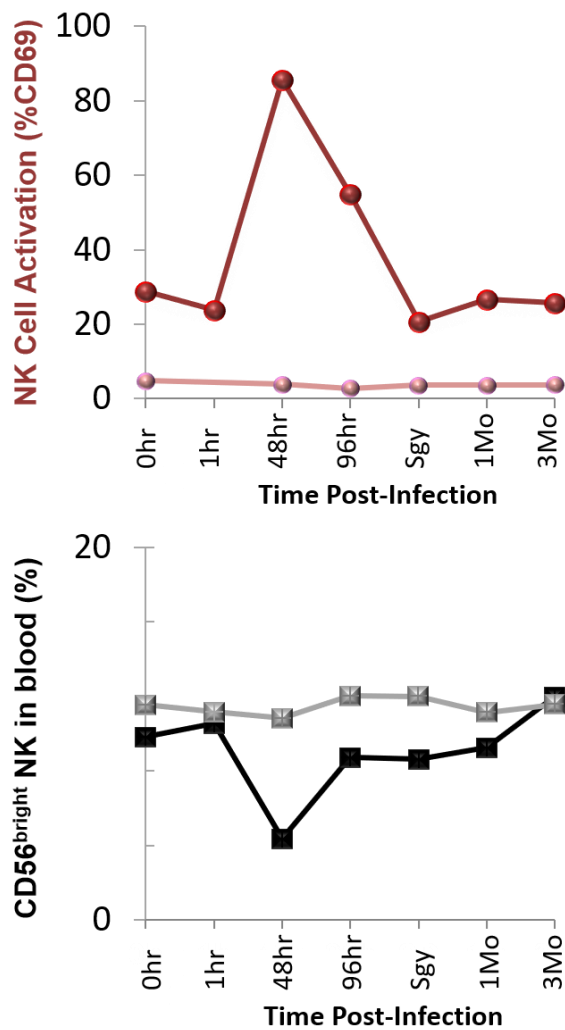
Figure 4.7 CD56^{bright} NK cell dynamics in human blood following reovirus treatment

Data generated by Yasser El-Sherbiny, showing *in vivo* peripheral blood NK cell dynamics during a clinical trial of intravenous reovirus (EUDRACT number 2007/000258-29). 10 patients received multiple doses of reovirus, as detailed in (El-Sherbiny et al., 2015). **Top graph**: CD69 expression on NK cells, from blood taken at the specified time points (also published in (El-Sherbiny et al., 2015)). Healthy control CD69 expression is in light red, patient CD69 expression in dark red. **Bottom graph:** Mean percentage of CD56^{bright} cells within total NK cells, from the same samples (unpublished). CD56^{bright} population was determined by flow cytometric staining of CD56 and CD16. Healthy control CD56^{bright} is in grey, patient CD56^{bright} in black.
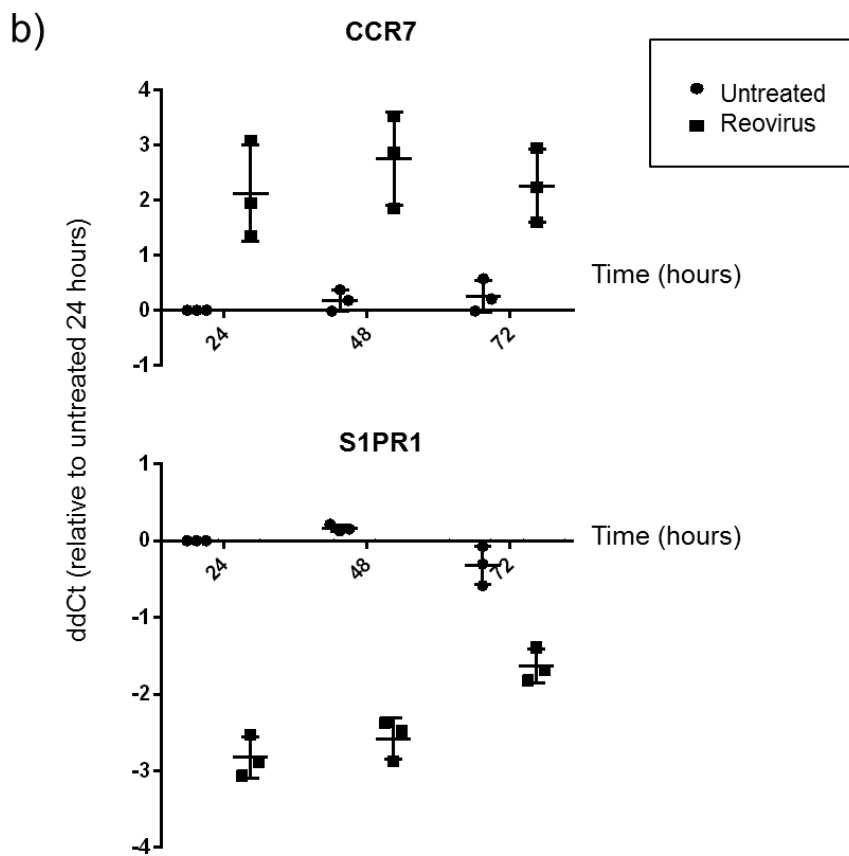
Figure 4.8 Expression of transcripts involved in lymphocyte homing to lymph nodes

a) Lymph node homing associated transcripts and fold change expression in reovirus treated PBMC-NK cells relative to untreated PBMC-NK (data from microarray). **b)** Expression of CCR7 and S1PR1 transcripts in untreated and reovirus treated PBMC-NK cells, at three separate time points, measured by qRT-PCR. Relative differences were calculated by the ddCt method, normalising to ABL1 expression. Shown above are the ddCt values, relative to the 24 hour untreated sample, in three separate donors.

Next, the expression of these transcripts was measured separately in the CD56^{dim} and CD56^{bright} populations of NK cells. In Figure 4.7, CD56^{bright} NK cells were selectively lost from the blood *in vivo* during a clinical trial . This subset of NK cells was therefore expected to selectively regulate the lymph node homing receptors. PBMC were treated with reovirus as before for 48 hours, but this time NK cell isolation by magnetic labelling was followed by fluorescence activated cell sorting (FACS), to further separate NK cells into CD56^{dim} and CD56^{bright} populations (figure 4.9a). For FACS, NK cells were separated according to CD16 and CD56 expression, reproducing the staining strategy used in the *in vivo* study in Figure 4.7. In both donors analysed, the expression of CCR7 mRNA in untreated cells was higher in the CD56^{bright} than in CD56^{dim} NK cells (Figure 4.9b), which matched findings from previous studies (Campbell et al., 2001; Berahovich et al., 2006). However, unexpectedly reovirus treatment did not increase expression of CCR7 mRNA in the CD56^{bright} population, only in the CD56^{dim} population. S1PR1 mRNA expression was slightly lower in untreated CD56^{bright} than CD56^{dim} NK (reflecting the preference of CD56bright NK cells for the lymph nodes over the blood), but there was no consistent difference between the two populations when treated with reovirus.
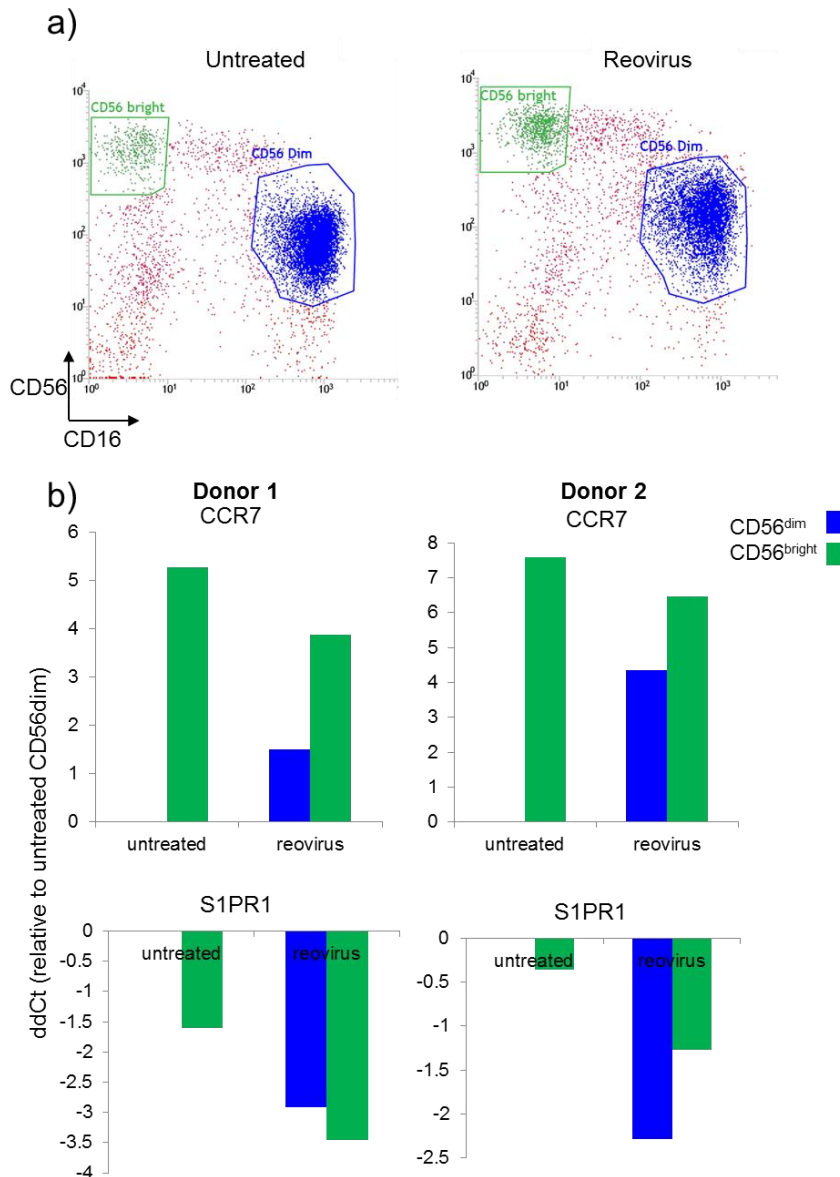
Figure 4.9 Expression of lymph node homing transcripts in CD56^{dim} and CD56^{bright} NK cells

a) Flow cytometry cell sorting to isolate CD56^{dim} CD16+ and CD56^{bright} CD16- NK cells for real time PCR analysis of transcript expression. **b)** Expression of CCR7 and S1PR1 transcripts in untreated and reovirus treated PBMC-NK cells, sorted into separate CD56^{dim} CD16+ and CD56^{bright} CD16- NK cell populations. PBMC were cultured for 48 hours before NK isolation, and transcript expression was measured by real time PCR. Relative differences were calculated by the ddCt method, normalising to ABL1 expression. Shown above are the ddCt values, relative to the untreated CD56^{dim} CD16+ sample, in two separate donors.

In order to validate these observations at protein level, CCR7 expression was analysed by flow cytometry. PBMC cultured with or without reovirus were stained using a two-step method, using a primary antibody against CCR7 followed by a secondary fluorochrome conjugated antibody, and finally with antibodies against surface markers. CD56^{dim} and CD56^{bright} NK cells were gated as above, separated by CD56 dim/bright expression and CD16 expression (Figure 4.10a). CCR7 expression was observed on a proportion of T cells, typically 70 % of CD3+ lymphocytes. However, NK cells were negative for CCR7 expression, even the CD56^{bright} population. This was surprising as sorted CD56^{bright} NK cells had strikingly higher expression of CCR7 mRNA than CD56^{dim} NK cells (Figure 4.9). To rule out problems with reagents, the same experiment was repeated with a new antibody against CCR7 (antibody 2), which was a different clone and directly conjugated with a fluorochrome. Again, a proportion of T cells were positive for CCR7 but both populations of NK cells were negative. The median fluorescence values obtained from antibody 1 and antibody 2 are shown in Figure 4.10b. The lack of CCR7 surface expression on CD56^{bright} NK cells does not reflect the results of previous studies, suggesting that the approach used here to detect cell surface CCR7 is not optimal. Despite this, mRNA expression data suggests that CCR7 is probably not the trigger for the selective loss of CD56^{bright} NK from the blood of patients, as reovirus treatment does not upregulate expression in this subset. However S1PR1 mRNA expression did decrease in both subsets when treated with reovirus, so may contribute to lymph node homing of CD56^{bright} NK cells.
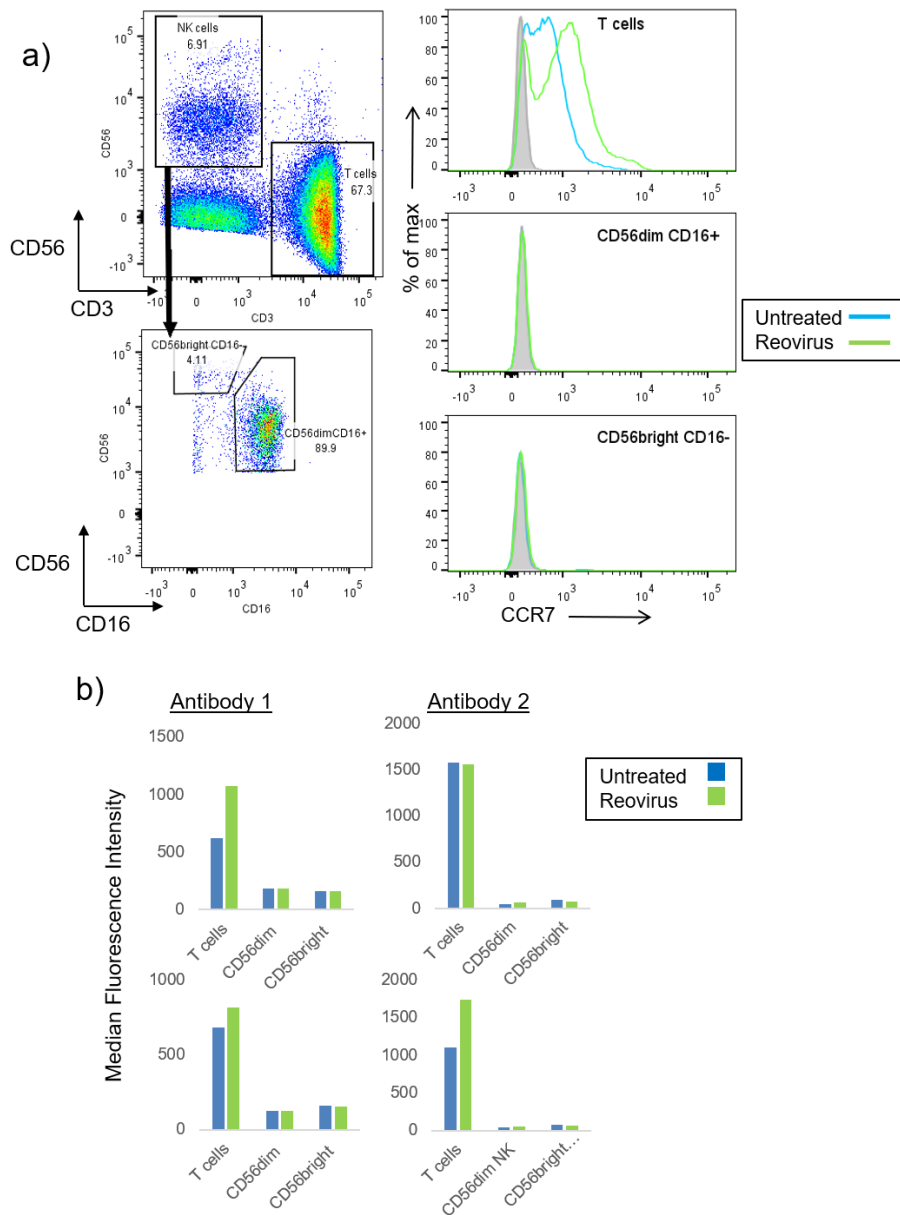
Figure 4.10 CCR7 protein levels on the surface of T cells, CD56^{dim} and CD56^{bright} NK cells

a) Histograms showing flow cytometry indirect surface staining with an antibody against CCR7, comparing T cells, CD56^{dim} CD16+ NK cells and CD56^{bright} CD16- NK cells within PBMC (gating shown for CD56^{dim} and CD56^{bright} populations). CCR7 positive gate was set on 2 % of the secondary only control. **b)** CCR7 median fluorescence staining intensities with two separate antibodies, antibody 1 and antibody 2. PBMC from 4 separate donors were cultured either with or without reovirus at an MOI of 1, then CCR7 expression on the surface of lymphocyte subsets was quantified by flow cytometry.

4.2.5 Reovirus treatment upregulates cell cycle pathways

The microarray data showed that reovirus upregulated transcripts were enriched for cell cycle associated processes (Figure 4.3), suggesting that reovirus treatment might regulate NK cell proliferation. The top cell cycle process in the enrichment contained S phase associated proteins, involved in checkpoint control or triggering DNA replication. Reovirus treatment enhanced expression of many pro-proliferation S phase transcripts; the full list is shown in Appendix 1. Two transcripts from this list, MCM4 and CDK2, and an additional cell cycle associated gene, CCNB1 (cyclin B1), were tested by qRT-PCR, which confirmed significant upregulation of MCM4 and CDK2 following reovirus treatment (Figure 4.11a). Cyclin B mRNA expression was higher on average in reovirus treated NK cells, but this difference was not significant when tested by paired T test. MCM4 is a subunit of the minichromosome maintenance (MCM) complex, involved in DNA replication licensing, while CDK2 and Cyclin B are involved in checkpoint control of the cell cycle. These transcripts are all upregulated in NK cells in response to IL-15, which is mitogenic for NK cells (Helen Close microarray data), indicating that their expression is indeed associated with NK cell proliferation. I investigated whether expression of cell cycle associated transcripts differed between subsets of NK cells. Using RNA from sorted CD56^{dim} and CD56^{bright} NK cells (Figure 4.9), MCM4 expression levels were measured by qRT-PCR. The 2 donors tested showed the same pattern of expression; in reovirus treated cells, MCM4 was upregulated more in CD56^{bright} NK cells than in CD56^{dim} NK cells (Figure 4.11b). Therefore, for cell cycle associated genes, it is likely that the fold changes reported by the microarray are primarily due to increased transcripts in the CD56^{bright} population, triggered by reovirus treatment.
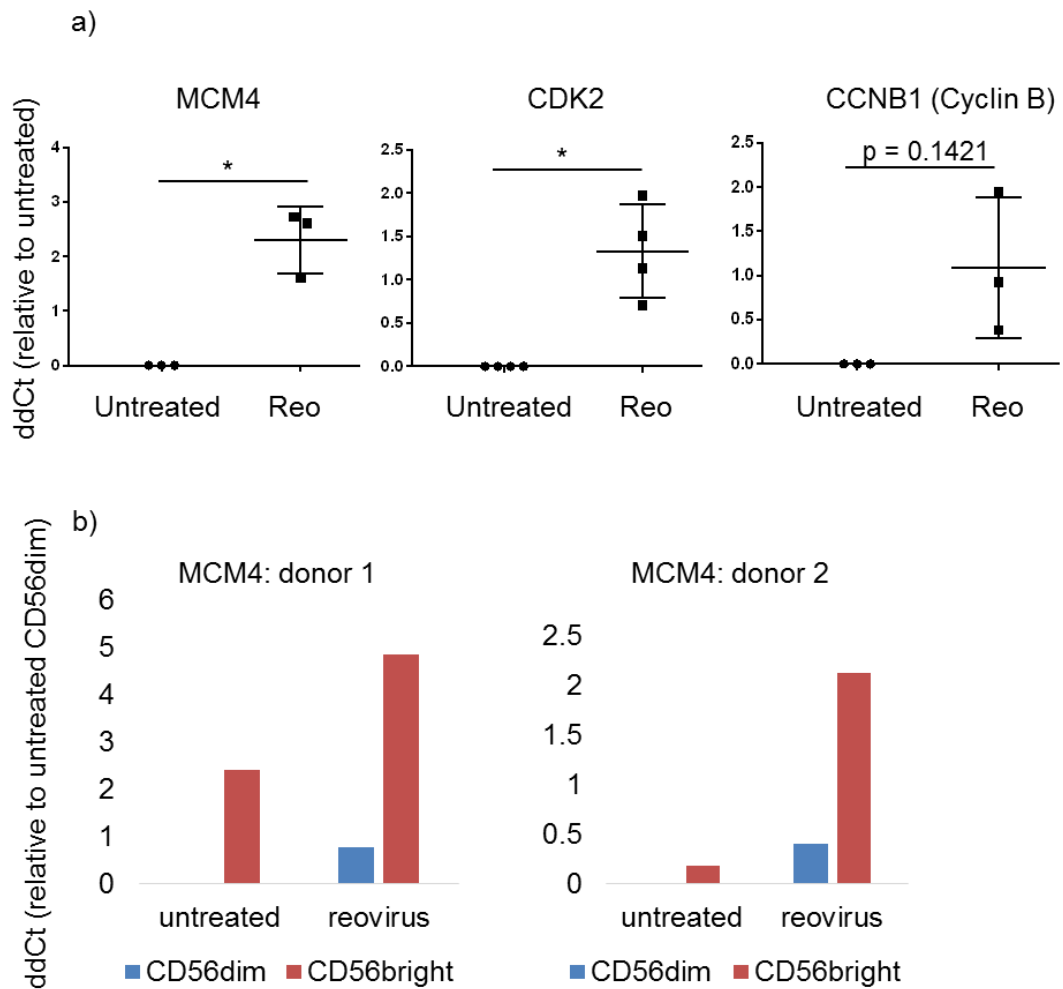
Figure 4.11 Expression of transcripts involved in cell cycle progression

a) Expression of MCM4, CDK2 and CCNB1 transcripts in PBMC-NK cells cultured with or without reovirus at an MOI of 1 for 48 hours, measured by qRT-PCR. Relative differences were calculated by the ddCt method, normalising to ABL1 expression. Shown above are the ddCt values, relative to the untreated sample, in three separate donors. Differences between mean ddCt values from untreated and reovirus treated samples were tested by paired T test. * p < 0.05. **b)** MCM4 transcript expression in untreated and reovirus treated PBMC-NK cells, sorted into separate CD56^{dim} CD16+ and CD56^{bright} CD16- NK cell populations (as in figure 4.8). PBMC were cultured for 48 hours before NK isolation, and transcript expression was measured by qRT-PCR. ddCt values are calculated relative to the untreated CD56^{dim} CD16+ sample, in two separate donors.

To test whether these changes in mRNA were reflected at the protein level, expression of MCM4, CDK2 and Cyclin B was analysed by Western Blot (Figure 4.12). MCM4 protein was detected in untreated NK cells and was highly upregulated by IL-15 treatment, as expected. Furthermore, quantification of band densities confirmed that MCM4 was reproducibly upregulated by reovirus at 48 hours (Figure 4.12a); this timepoint matches that used in the microarray analysis, demonstrating that the reovirus-mediated induction of MCM4 gene expression was accompanied by increased expression of the protein. However, at 72 hours the differences were not as clear and expression of MCM4 in both untreated and reovirus treated NK cells was variable at this time-point. Untreated NK cells were not expected to proliferate in culture, however in one donor, untreated NK cells upregulated MCM4 expression between 48 and 72 hours. It is possible that primary cells from some donors may be more sensitive than others to factors in the growth medium, or NK cells might be proliferating in response to endogenous growth factors (e.g. as the result of a sub-clinical infection in the donor). Cyclin B and CDK2 protein levels were also tested, shown on the same blot (Figure 4.12b). The positive control, IL-15 treatment, upregulated both of these proteins. However, levels of CDK2 and Cyclin B protein appeared similar between untreated and reovirus treated NK cells. This suggests that these molecules may not be upregulated at the protein level despite reovirus-induced expression of their respective genes. Alternatively, some cell cycle proteins might only be upregulated in the minority CD56^{bright} population, making detection difficult within total NK cells. Therefore, I next tested the expression of proteins which are detectable by flow cytometry. This enabled the separation of CD56^{dim} and CD56^{bright} NK cells during analysis, without needing an expensive isolation step beforehand. The proteins PCNA and Ki67 are markers associated with proliferation, and were both significantly upregulated by reovirus treatment according to the transcriptome profile: PCNA 3.35 fold and Ki67 8.7 fold. PBMC cultured with or without reovirus were stained intracellularly for total PCNA (Figure 4.13) or Ki67 (Figure 4.14). IL-15 was again tested as a positive control and, as expected, IL-15 highly upregulated both markers in NK cells, more so in the CD56^{bright} population. A gate was set during analysis, to separate PCNA/Ki67 low cells from PCNA/Ki67 high cells. Reovirus treatment increased the mean percentage of PCNA high NK cells in both subsets, although this did not reach statistical significance according to paired T tests. In contrast, the mean percentage of Ki67 high NK cells did not increase in response to

reovirus. This was surprising as Ki67 mRNA was more highly upregulated than PCNA. This suggests that Ki67 mRNA expression may not reflect the level of its protein in NK cells. Overall, reovirus treatment appears to upregulate some proliferation associated proteins, but not others.
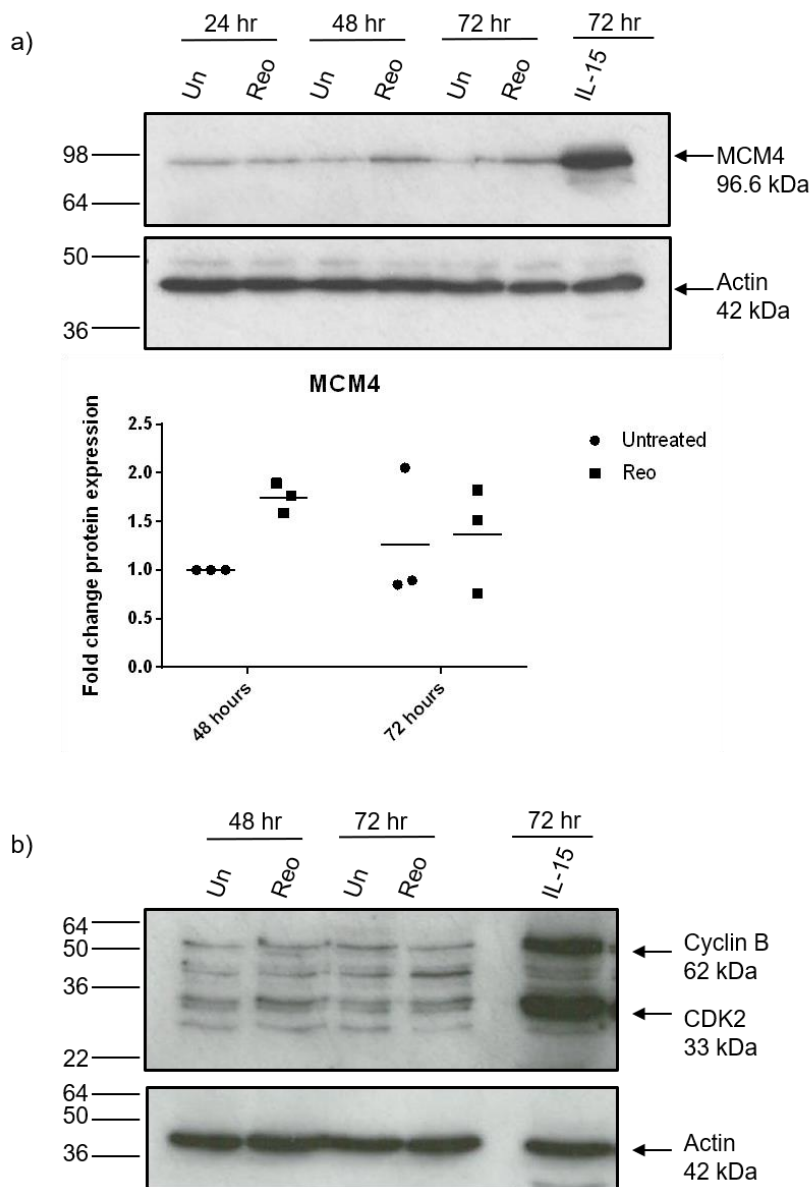
Figure 4.12 Expression of proteins involved in cell cycle progression: Western Blot

NK cells were magnetically isolated after culturing PBMC with or without reovirus at an MOI of 1, or with 10 ng/ml IL-15, for either 24, 48 or 72 hours (numbered 1 to 7). Protein expression of MCM4, cyclin B and CDK2 were analysed by Western Blot. **a)** Top: MCM4 blot example. Bottom: MCM4 expression was analysed in 3 separate donors, and normalised to β actin expression, using ImageJ. The graph shows protein expression relative to the 48 hour untreated sample. **b)** Cyclin B and CDK2 expression was analysed together. Representative of 3 donors.

118
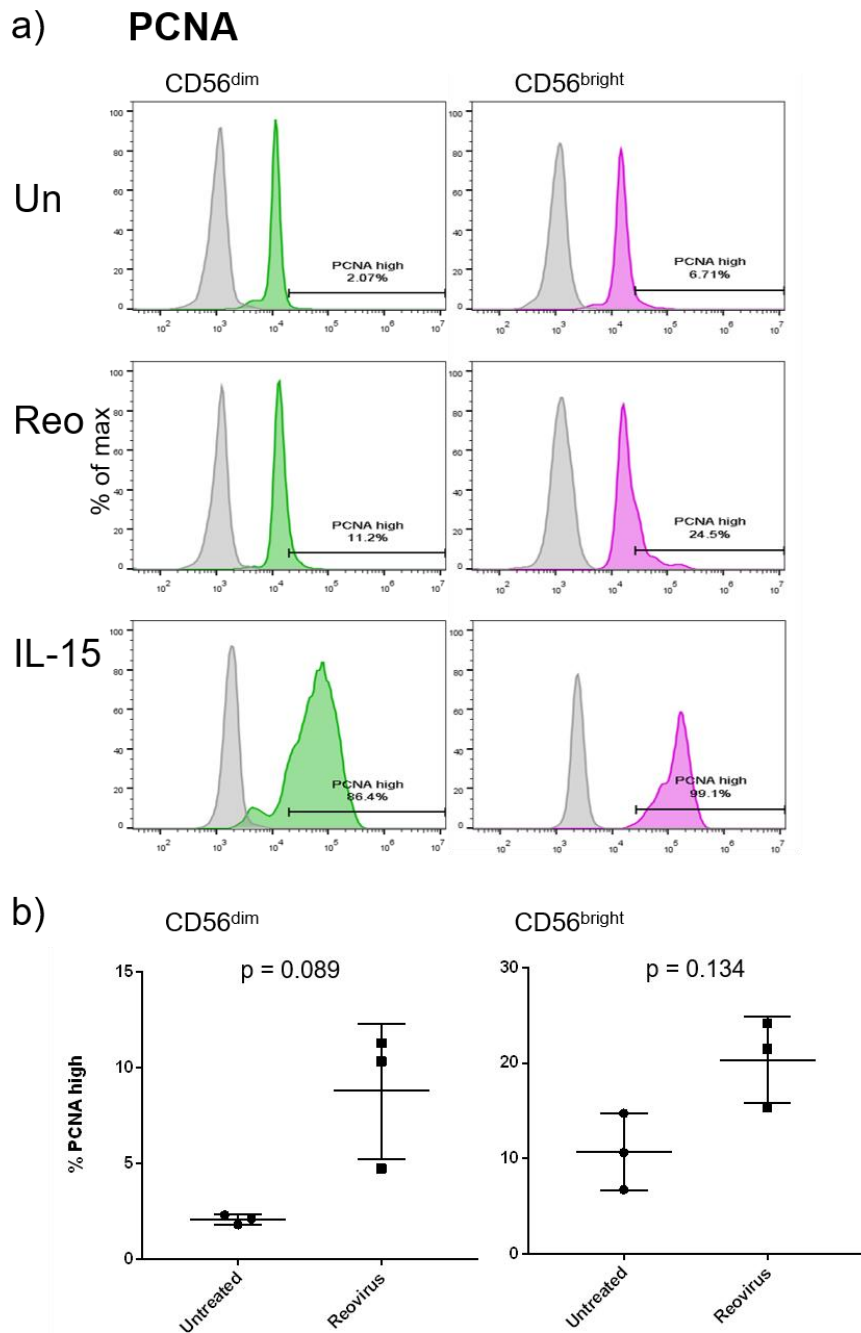
Figure 4.13 Expression of PCNA protein in CD56^{dim} and CD56^{bright} NK cells

PBMC were cultured with or without reovirus at an MOI of 1, or with 10 ng/ml IL-15, for 48 hours. Protein expression of PCNA was analysed in CD56^{dim} and CD56^{bright} NK cell populations by intracellular flow cytometry. **a)** Representative histograms from 1 of 3 separate donors, with gating separating PCNA low from PCNA high cells. Grey histograms are isotype controls. **b)** % PCNA high cells in each subset are plotted for 3 separate donors. Differences between mean % values were tested by paired T test.

a) **Ki67**
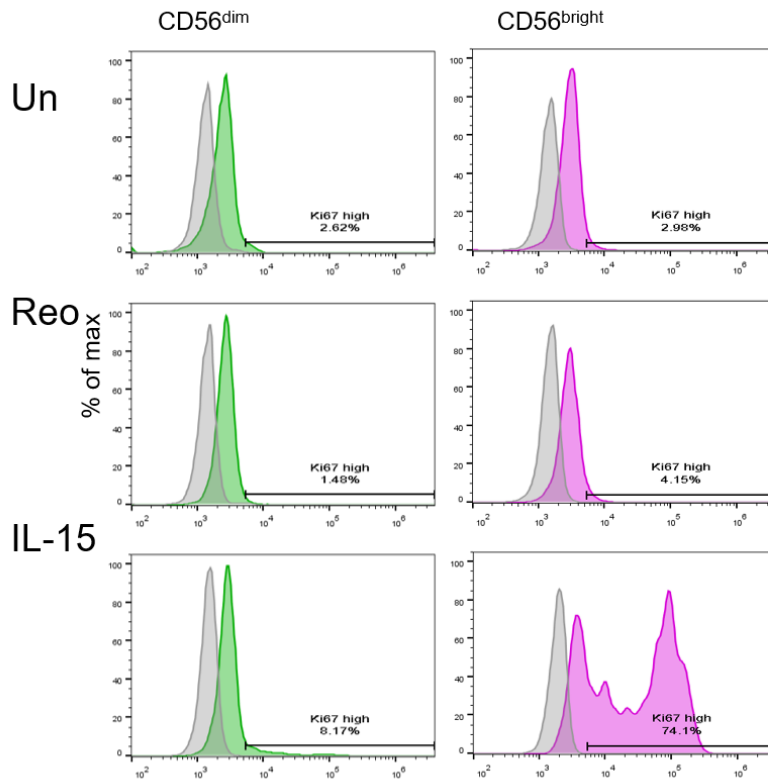
b)
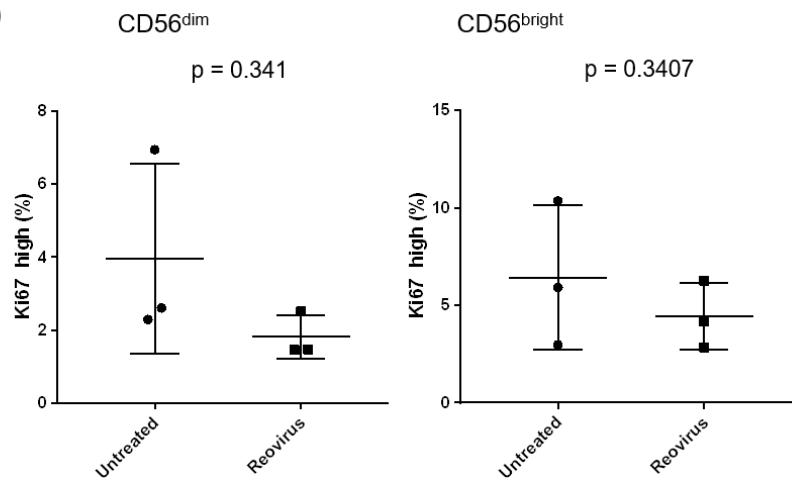
Figure 4.14 Expression of Ki67 protein in CD56^{dim} and CD56^{bright} NK cells

PBMC were cultured with or without reovirus at an MOI of 1, or with 10 ng/ml IL-15, for 48 hours. Protein expression of Ki67 was analysed in CD56^{dim} and CD56^{bright} NK cell populations by intracellular flow cytometry. **a)** Representative histograms from 1 of 3 separate donors, with gating separating Ki67 low from Ki67 high cells. Grey histograms are isotype controls. **b)** % Ki67 high cells in each subset are plotted for 3 separate donors. Differences between mean % values were tested by paired T test.

4.3 Discussion

In the previous chapter, I showed that reovirus treated NK cells acquired an activated phenotype, with increased CD69 expression. Whilst CD69 is a useful, broad marker of NK cell activation, NK cells can be activated by many different stimuli, resulting in different responses. As observed in this study, both reovirus and IL-15 upregulate CD69, but their effects on the NK cell transcriptome are distinct. In this chapter, whole transcriptome profiling revealed a wide range of reovirus induced changes in NK cells.

Functional enrichment analysis was a useful method for analysing such a large dataset (Figure 4.3) and can help discover unexpected upregulated pathways. In this case, interferon signalling was the top enriched function, which was unsurprising given the importance of interferon in regulating anti-viral responses. Comparison with previous studies revealed similarities between the reovirus-induced gene expression analysed here and interferon induced transcriptomes (Figure 4.4, microarray data from Metacore repository). Together, these results support the model proposed in chapter 3, in which interferon acts directly on NK cells. Most of the most highly upregulated genes are interferon stimulated genes such as IFI44L and RSAD2. Sustained high levels of STAT1 activation (chapter 3) probably leads to accumulation of these transcripts, such that NK cells acquire an anti-viral state. Comparison with previous microarray studies was useful, but does have limitations. Ideally, comparison should be between datasets produced with identical microarrays. Otherwise, it is not clear whether transcriptome differences are due to biological differences, or differences in probe lists (including the coverage of newly annotated genes) or probe location within the gene. If costs were unlimited, it would be interesting to run the experiment again, and compare reovirus treatment with interferon treatment, or reovirus treated NK cells with reovirus treated T cells or other cell types. This could identify pathways unique to reovirus treatment, or unique to NK cells.

Since IL-15 transcriptome data from an identical array was available, I used this to compare reovirus upregulated genes with IL-15 regulated genes specific to NK cells (Figure 4.5). Out of 1431 IL-15 upregulated genes, only 182 were shared with the list of reovirus upregulated genes. IL-15 generally upregulated cell cycle associated transcripts while reovirus treatment upregulated interferon signalling and innate anti-viral immune responses. Clearly, IL-15 and reovirus have distinct effects on NK cells. The 182 overlapping transcripts were enriched for cell cycle processes. Similar sets of cell cycle processes were highlighted in the first enrichment analysis, in the list of reovirus upregulated transcripts. Reovirus treatment might trigger NK cell proliferation, as similar sets of cell cycle transcripts are upregulated by virus treatment and by IL-15, a cytokine known to promote NK cell division. However, IL-15 upregulated cell cycle associated transcripts to a much higher degree than reovirus. It is possible that both type I IFNs and IL-15 are acting on NK cells during reovirus treatment, leading to downstream effects of both cytokines. However the lack of detectable STAT5 activation seen in chapter 3 does not support this hypothesis. Possibly, another stimulus is triggering the upregulation of cell cycle associated transcripts during reovirus treatment.

Transcriptome profiling identified a number of expected as well as unexpected changes in mRNA expression, which were then followed up with validation experiments. Reovirus treatment of PBMC enhances NK cell degranulation against cancer cell targets (chapter 3), which could be explained by altered expression of activating or inhibitory receptors, enhanced expression of degranulation machinery, or some other signalling pathway enhancement. Reovirus induced changes in NK activating receptor expression has previously been assessed in patient PBMC samples and *in vitro* treated PBMC, but no significant changes were observed (El-Sherbiny et al., 2015). The expression of GZMB mRNA increased with reovirus treatment, but intracellular granzyme B protein did not significantly increase when assessed by flow cytometry (Figure 4.6). NK cell granzyme B protein levels at rest were already high, relative to isotype control binding and to non-NK cell levels (not shown). Indeed, one reason that NK cells are able to respond very rapidly to infection and cancer is because they are "pre-armed" with cytotoxic proteins, unlike T cells

which induce granzyme B expression upon activation. Rather than increasing granzyme B concentration in the cell, reovirus exposed NK cells may enhance some other process, to enhance granule dependent killing of target cells; this could include regulation of the granule exocytosis pathway or the activation of granzyme molecules which are synthesised as inactive zymogens requiring proteolytic processing (Meade et al., 2006). Transcripts encoding components of the granule independent killing machinery were also upregulated by reovirus treatment. The death receptor ligand TRAIL was upregulated at the mRNA level, and TRAIL protein was upregulated on the surface of NK cells (Figure 4.6). IL-15 stimulation did not upregulate TRAIL expression to the same extent, suggesting this is a response unique to viral activation of NK cells. Indeed, the TRAIL gene promoter contains an ISRE, a type I interferon responsive element, and TRAIL upregulation on NK cells has been implicated in the control of viral infections (Sato, K. et al., 2001). The upregulation of NK cell TRAIL by oncolytic viruses could be an advantage during therapy, as high expression of TRAIL receptors has been reported on some cancer types including melanoma and colon cancer tissue (Daniels et al., 2005), as well as colon cancer and lung cancer cell lines (Kim, K.H. et al., 2000). Furthermore, TRAIL protein has been proposed as a anti-cancer therapy, though clinical trials have proved negative to date (Lemke et al., 2014).

The transcriptome profile data also provided an opportunity to investigate a poorly studied function of NK cells; migration. Although there have been numerous studies of mouse NK cell migration, there are few regarding human NK cells. The CD56^{bright} and CD56^{dim} NK cell subsets preferentially locate to different tissues. In the blood, CD56^{dim} outnumber CD56^{bright} NK cells, whereas in the lymph nodes the opposite is observed (Cooper et al., 2001; Fehniger et al., 2003). However, these subsets do not exist in mice (although equivalent populations have been suggested, as discussed in section 1.2.4). Furthermore, oncolytic virus studies have mainly focused on the cytotoxic capabilities of NK cells and have not considered the effects of viral treatment on NK cell distribution. Unpublished data from this lab (performed by Yasser El-Sherbiny) showed that CD56^{bright} NK cells transiently disappear from the blood of patients receiving reovirus infusions (data summarised in Figure 4.7). It was

hypothesised that this subset was migrating out of the blood into secondary lymphoid tissue. CD56^{bright} NK cells are present in higher proportions in the lymph nodes than in the blood, where they are thought to regulate T cell responses through IFN-γ release (Fehniger et al., 2003). Therefore, increased numbers of CD56^{bright} NK cells in the lymph nodes might enhance adaptive immune responses during oncolytic virus therapy. In the model used here, reovirus treatment of PBMC led to increased levels of CCR7 and decreased levels of S1PR1 mRNA in a mixed population of NK cells. However when NK cells were sorted to separate the CD56^{bright} and CD56^{dim} subsets, enhanced CCR7 expression was only observed in the CD56^{dim} population. CCR7 expression remained higher in the CD56^{bright} subset, both at rest and during reovirus treatment. Thus, even though CD56^{dim} CCR7 mRNA increased, it never reached the levels found in the CD56^{bright} population. Perhaps CD56^{bright} NK cells have reached a maximum expression level and increases are only seen in the CD56^{dim} subset. However this observation does not help to explain why the CD56^{bright} subset was selectively lost from the blood in the clinical trial. Neither CCR7 nor S1PR1 mRNA expression was selectively altered in the CD56^{bright} subset.

As CCR7 mRNA levels were already elevated in CD56^{bright} compared to CD56^{dim} NK cells, there may be an mRNA pool ready to be rapidly translated following stimulation. Surface protein levels were tested by flow cytometry, but CCR7 could not be detected on either subset of NK cells after 48 hours culture, either with or without reovirus. This was surprising, as several studies have determined CCR7 expression on the surface of CD56^{bright} NK cells (Campbell et al., 2001; Berahovich et al., 2006). CCR7 was clearly detectable on a proportion of T cells, and two separate antibodies gave the same result, suggesting that the methodology and reagents were robust. However, PBMC were cultured for two days before staining, whereas previously published studies analysed freshly isolated PBMC (Campbell et al., 2001; Berahovich et al., 2006). It is possible that culture of primary NK cells leads to loss of surface CCR7; when Berahovich et al. analysed CCR7 expression on NK cell lines, only 1 out of 3 was positive by flow cytometry (Berahovich et al., 2006). Chemokine receptor internalisation is a widely reported phenomenon, and might be responsible for the lack of cell surface expression. It would be interesting to study NK cell

chemotaxis towards lymph node cytokines following *in vitro* reovirus treatment, however the experimental model would need to be further validated due to these inconsistencies with previous studies. It is unclear whether *in vitro* culture of PBMC is an appropriate method for the study of chemokine receptors and chemotaxis.

S1PR1 mRNA was downregulated in both CD56^{dim} and CD56^{bright} NK subsets during reovirus treatment. The ligand for this receptor, Sphingosine-1-Phosphate (S1P), is present in higher concentrations in the blood than other tissue compartments. This concentration gradient promotes egress of lymphocytes from the lymph nodes into the blood (Matloubian et al., 2004). Therefore, downregulation of S1P receptors might slow the egress of lymphocytes from lymph nodes (allowing NK cells to act in the lymph node, for example by providing IFN-γ to skew Th1 responses). CD69 has also been implicated in the control of lymphocyte egress from lymph nodes, by inhibiting the action of S1PR1 (Shiow et al., 2006). NK cell CD69 is clearly upregulated by reovirus treatment (chapter 3) and transient CD69 upregulation overlaps with the loss of CD56^{bright} NK cells from the blood of patients (Figure 4.7). The downregulation of S1PR1 combined with upregulation of CD69 may therefore enhance retention of NK cells in the lymph nodes. Since the S1P gradient does not exist solely in lymph nodes, NK cells might be transiently retained in other tissues as well, depending on additional homing signals. In the clinical trial, the patients receiving reovirus were being treated for colorectal cancer, so NK cells might have homed to the cancerous tissue (where signs of reovirus replication were observed (Adair et al., 2012)). Although CD69 upregulation and S1PR1 mRNA downregulation were not specific to CD56^{bright} NK cells, this subset does express higher levels of many chemokine receptors, including CCR7 transcripts as I confirmed here. Therefore, the reason why only CD56^{bright} NK cells are lost from the blood could be because of an innate migratory ability, causing this subset to leave the periphery, followed by an enhanced retention in lymph node (or tissue) triggered by changes in CD69 and/or S1PR1. To test these hypotheses, *in vivo* study would be required. A mouse study would be ideal for tracking changes in a controlled way, however information about the human CD56^{bright} and CD56^{dim} subsets would be lost.

Finally, cell cycle associated transcript expression was investigated further, after functional enrichment identified cell cycle processes were upregulated by reovirus. Compared with some of the interferon stimulated genes (e.g. IFI44L, up 128.98 fold), cell cycle transcripts were relatively weakly upregulated (e.g. MCM4, up 2.08 fold). Real time PCR on a small selection of genes confirmed modest upregulation of transcripts associated with DNA replication or cell cycle progression. However, when NK cells were sorted into CD56^{dim} and CD56^{bright} subsets, expression of MCM4 was much more highly upregulated in the CD56^{bright} population. Therefore, transcriptome profiling on whole NK cells probably underestimates the enhancement of these pathways in the CD56^{bright} subset. CD56^{bright} NK cells are known to proliferate more than the CD56^{dim} subset in response to IL-2, which has been explained by their expression of the high affinity IL-2 receptor (Caligiuri et al., 1990), now known as the IL-2Rαβγ. CD56^{bright} NK cells are also the more proliferative subset under other conditions, such as pDC induced proliferation (Romagnani et al., 2005) or IL-4 and IL-7 induced proliferation (Robertson et al., 1993). A recent paper showed that CD56^{bright} NK cells are more metabolically active than the CD56^{dim} subset (Keating et al., 2016), which might explain their enhanced ability to proliferate in response to a range of stimuli. Protein expression validation confirmed upregulation of some proliferation associated markers in response to reovirus, but not others. Of those that were upregulated (MCM4, PCNA), the changes induced by reovirus were small compared to the effects of IL-15, but this was expected considering the comparative analysis of the reovirus and IL-15 transcriptome profiles. Flow cytometry allowed the separate analysis of PCNA and Ki67 levels in CD56^{dim} and CD56^{bright} NK cells. As expected, there was higher proportion of PCNA high cells in the CD56^{bright} subset. Flow cytometry also allowed single cell level of analysis of protein levels, which revealed that the majority of NK cells at rest have uniform levels of PCNA or Ki67, with a small percentage of cells staining more strongly. PCNA is a component of DNA replication machinery, is used as an S phase marker (Landberg and Roos, 1991) and PCNA high cells are probably cells in (or about to enter) S phase. Ki67 is thought to function during mitosis (Cuylen et al., 2016), and accumulates later in the cell cycle (Sobecki et al., 2017). This could explain why I observed higher proportions of PCNA high cells compared to Ki67 high cells at the same time-point. Surprisingly, intracellular protein levels of Ki67 did not increase with reovirus treatment. The

proportion of Ki67 high cells in reovirus treated samples was typically less than untreated samples, although this was not significantly significant. This was despite an 8 fold upregulation of Ki67 mRNA in reovirus samples, when measured by transcriptome profiling. These apparently conflicting results suggest that reovirus mediated effects on NK cell proliferation may be more complex than originally predicted.

In conclusion, transcriptome profiling both confirmed the expected – that interferon signalling is the dominant pathway activated by reovirus – and revealed new pathways to explore further. Reovirus treatment influenced the expression of transcripts involved in granule independent cytotoxicity, lymph node homing, and proliferation; functions which could be important for optimal therapeutic effect of NK cells during oncolytic virus therapy. In the final chapter, I have investigated the effects of reovirus on NK cell proliferation.

Chapter 5. Regulation of NK cell proliferation by reovirus

5.1 Introduction

In the previous chapter, I analysed the transcriptional responses of NK cells in PBMC treated with reovirus. Gene expression profiling revealed an upregulation of cell cycle associated transcripts in reovirus treated NK cells, suggesting that reovirus may affect NK cell proliferation. NK cell expansion has been reported in some viral infection models, the most widely studied example being the MCMV mouse model, and in a few human viral infections, but not in others. The mechanisms underlying NK cell proliferation differ across types of viruses; MCMV induces clonal proliferation through the Ly49 receptor (Dokun et al., 2001), while hantavirus induces IL-15 on endothelial cells to trigger human NK cell proliferation (Bjorkstrom et al., 2011; Braun et al., 2014). Clearly, not all viruses affect NK cell proliferation equally. Furthermore, it is difficult to predict how intravenous virus therapy will impact on NK cell turnover or expansion, as little is known about NK proliferation in the blood. Therefore, it was important to study how NK cells within PBMC might proliferate in response to reovirus treatment. In this chapter, I have used proliferation assays to study how reovirus affects human NK cell division, and investigated the impact of reovirus treatment on signalling pathways that drive proliferation.

5.2 Results

5.2.1 Reovirus treatment does not induce NK cell proliferation *in vitro*

To study proliferation *in vitro*, PBMC isolated from healthy donors were labelled with carboxyfluorescein succinimidyl ester (CFSE) (Section 2.3.8). CFSE binds covalently to free amines on the cell surface and inside of cells, and emits a bright signal when analysed by flow cytometry. Upon cell division, the CFSE inside the cell is diluted by half – allowing the tracking of cell division events in a population. Tracking of lymphocyte proliferation usually requires longer term culture of cells, in order to visualise multiple divisions. I cultured CFSE labelled PBMC for 5 days, as in (Romagnani et al., 2005). As the CFSE dilution assay is a flow cytometry based method, it allows the simultaneous analysis of separate subsets of cells. This was ideal for the analysis of NK cell within PBMC. In the previous chapter, mRNA expression analysis of sorted CD56^{dim} and CD56^{bright} NK cells revealed much higher cell cycle transcript upregulation in the CD56^{bright} population. In order to assess proliferation in both of these NK cell subsets, PBMC were stained with CD3, CD56 and CD16 antibodies. The gating for this experiment is shown in Figure 5.1a. Untreated cells are not expected to proliferate; the majority of untreated NK cells are found in a peak of undivided cells. A gate was drawn to separate this peak of undivided cells from the less brightly staining, divided cells. The gate was positioned at the edge of the undivided peak, in untreated cells. Within IL-15 treated PBMC, proliferation of NK cells was observed, with clear peaks of dividing cells. CD56^{bright} NK cells proliferated more than the CD56^{dim} population in response to IL-15, which is consistent with the pattern of Ki67 expression shown in Figure 4.14. In contrast, reovirus treated cells did not proliferate at this time-point. Across 3 separate donors, there were no statistically significant differences between untreated and reovirus treated cells, although in CD56^{bright} NK cells the mean level of proliferation was actually lower in reovirus treated cells than untreated cells (Figure 5.1b).

It was possible that reovirus treatment did induce NK cell proliferation, but at a later time-point. However, when PBMC were kept in culture for longer, the viability of reovirus

treated lymphocytes dropped dramatically (Figure 5.2). This meant that longer term culture experiments were not possible, and also suggested that reovirus treatment might actually activate anti-survival signals in lymphocytes, rather than pro-survival, pro-proliferation signals.
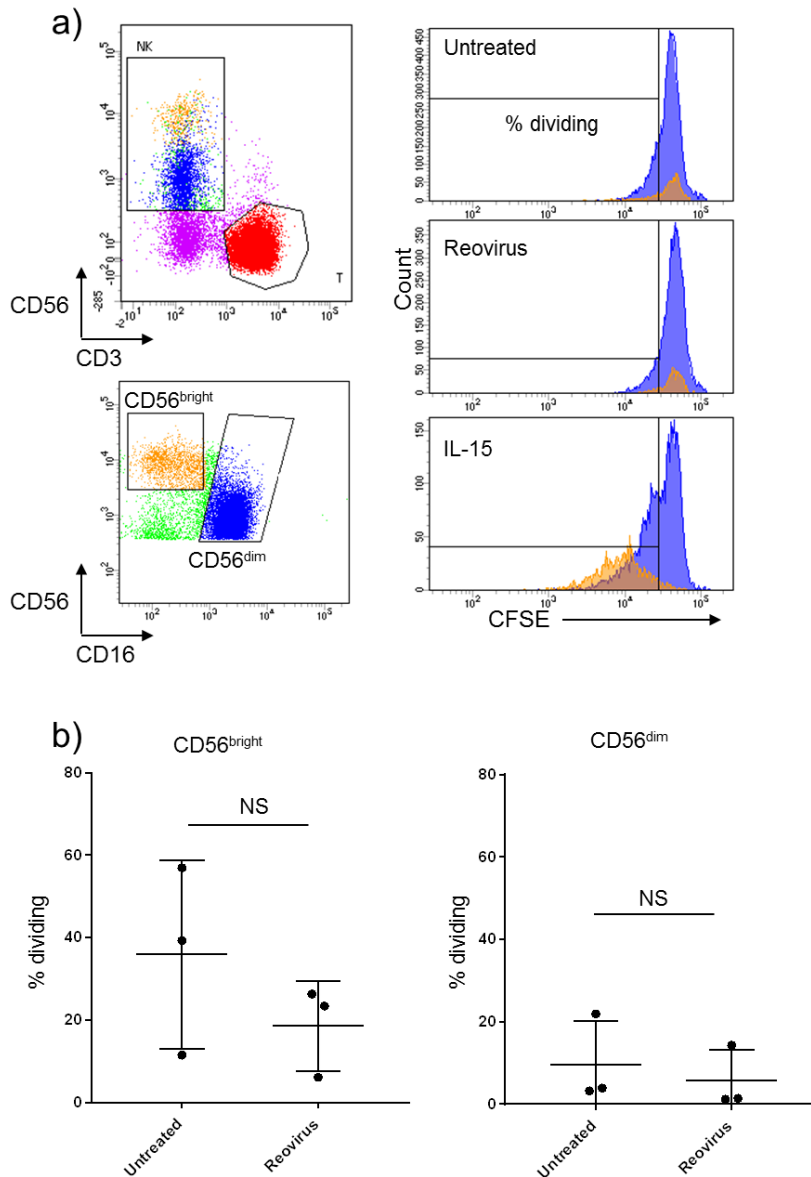
Figure 5.1 NK cell proliferation during *in vitro* reovirus treatment

a) PBMC were labelled with 0.2 µM CFSE, then cultured for 5 days either with or without reovirus at an MOI of 1, or 10 ng/ml IL-15. After 5 days, PBMC were stained with viability dye to exclude dead cells, and surface markers and dilution of CFSE were analysed by flow cytometry. Left hand dot plots show gating of NK cells within PBMC, and gating of CD56^{dim} and CD56^{bright} cells within total NK cells. Right hand histograms are CFSE dilution plots. Cells falling to the left of the gate are classed as dividing. **b)** Percentage of CD56^{bright} (left) and CD56^{dim} (right) NK cells classed as dividing by the CFSE dilution assay above, from 3 separate donor PBMC. Paired T test results are shown. Differences between treatment means were tested by paired T test. NS = not significant.
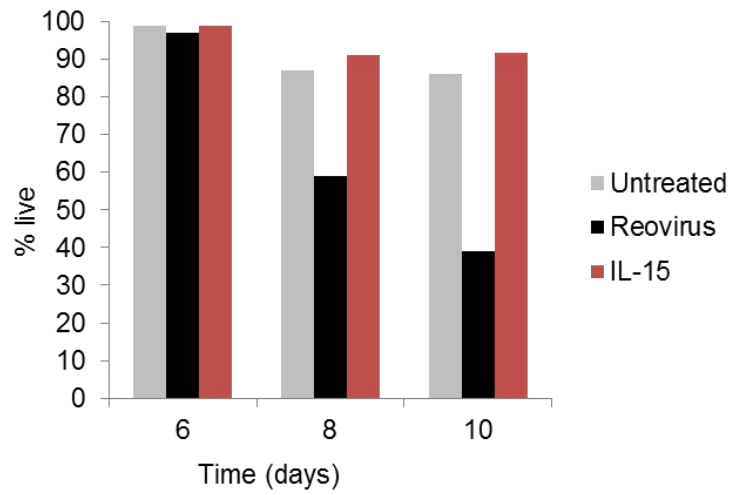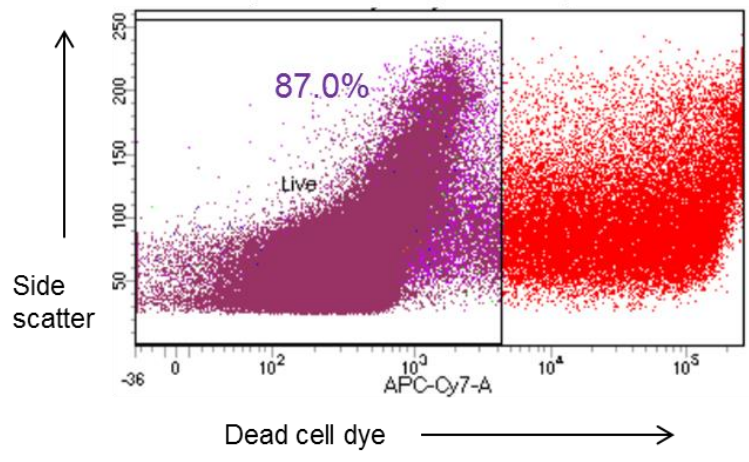
Figure 5.2 Long term culture of CFSE labelled PBMC

PBMC were labelled with 0.2 µM CFSE, then cultured alone, with reovirus at an MOI of 1, or with 10 ng/ml IL-15, for 6, 8 or 10 days. Viability of lymphocytes within PBMC was analysed by viability dye staining. Cells within the gate (staining dimly for the viability dye) were classed as live lymphocytes, whereas cells falling outside of the gate (staining brightly for the viability dye) were classed as dead. Representative of 2 donors.

5.2.2 Reovirus pre-treatment inhibits IL-15 induced proliferation

Although reovirus treatment induces the expression of several cell cycle genes (Chapter 4), reovirus treatment alone did not trigger NK cell proliferation (Figure 5.1). Reovirus alone might not be a strong enough stimulus to initiate cell division. In some cases, certain cytokines are able to augment proliferation, but only in combination with other stimuli (Robertson et al., 1993). Potentially, reovirus might prime NK cells for enhanced proliferation in response to a second stimulus, such as IL-15. The cytokine IL-15 has been used throughout this study as a positive control for proliferation, and it plays an important role in NK cell homeostasis (Ranson et al., 2003). Therefore, I tested whether reovirus pre-treatment affected NK cell proliferation in response to IL-15. CFSE labelled PBMC were primed with reovirus for 4 hours before stimulation with IL-15 for 5 days. Surprisingly, reovirus priming did not enhance NK cell proliferation, but instead inhibited proliferation in response to IL-15 (Figure 5.3). In the CD56^{bright} subset, reovirus pre-treatment significantly reduced the mean proportion of dividing cells; this difference was also observed in the CD56^{dim} subset but the differences were not statistically significant. Thus, although reovirus treatment upregulated markers of proliferation in NK cells (chapter 4), the functional consequence of treatment was actually to inhibit *in vitro* proliferation.

While CFSE is a good indicator of cell division, it does not reveal anything about cell cycle phase. Therefore, propidium iodide (PI) staining of DNA was performed, to test how reovirus treatment affected cell cycle progression. Previous work in our group determined 72 hours as an optimal time-point to detect S phase in IL-15 treated NK cells using PI staining. The dye PI intercalates between DNA or RNA bases in a quantitative manner (similar to ethidium bromide); after RNase treatment, PI staining indicates the total DNA content of each cell when analysed by flow cytometry. However, this method of DNA staining requires ethanol fixation which is incompatible with cell surface antigen staining. Hence, for these experiments, NK cells were treated with reovirus and/or IL-15 within the context of PBMC and then purified by magnetic labelling before the staining process. After doublet exclusion (Figure 5.4a), PI staining was analysed in histogram format using Modfit software, which fits G0/G1 and G2 peaks to the data and defines S phase cells. After 72 hours culture with IL-15 alone, S phase and G2 cells were clearly

observed. However when PBMC were pre-treated with reovirus before IL-15 stimulation, the proportion of NK cells in S phase was dramatically reduced. The duration of reovirus treatment did not change the result; cell cycle progression was inhibited with 4 hour, 24 hour or 48 hour pre-treatments with reovirus (Figure 5.4). The proportion of cells in each cell cycle compartment was quantified by Modfit, shown in figure 5.4b. Reovirus pre-treatment led to an accumulation of cells in G0/G1 phase, relative to treatment with IL-15 alone (Figure 5.4b). Therefore, reovirus treatment inhibited NK cell proliferation by blocking progression into S phase.
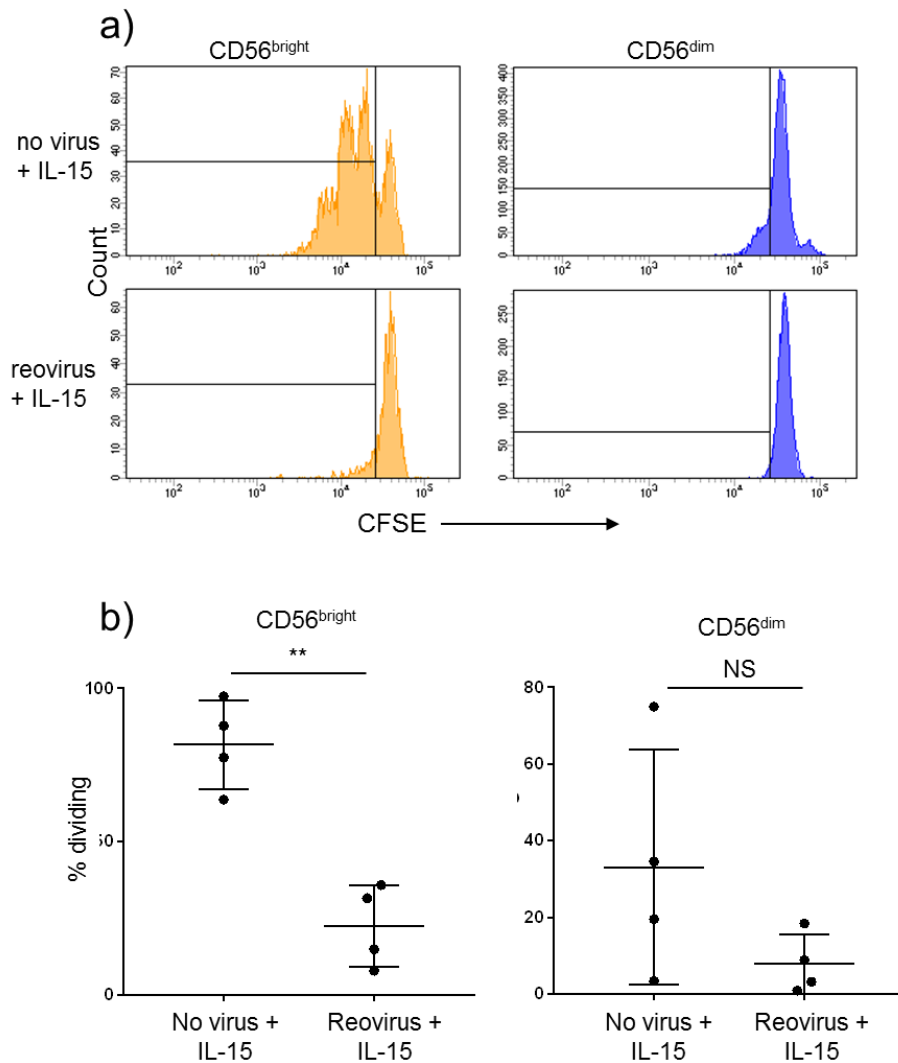
Figure 5.3 Effect of reovirus priming on IL-15 induced NK cell proliferation

a) PBMC were labelled with 0.2 µM CFSE, then primed for 4 hours with reovirus at an MOI of 1 or cultured without virus. 10 ng/ml IL-15 was then added directly to all samples and cells were cultured for a further 5 days. After 5 days, PBMC were stained as in figure 5.1. Histograms show CFSE dilution of CD56^{dim} and CD56^{bright} NK cells. **b)** Percentage of CD56^{bright} (left) and CD56^{dim} (right) NK cells classed as dividing by the CFSE dilution assay above, from 4 separate donor PBMC. Differences between treatment means were tested by paired T test. ** $p < 0.01$. NS = not significant
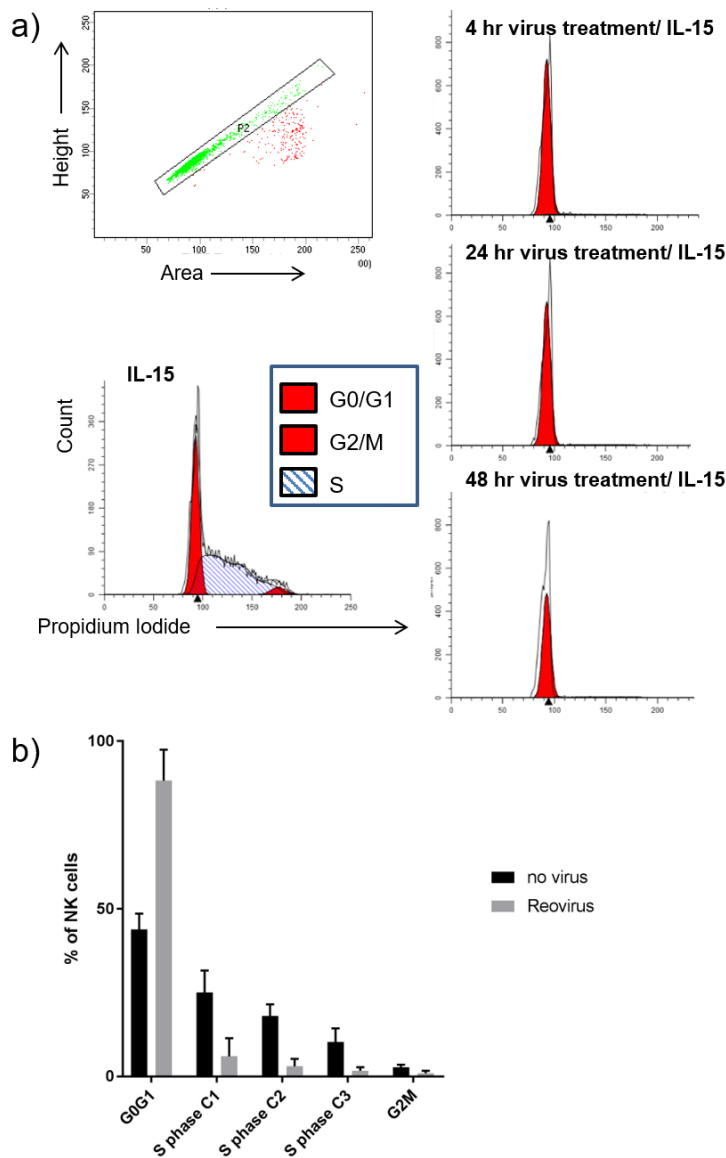
Figure 5.4 Effect of reovirus priming on cell cycle progression

a) PBMC were either treated with 10 ng/ml IL-15 for 3 days, or primed with reovirus at an MOI of 1 for 4, 24 or 48 hours, followed by IL-15 treatment for 3 days. NK cells were then isolated by magnetic labelling, fixed and DNA stained with propidium iodide (PI). Staining was analysed by flow cytometry, which required doublet exclusion by height Vs area of signal (top left). PI cell cycle profiles were analysed using Modfit software. **b)** The bar graph shows percentage of NK cells in each cell cycle compartment, after 3 days culture with 10 ng/ml Il-15 (no virus), or 3 days culture with IL-15 after 4 hours priming with reovirus at an MOI of 1 (Reovirus). Values were calculated by Modfit software. Bar graph shows mean values plus standard deviation for 3 separate donor PBMC.

As shown in chapter 3, PBMC treated with reovirus secreted high concentrations of IFN-α, a cytokine long known to inhibit the proliferation of virus infected cells, as part of its broad antiviral activity (Sangfelt et al., 2000). The effect of IFN-α on lymphocyte proliferation is more controversial, but some studies have shown that IFN-α inhibits the IL-2 induced proliferation of T cells and NK cells (Erickson et al., 1999; Jewett and Bonavida, 1995). Therefore, high levels of IFN-α in reovirus treated PBMC might inhibit NK cell proliferation, and block any pro-proliferation signals that may be present. To test this, I cultured PBMC in reovirus conditioned media, filtered to remove virus particles. Reovirus conditioned media had a similar effect to live reovirus treatment, inhibiting NK cell proliferation in response to IL-15 (Figure 5.5). When cultured in reovirus conditioned media, there were fewer cell division events – which was most striking in the CD56^{bright} NK subset. This suggested that soluble factors released into the media in response to reovirus treatment were responsible for blocking proliferation. To test whether IFN-α was the factor responsible, a cocktail of antibodies blocking the action of IFN-α was utilised. Inclusion of type I IFN blocking antibodies prevented the inhibition of proliferation by reovirus conditioned media, with the CFSE histograms for both untreated CM and reovirus CM conditions appearing very similar. In contrast, inclusion of isotype control antibodies did not prevent inhibition of proliferation. Therefore, type I IFN released by reovirus stimulated PBMC was responsible for inhibiting NK cell proliferation in response to IL-15.
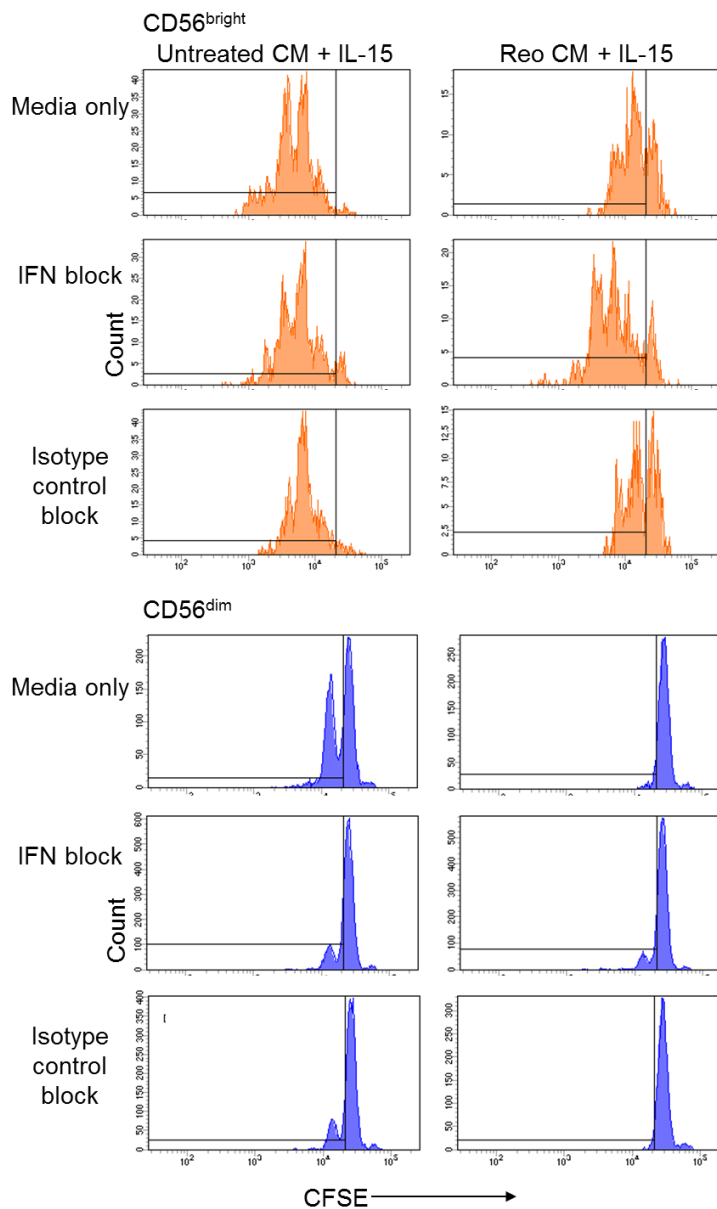
Figure 5.5 Effect of type I interferon neutralisation on IL-15 induced NK cell proliferation

PBMC were labelled with 0.2 µM CFSE and resuspended in conditioned media from either untreated PBMC (untreated CM) or Viresolve filtered conditioned media from reovirus treated PBMC (Reo CM). The samples were split and some were treated with IFN-blocking antibody cocktail and some with isotype control blocking cocktail. 10 ng/ml IL-15 was then added directly to all samples and cells were cultured for 5 days. After 5 days, PBMC were stained as in figure 5.1. Histograms show CFSE dilution of CD56bright and CD56dim NK cells, representative of 3 separate donors.

5.2.3 Type I interferon inhibitory effects on NK cell proliferation

The results above show that type I IFN, released from reovirus treated PBMC, inhibited proliferation of IL-15 stimulated NK cells, but it was unclear whether this inhibitory effect was specific to IL-15. The cytokine IL-12 is also reported to contribute to NK cell proliferation, although it is not as strong a stimulus as IL-15 (Vitale et al., 2002). To compare the effects of distinct proliferative cytokines, purified NK cells from healthy donors were cultured in combinations of IFN-α with IL-15 or IL-12, then subjected to cell cycle analysis by PI staining (Figure 5.6). IL-12 treatment increased the proportion of S phase cells, although the increase was small relative to IL-15 treated cells (33% in S phase for IL-15, but only 6% for IL-12). Addition of IFN-α to both IL-12 treated NK cells and IL-15 treated cells decreased the S phase fraction.

NK cells from the same experiment were also analysed for mRNA expression of cell cycle associated transcripts, using quantitative real time PCR. Both IL-12 and IL-15 increased the expression of MCM4, CDK2 and Cyclin A and B transcripts (Figure 5.7). However, IFN-α inhibited expression of these transcripts, both in IL-12 treated and IL-15 treated NK cells, and even reduced expression in otherwise untreated cells. These results, together with the proliferation assays above, demonstrate that IFN-α mediated inhibition of proliferation is not specific to IL-15 based proliferation and that IFN-α inhibits expression of cell cycle genes. On the other hand, reovirus treatment – which clearly induces IFN-α release – triggered the upregulation of cell cycle gene expression. The possible reasons for this inconsistency were explored further in section 5.2.6.

Lastly, a similar experiment was conducted to analyse the dose response to IFN-α. Since IFN-α has been reported to promote lymphocyte proliferation in some cases (Curtsinger et al., 2005), I next tested the possibility that low concentrations might promote NK cell proliferation, while high concentrations (such as those resulting from reovirus treatment of PBMC) might activate different pathways to inhibit proliferation. However, all of the tested concentrations of IFN-α inhibited proliferation of IL-15 treated NK cells, as determined by the proportion of cells in S phase (Figure 5.8). Similarly, all dilutions of the reovirus conditioned media inhibited proliferation.

In certain cell lines, treatment with IFN-I has been shown to upregulate expression of cell cycle inhibitory proteins, including INK4 proteins and CIP/KIP proteins such as p19 and p21 (Sangfelt et al., 2000) These families of proteins inhibit the action of cyclin dependent kinases (CDKs), therefore inhibiting progression through the cell cycle. Expression of these factors was examined in the transcriptome profiles from untreated and reovirus treated NK cells (chapter 4). However, no significant changes were observed in a range of INK4 and CIP/KIP transcripts (Table 5.1).
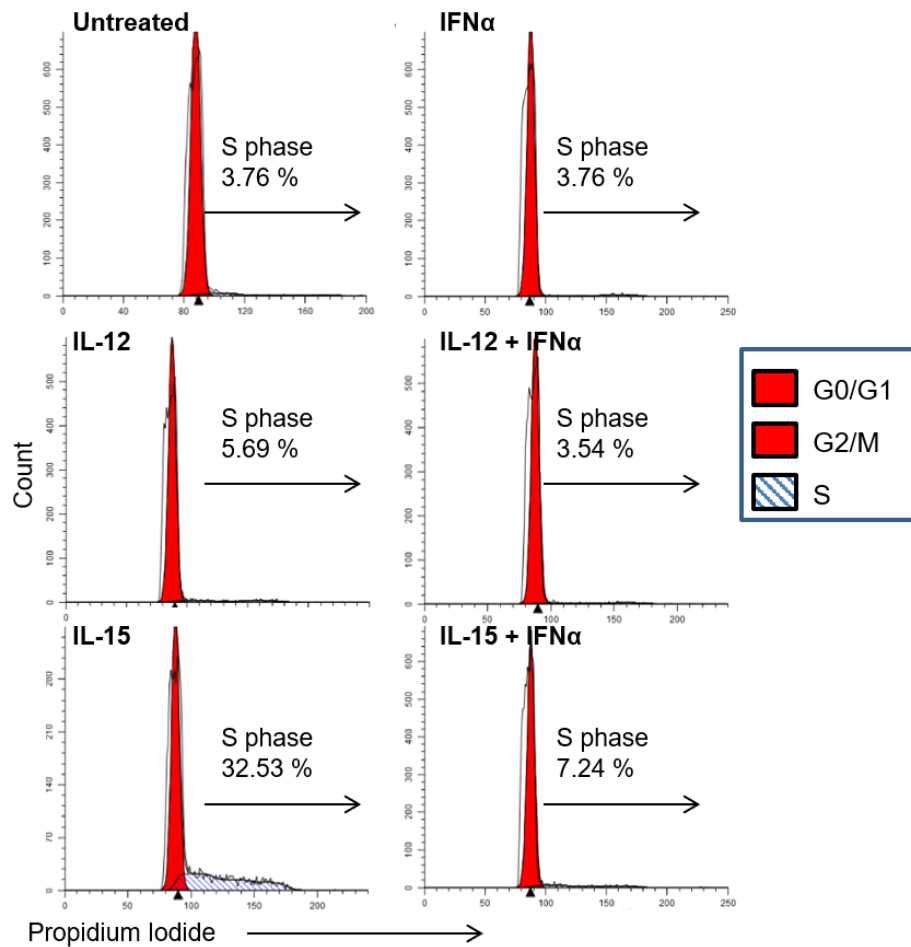
Figure 5.6 NK proliferation during treatment with different cytokine combinations

Purified NK cells were cultured with the combinations of cytokines above, all at 100 ng/ml, for 3 days. Samples were then fixed and DNA stained with propidium iodide (PI). Staining was analysed by flow cytometry and cell cycle profiles were analysed using Modfit software, to calculate percentages of NK cell in S phase for each sample. The results above are representative of three donors.
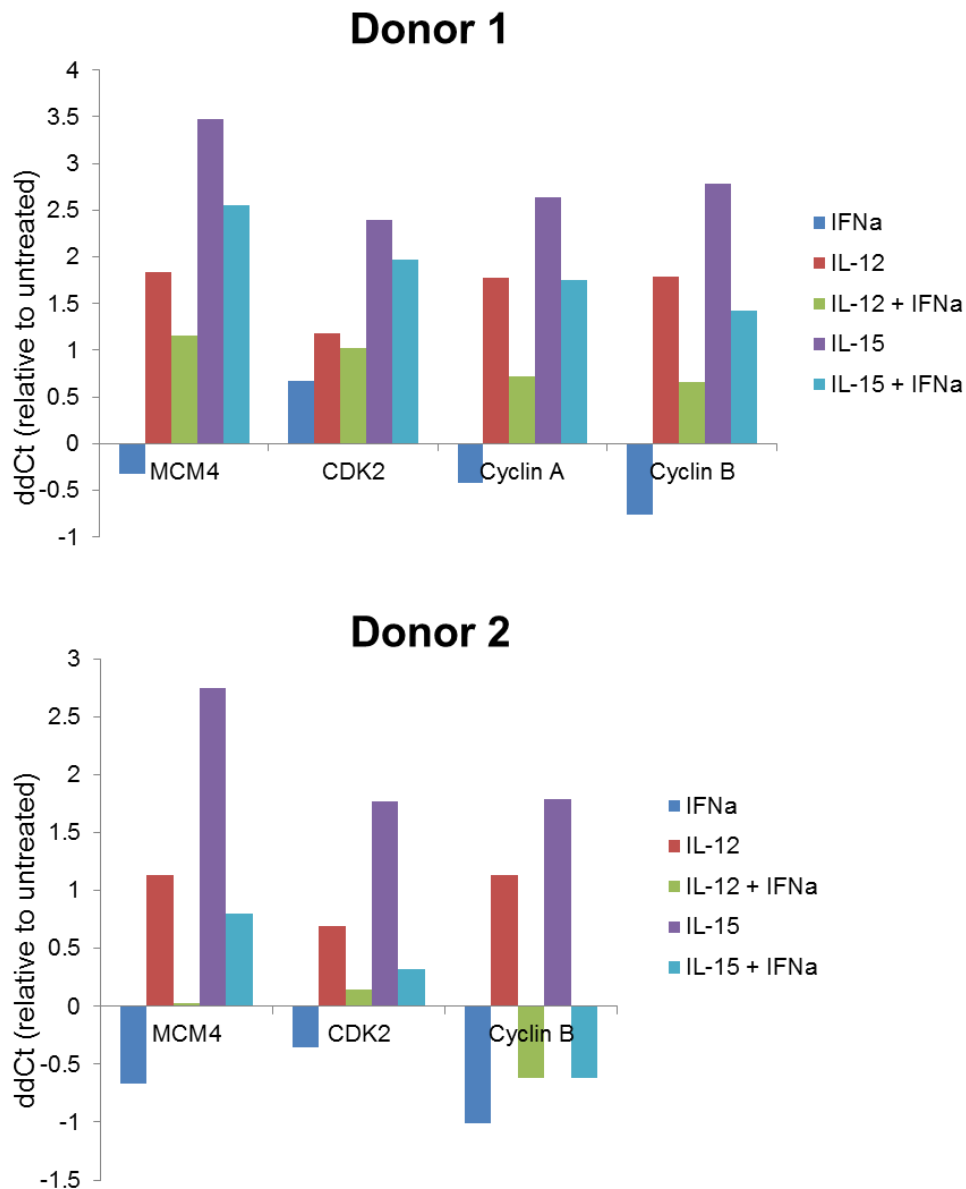
Figure 5.7 Expression of cell cycle associated transcripts after treatment of NK cells with different cytokine combinations

Purified NK cells were cultured with the combinations of cytokines above, all at 100 ng/ml, for 3 days. Expression of MCM4, CDK2, CCNA2 (Cyclin A) and CCNB1 (Cyclin B) transcripts was measured by real time PCR. Relative differences were calculated by the ddCt method, normalising to ABL1 expression. Shown above are the ddCt values, relative to the untreated sample, in 2 separate donors.
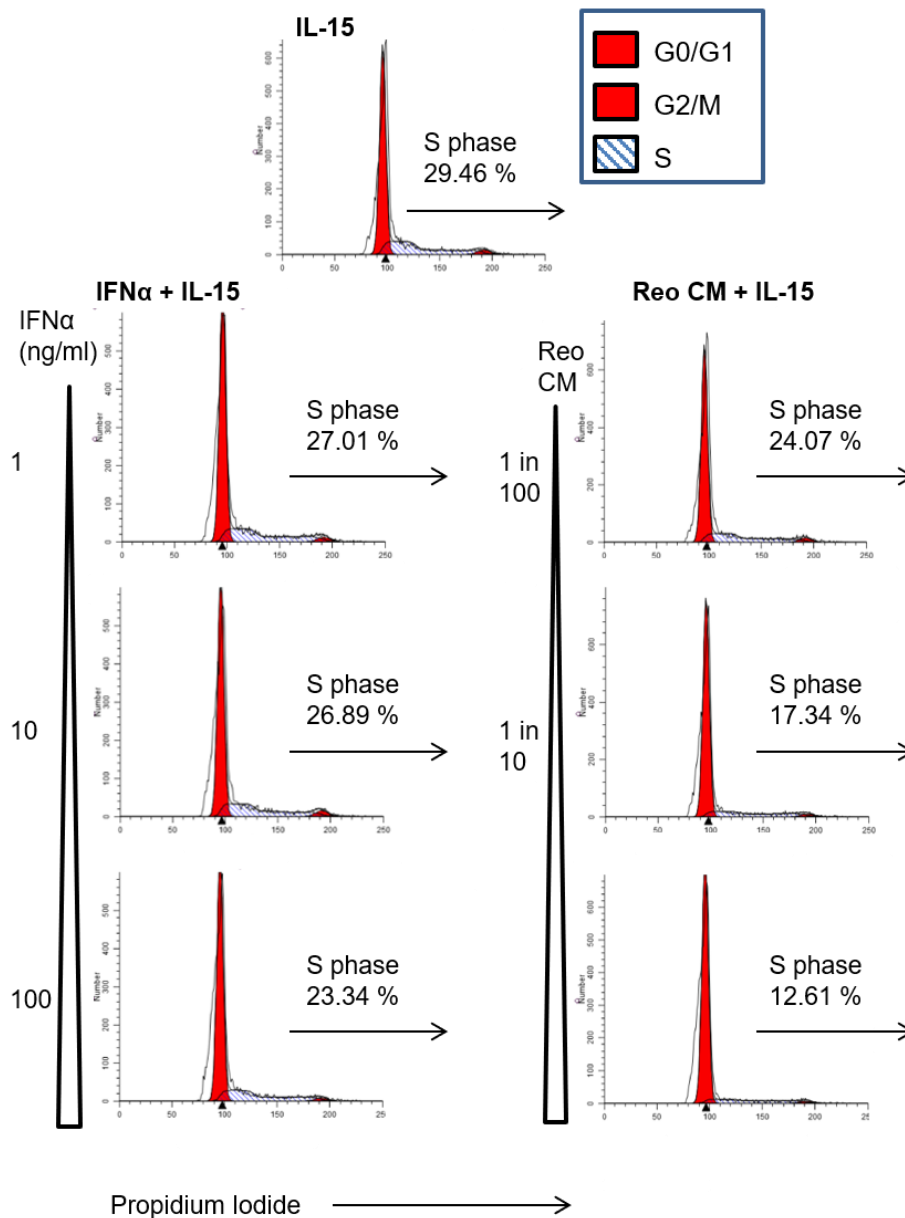
Figure 5.8 Effect of IFN-α concentration on NK cell proliferation

Purified NK cells were cultured with 10 ng/ml IL-15 plus increasing concentrations of IFNα, or decreasing dilutions of reovirus conditioned media (Viresolve filtered) for 3 days. Samples were then fixed and DNA stained with propidium iodide (PI). Staining was analysed by flow cytometry and cell cycle profiles were analysed using Modfit software, to calculate percentages of NK cell in S phase for each sample. The experiment was performed in one donor.

INK4 proteins

Fold Change (linear) (Reo vs. Resting)	FDR p-value (Reo vs. Resting)	Gene Symbol	Description
1.05	0.540408	CDKN2D	cyclin-dependent kinase inhibitor 2D (p19, inhibits CDK4)
1.03	0.986728	CDKN2A	cyclin-dependent kinase inhibitor 2A; cyclin-dependent kinase inhibitor 2A (melanoma, p16, inhibits CDK4)
1.03	0.319032	CDKN2B	cyclin-dependent kinase inhibitor 2B (p15, inhibits CDK4)
-1.13	0.243265	CDKN2C	cyclin-dependent kinase inhibitor 2C (p18, inhibits CDK4)

CIP/KIP proteins

Fold Change (linear) (Reo vs. Resting)	FDR p-value (Reo vs. Resting)	Gene Symbol	Description
1.16	0.275991	CDKN1A	cyclin-dependent kinase inhibitor 1A (p21, Cip1)
1	0.757898	CDKN1C	cyclin-dependent kinase inhibitor 1C (p57, Kip2)
-1.01	0.391143	CDKN1C	cyclin-dependent kinase inhibitor 1C (p57, Kip2)
-1.02	0.91586	CDKN1B	cyclin-dependent kinase inhibitor 1B (p27, Kip1)
-1.09	0.510175	CDKN1B	cyclin-dependent kinase inhibitor 1B (p27, Kip1)

Table 5.1 Expression of potential anti proliferative transcripts during reovirus treatment

Fold change expression of INK4 family and CIP/KIP family transcripts in reovirus treated PBMC-NK cells relative to untreated PBMC-NK . Data from microarray.

5.2.4 Effects of reovirus treatment on IL-15 signalling

During the proliferation analysis, I observed that reovirus pre-treatment had additional effects on NK cells treated with IL-15. IL-15 stimulated NK cells upregulate expression of cell surface CD56, which can be observed by flow cytometry (Figure 5.9). However, in PBMC pre-treated with reovirus conditioned media, this upregulation of CD56 was inhibited. Addition of IFN-I blocking antibodies into the conditioned media rescued CD56 upregulation, while isotype control blocking antibodies did not (Figure 5.9). This suggested that reovirus induced IFN-I has wider inhibitory effects on NK cells, other than the inhibition of proliferation. One possibility was that reovirus treatment interferes with signalling downstream of IL-15 (or other proliferative cytokines).
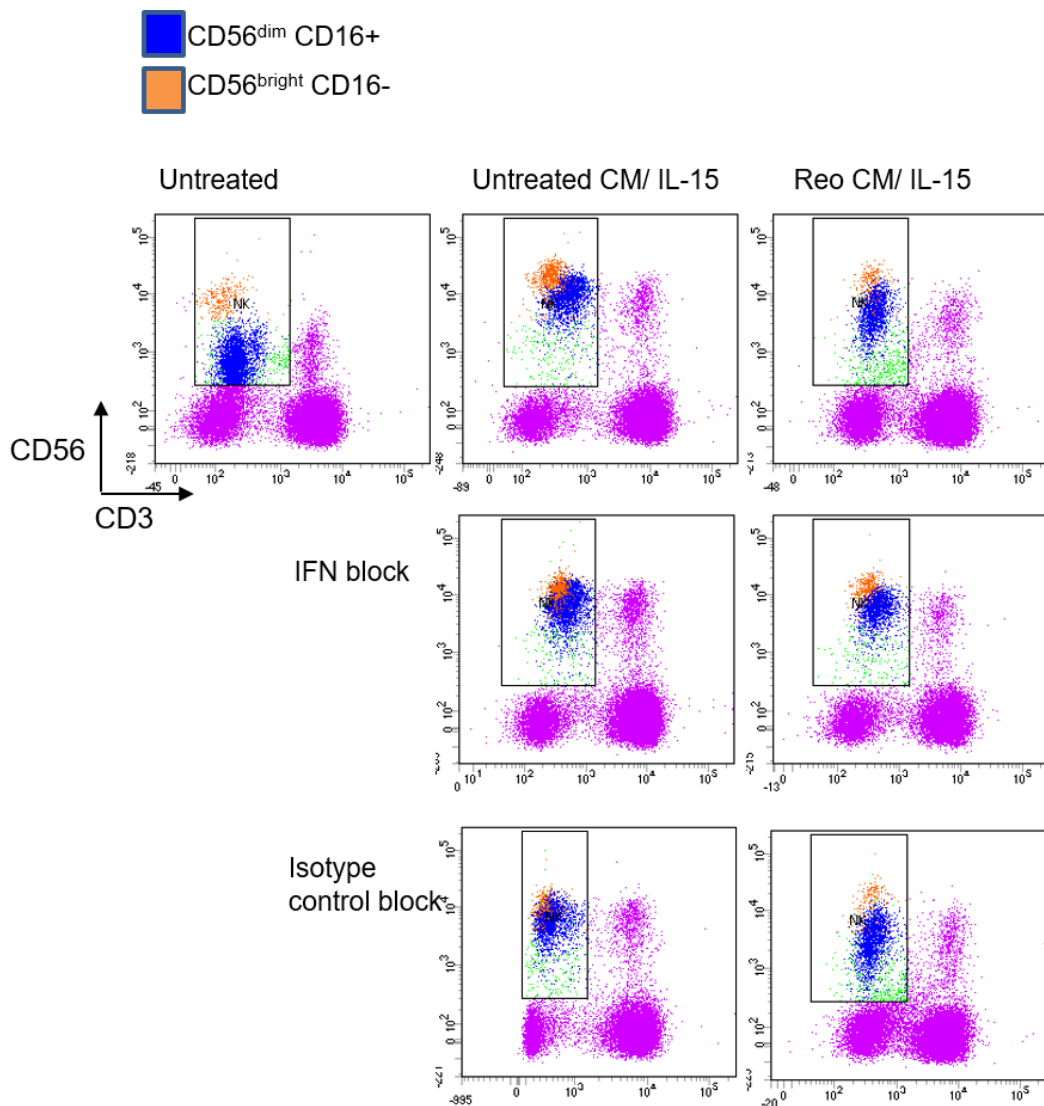
Figure 5.9 Effect of reovirus conditioned media on IL-15 induced NK surface phenotype

CFSE labelled PBMC were cultured in conditioned media plus 10 ng/ml IL-15 for 5 days, with the addition of type I interferon blocking cocktail (IFN block) or isotype control blocking cocktail (Isotype control block). A sample left untreated for 5 days was also included for comparison. After 5 days, surface staining for CD56, CD3 and CD16 was analysed by flow cytometry. Shown above are lymphocyte CD3/CD56 dot plots for each sample, with back gating of the CD56dim CD16+ NK population (dark blue) and the CD56bright CD16- NK population (orange).

To test whether reovirus pre-treatment affects IL-15 signalling, intracellular staining of phosphorylated proteins was utilised. PBMC were pre-treated with reovirus for 48 hours, enough time for IFN-I to accumulate in the media and IFN-I mediated changes to take place. After 48 hours, PBMC were then stimulated with IL-15 for 30 minutes, to enable optimum detection of rapid phosphorylation events. IL-15 is known to activate several different signalling pathways, including JAK/STAT pathways as well as mTOR and PI3K-Akt signalling (section 1.1.7). Therefore, a range of molecules were tested for phosphorylation: STAT1 and STAT5 tyrosine phosphorylation (as in chapter 3), serine phosphorylation of mTOR (as a marker of mTOR activity), and serine phosphorylation of Akt, which is downstream of PI3K activation. Levels of phosphorylation were quantified by reporting the median fluorescence intensity (MFI) of NK cells within PBMC, both in unstimulated and IL-15 stimulated cells (Figure 5.10). STAT1 phosphorylation was induced by reovirus pre-treatment, as reported in chapter 3. STAT1 phosphorylation in reovirus treated cells was enhanced following IL-15 stimulation, whereas STAT1 activation in non-virus treated cells did not change. This was clearest at 10 ng/ml of IL-15, where there was a statistically significant difference between non-primed and reovirus primed pSTAT1 levels. STAT1 is not typically phosphorylated downstream of IL-15 (as demonstrated in chapter 3, Figure 3.7), but high levels of STAT1 present in reovirus treated cells (the transcriptome profile showed a 17.36 fold upregulation of STAT1 transcripts in reovirus Vs untreated NK cells), could increase the probability of STAT1 phosphorylation. STAT5 phosphorylation was induced by IL-15, consistent with previous experiments (Figure 3.7), but STAT5 phosphorylation levels did not significantly differ between non-primed and reovirus primed NK cells. mTOR phosphorylation was also induced by IL-15, but similarly did not change between non-primed and reovirus primed cells. In contrast, reovirus pre-treatment had a statistically significant effect on Akt phosphorylation. In PBMC stimulated with IL-15, reovirus primed NK cells contained lower levels of phosphorylated Akt than non-virus primed cells. Without addition of IL-15, levels of phosphorylated Akt were similar between non-primed and virus primed NK cells. These results suggest that reovirus treatment promotes changes in NK cells that selectively interfere with Akt signalling but not STAT5 signalling, downstream of IL-15. This could contribute to the inhibition of proliferation observed in reovirus treated cells.
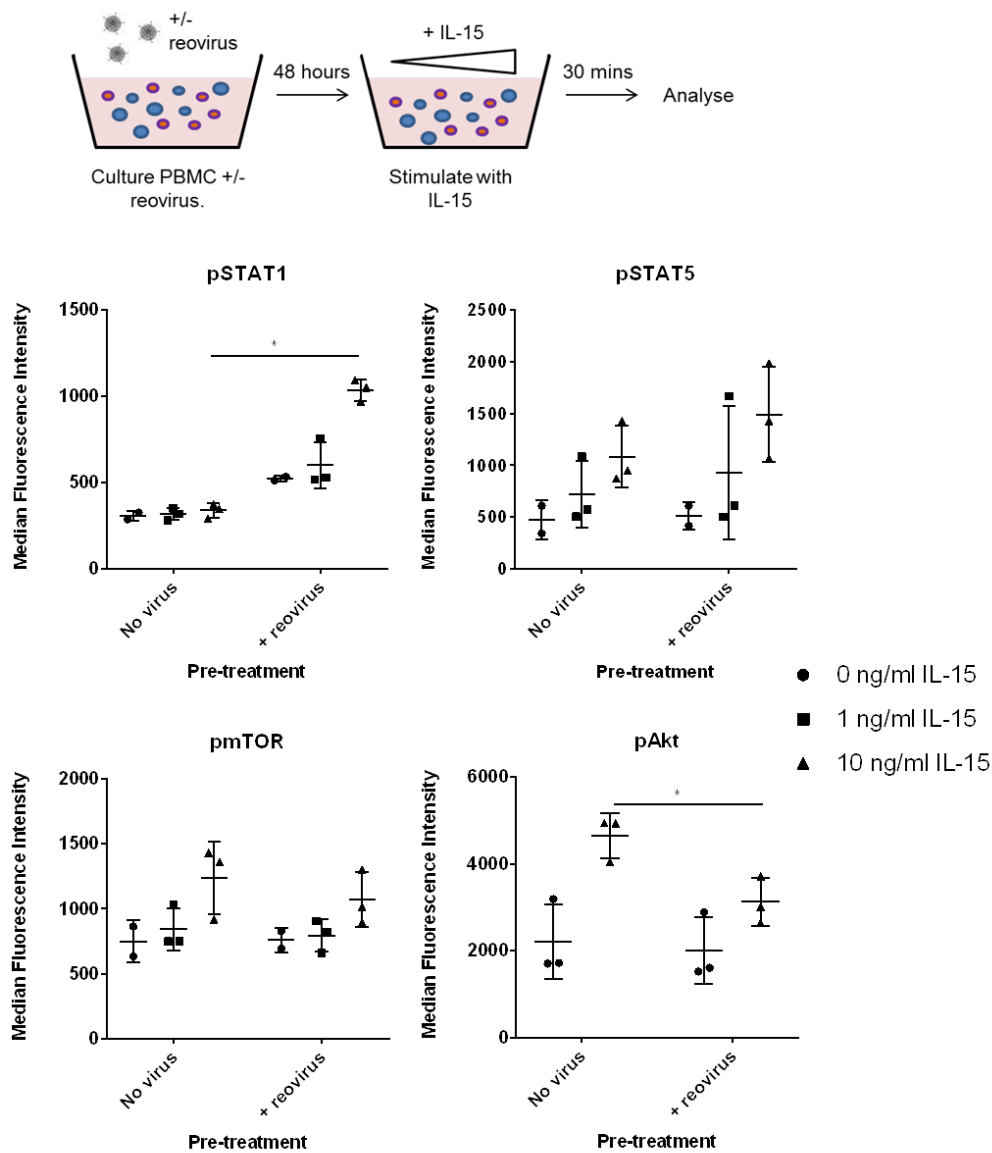
Figure 5.10 Phosphorylation of signalling proteins in response to IL-15, following priming with reovirus

PBMC were cultured for 48 hours alone (no virus) or primed with reovirus at an MOI of 1 (+ reovirus). After 48 hours, 10 ng/ml IL-15 was added directly to all samples for 30 minutes. NK cells within PBMC were evaluated for levels of phosphorylated STAT1, STAT3, STAT5, mTOR and Akt by intracellular flow cytometry. Graphs show median fluorescence intensities for 2 or 3 separate donors. The effect of IL-15 concentration and effect of virus on MFI were tested by 2 way repeated measures ANOVA. When the effect of virus was statistically significant, post hoc Sidak multiple comparison test was applied, to identify statistically significant differences between "no virus" and "reovirus" MFI values.

148

To further investigate the mechanisms of proliferation inhibition, the expression of cell cycle associated proteins was tested in PBMC cultured with or without virus, followed by IL-15 stimulation. The aim was to test whether reovirus pre-treatment inhibited the upregulation of any of these proteins by IL-15. PCNA and Ki67 expression was measured by intracellular flow cytometry, gating on CD56^{dim} and CD56^{bright} NK cells within PBMC (Figure 5.11). Reovirus pre-treatment inhibited the expression of both PCNA and Ki67 in response to IL-15. Inhibition of PCNA expression was evident in both NK cell subsets, but Ki67 inhibition was clearest in the CD56^{bright} subset. Protein expression of MCM4, Cyclin B and CDK2 was measured by Western Blot, using lysates from total NK cells isolated from PBMC. A similar result was observed; reovirus primed cells contained lower levels of all three proteins than non virus primed cells. Therefore, reovirus treatment prevented the accumulation of cell cycle associated proteins triggered by IL-15 stimulation. This finding appears to contradict the results of transcriptome profiling, which showed that reovirus treatment increased the transcript expression of Ki67, PCNA, MCM4, CDK2 and Cyclin B (appendix 1 and chapter 4, Figure 4.11). A possible explanation could be that reovirus triggers the activation of two pathways: one that promotes proliferation, and the other inhibiting proliferation through the release of IFN-I. The first pathway may trigger the upregulation of cell cycle transcripts, while IFN-I released into the media would act to repress transcription of these genes. In this hypothetical situation, it is unlikely that all cell cycle gene expression would be repressed by IFN-I, resulting in an apparent upregulation of these transcripts in reovirus treated NK cells.
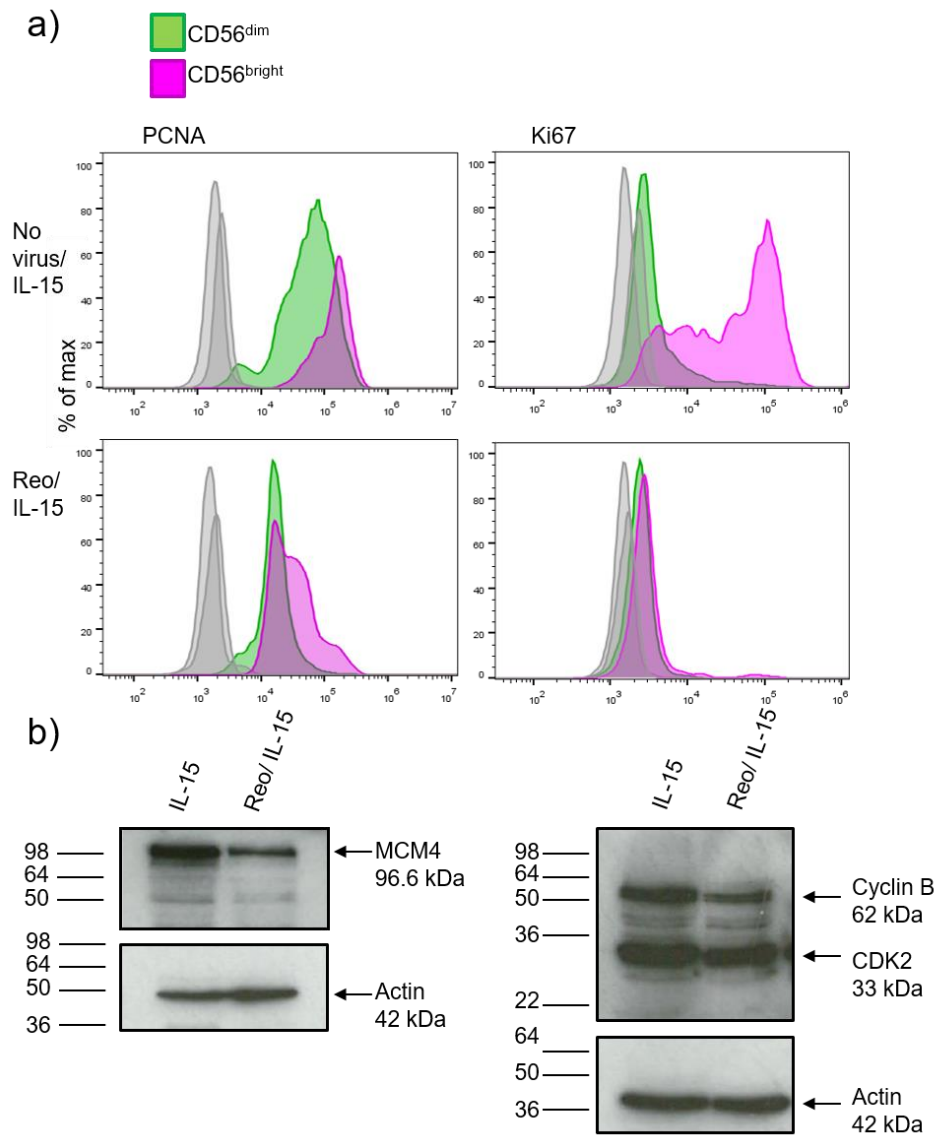
Figure 5.11 Expression of cell cycle associated proteins in IL-15 treated NK cells, following priming with reovirus

PBMC were cultured for 4 hours alone (no virus) or primed with reovirus at an MOI of 1 (Reo). 10 ng/ml IL-15 was then added directly to all samples for 48 hours (a) or 3 days (b). a) NK cells within PBMC were assessed for levels of PCNA and Ki67 by intracellular flow cytometry. Green=CD56^{dim} NK cells. Purple=CD56^{bright} NK cells. b) Expression of MCM4, Cyclin B and CDK2 was assessed by Western Blot, after isolation of total NK cells from PBMC by magnetic labelling.

5.2.5 Proliferation of NK cells from patients with an IFN-I driven disease

The evidence shown above suggests that IFN-I, released by PBMC exposed to reovirus, is a potent inhibitor of NK cell proliferation in culture. However, the *in vivo* effects of IFN-I on peripheral NK cell proliferation are not clear. It was hoped that blood samples from cancer patients receiving reovirus as part of a clinical trial might be used to address the effects of reovirus on human NK cell proliferation in vivo. However, suitable samples were not forthcoming during this work and an alternative approach was attempted. Systemic lupus erythematosus (SLE) is an autoimmune disease associated with high IFN-I activity (Kaul et al., 2016). Upregulation of an IFN-I signature in the blood during SLE has been widely reported (Baechler et al., 2003; Bennett et al., 2003; Crow et al., 2003). I hypothesised that NK cell proliferation in response to IL-15 would be repressed in peripheral blood NK cells from patients with SLE, relative to healthy control NK cells, due to the activation of IFN-I signalling. To test this, PBMC isolated from patients with SLE (from blood donated at a local clinic) or healthy donors were stimulated *ex vivo* with IL-15. On the day of donation, phenotyping of PBMC populations was performed, to determine the proportions of NK cells and T cells, and to quantify expression of CD69 and the IFN-I inducible molecule Tetherin. Due to time constraints at the end of the project, I was only able to analyse 4 healthy donors and 4 patients with SLE. Gating of NK cells within PBMC on the day of donation is shown in Figure 5.12. Dead cell discrimination was included, but only for the last 5 of 8 donors. However, the viability of cells in the lymphocyte gate was consistently over 99%, so dead cells probably did not impact greatly on staining results. The proportion of NK cells and T cells within PBMC was not significantly different between healthy donors and patients with SLE (Figure 5.13). NK cell CD69 and Tetherin expression was also not significantly changed in patient blood, relative to healthy donors. However, there was a greater spread of Tetherin expression in NK cells from patients, consistent with SLE being a heterogeneous disease, with high IFN-I scores seen only in a subset of patients (Kirou et al., 2005).

Ex vivo proliferation of NK cells from patients and healthy donors was assessed by the CFSE dilution assay. PBMC isolated from blood donors was labelled with CFSE and split into two samples: one to be cultured alone, and the other to be cultured with IL-15. After

5 days, NK cells within PBMC were analysed by flow cytometry. Unlike previous experiments in the chapter, where the control (untreated) and treatment (reovirus) samples were matched, i.e. from the same pool of labelled PBMC, this time the control (healthy donors) and treatment (patients with SLE) were from separate samples. Each sample takes up slightly different concentrations of CFSE, so to avoid bias when setting the non dividing/dividing gate, Modfit software was used for analysis. Modfit fits peaks to the CFSE histograms and identifies generations of dividing cells, given the co-ordinates of the parent generation. Examples of Modfit analysis are shown in Figure 5.14 (top). A proliferation index value was calculated by the software, which measures how much the parent population has grown, taking into account the proportions of cells in each generation. Using this approach, a comparison of IL-15 stimulated PBMC from patients with SLE and healthy donors revealed no significant difference in proliferation index. It is possible that the high variability of responses might be linked to differences in disease severity or IFN score, however stratification of patients was not possible with such low numbers in this study. More samples would be required to explore this further.
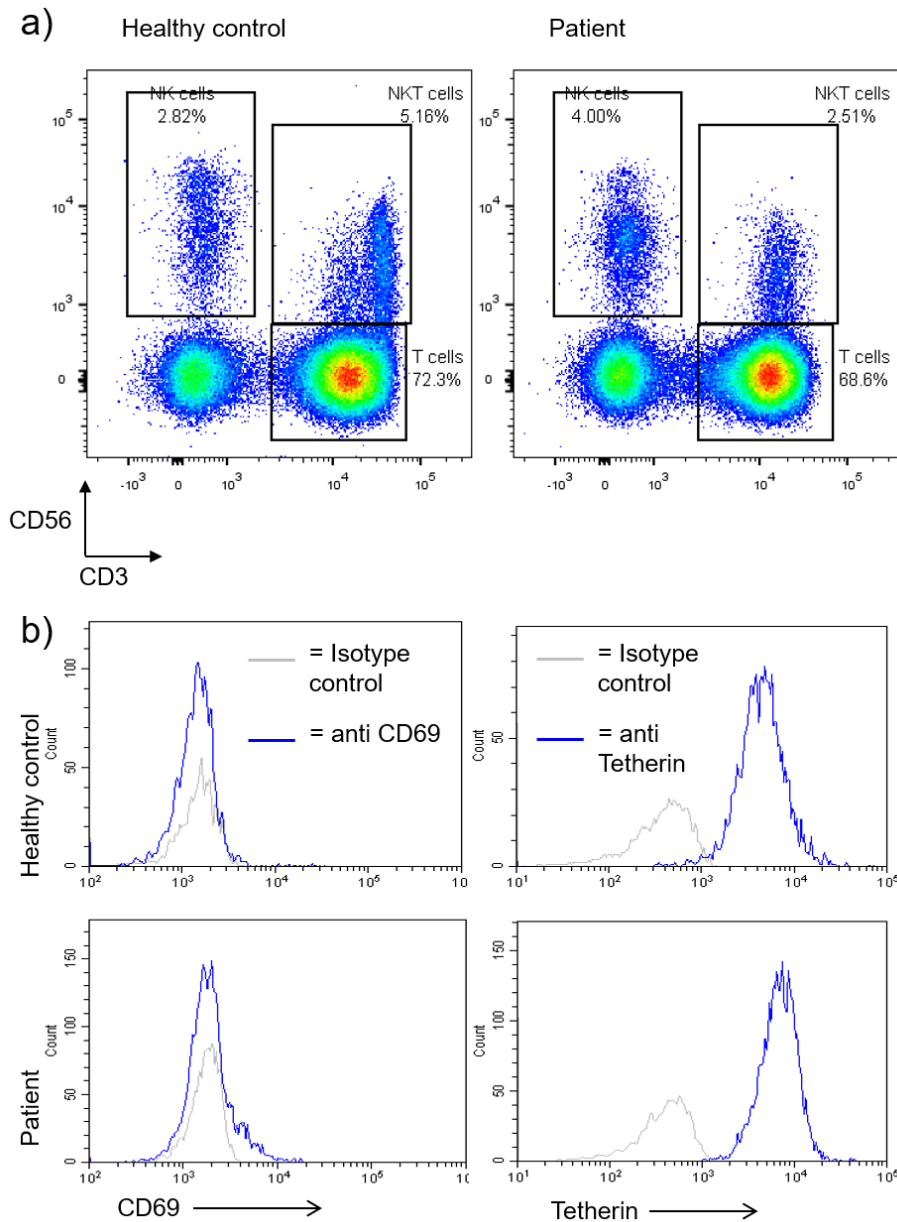
Figure 5.12 Flow cytometry analysis of PBMC from patients with SLE

PBMC were isolated from blood of healthy donors and patients with SLE, then surface stained with antibodies and analysed on the day of donation. a) Examples of lymphocyte subset staining. CD56 CD3 staining plots are shown for one healthy donor and onepatient, b) Examples of CD69 and Tetherin staining within NK cell gate.
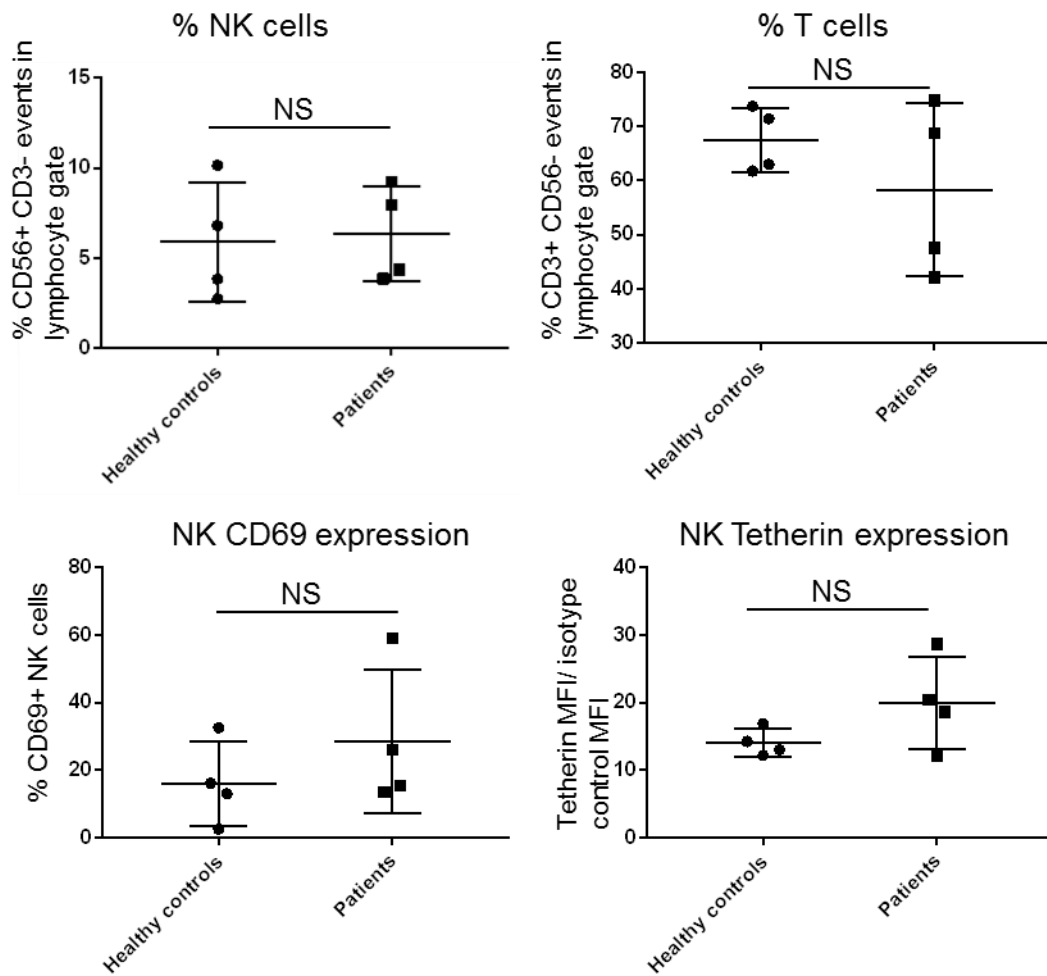
Figure 5.13 Phenotype of PBMC from patients with SLE

PBMC isolated from 4 healthy donors and 4 patients with SLE were surface stained and analysed by flow cytometry, on the day of donation. Samples were donated on 3 separate days. Top: proportions of NK cells (CD56+ CD3-) and T cells (CD3+ CD56-) within total lymphocytes. Bottom: CD69 and Tetherin expression on NK cells. Statistical differences between healthy controls and patients were tested by unpaired T test (NS = not significant).
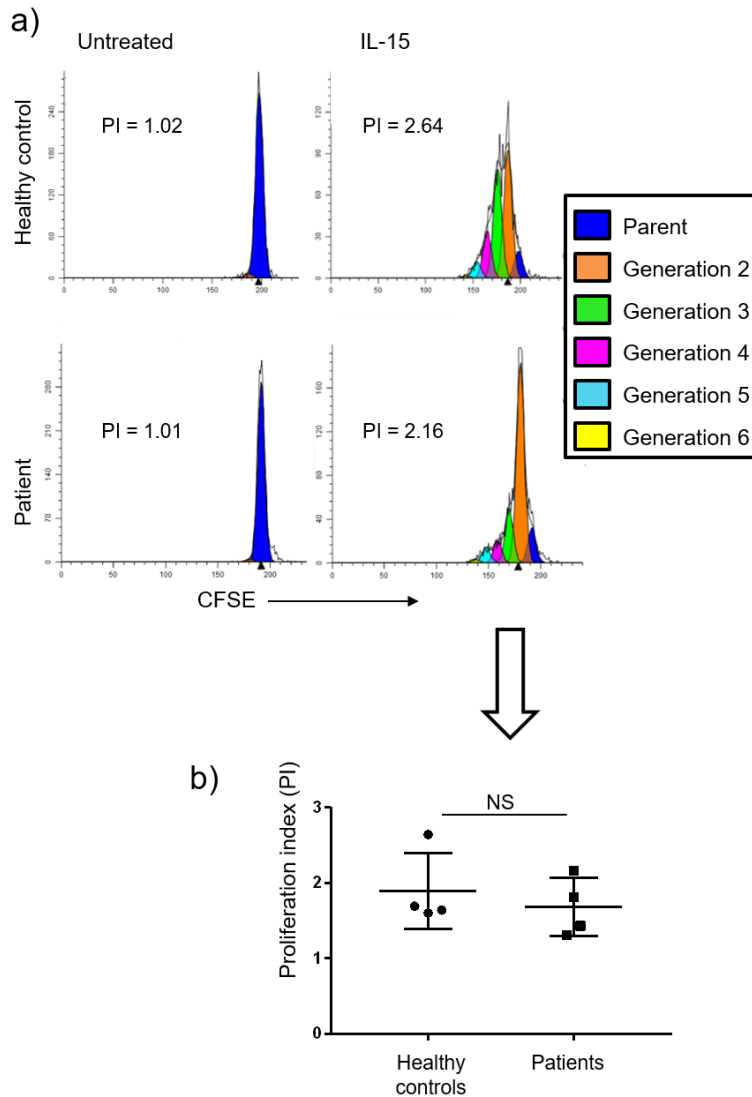
Figure 5.14 Proliferation of NK cells from patients with SLE

PBMC from healthy donors and patients with SLE were labelled with 0.2 µM CFSE, then cultured with or without 20 ng/ml IL-15. After 5 days, PBMC were stained with viability dye to exclude dead cells, and surface markers and dilution of CFSE were analysed by flow cytometry. a) CFSE plots for NK cells within PBMC were analysed using Modfit software, which estimated the proportion of events in each generation and calculated a proliferation index (PI). The parent generation peak was reset for each donor, using CFSE plots from untreated cells. b) Proliferation index values for NK cells within IL-15 stimulated PBMC. Statistical differences between healthy controls and patients were tested by unpaired T test (NS = not significant).

5.2.6 Why does reovirus treatment upregulate cell cycle machinery?

Pathway enrichment analysis and validation experiments suggested that reovirus treatment upregulated groups of cell cycle associated transcripts (chapter 4, section 4.2.5), however the results in this chapter show that reovirus treatment is actually inhibitory to NK cell proliferation. It was hypothesised that reovirus treatment activates a separate pro-proliferation pathway in NK cells (and that this pathway drives induction of the cell cycle genes), which is then opposed by the high levels of IFN-I in culture. The potential source of a pro-proliferation signal was unknown, but one possibility was that a soluble cytokine was responsible. Soluble cytokines released during reovirus treatment should be present in reovirus PBMC conditioned media. Therefore, the potential of reovirus induced cytokines to induce a pro-proliferation response was tested by culturing purified NK cells in conditioned media (filtered to remove virus), followed by analysis of MCM4 transcript expression. I tested conditioned media collected from PBMC at 24 hours and 48 hours of reovirus exposure, but neither appeared to upregulate MCM4 expression (Figure 5.15). This is in contrast to the effect of live reovirus on PBMC, which does upregulate NK cell MCM4 expression (Figure 4.11)

Alternatively, a cell to cell contact mechanism might be required for activation of the pro-proliferation signal. *Trans*-presentation of IL-15 is known to induce survival and proliferation of NK cells, and requires cell to cell contact (Dubois et al., 2002). Therefore I tested whether blocking IL-15 during reovirus treatment had any effect on the expression of cell cycle associated transcripts in NK cells. PBMC were cultured with or without reovirus, plus either anti-IL-15 blocking antibody, isotype control antibody, or nothing added. The IL-15 blocking antibody was separately validated by demonstrating inhibition of IL-15 stimulated CD69 expression in NK cells (data not shown). Reovirus treatment upregulated the expression of two cell cycle associated transcripts, CDK2 and CCNB1, consistent with what was shown previously in Figure 4.11. However, the addition of IL-15 blocking antibody did not inhibit these changes, in the one donor tested. These two experiments suggest that the pro-proliferation signal is probably not downstream of IL-15, or soluble factors present in reovirus conditioned media. This is consistent with the lack of STAT5 phosphorylation detected in chapter 3.
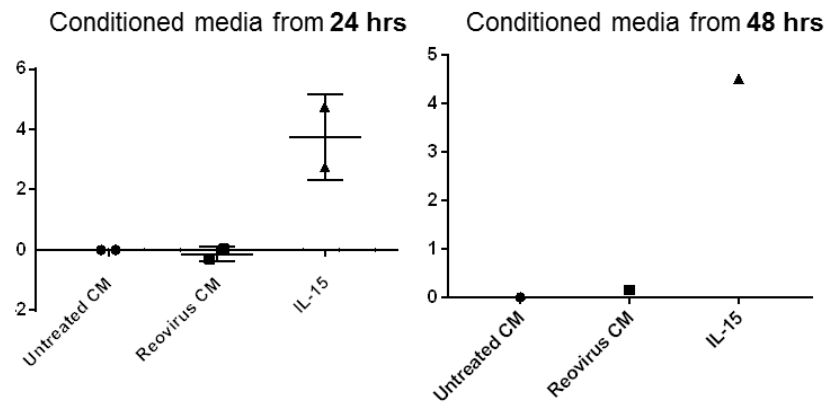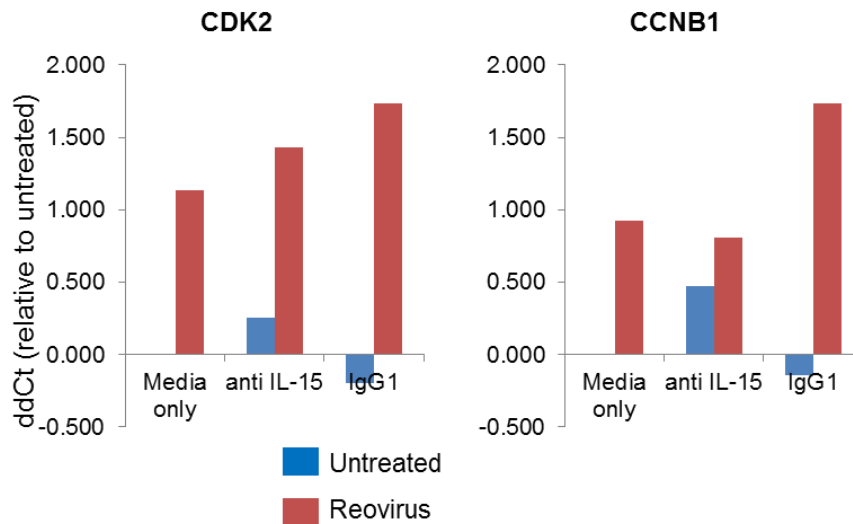
Figure 5.15 Potential mechanisms for cell cycle transcript upregulation induced by reovirus

mRNA transcript expression was measured by real time PCR and relative differences were calculated by the ddCt method, normalising to ABL1 expression. Shown above are the ddCt values, relative to the untreated sample in each case. **a)** MCM4 transcript expression in purified NK cells, cultured in either conditioned media from untreated PBMC (untreated CM) or Viresolve filtered conditioned media from reovirus treated PBMC (Reovirus CM). NK cells were cultured for 48 hours. **b)** Effect of IL-15 neutralisation on the upregulation of CDK2 and CCNB1 (Cyclin B) transcript expression. PBMC were cultured with or without reovirus, plus the addition of IL-15 blocking antibody or a matched isotype control. PBMC were cultured for 48 hours, then NK cells were isolated by magnetic labelling, for transcript analysis.

5.3 Discussion

Understanding the role of the innate immune system in the host response to oncolytic viruses (OVs) is important for the development of improved therapeutic regimes using these agents. However, the majority of studies on NK cell responses to OVs have focused on their cytotoxic capability, and have not explored other aspects of NK cell biology. Expansion of NK cell numbers during therapy could be a great advantage. In the previous chapter, I showed that reovirus upregulated transcripts associated with cell cycle progression in NK cells, which prompted an investigation into NK cell proliferation during virus treatment.

Despite the upregulation of these transcripts, reovirus treatment did not trigger *in vitro* proliferation of NK cells, measured by dilution of CFSE. When combined with a second stimulus, IL-15, reovirus clearly inhibited NK cell proliferation, rather than enhancing it. Further experiments confirmed that IFN-I was responsible for the inhibition of proliferation. In the literature, IFN is known to exert anti-proliferative responses in many cell types, particularly transformed cells (Sangfelt et al., 2000). In most of these cases, IFN has been found to induce G1 phase arrest (Sangfelt et al., 1999; Erickson et al., 1999). Consistent with this, I showed in this chapter that reovirus treatment, through IFN-I, blocked NK cell progression into S phase when stimulated with IL-15. Suggested mechanisms for G1 arrest in cell lines stimulated with IFN include the upregulation of CDK inhibitor molecules including the CIP/KIP proteins and the INK4 proteins (Sangfelt et al., 2000). In particular, p21 is thought to be transcriptionally upregulated by IFN, shown in multiple cell lines (Sangfelt et al., 1997; Xaus et al., 1999). However, when I searched the reovirus NK transcriptome dataset, I did not find any significant changes in expression of a range of CIP/KIP and INK4 transcripts. A more detailed examination of transcript levels, at different time-points after reovirus addition, would be required to rule out transcriptional regulation of CDK inhibitors as a potential mechanism. Additionally, some more widely recognised interferon stimulated genes such as IFIT1 have been implicated in cell cycle arrest (Niu et al., 2016). IFIT1 was highly upregulated by reovirus treatment in NK cells, according to transcriptome profiling (93 fold upregulated, FDR p value = 0.005).

Interestingly, reovirus induced IFN-I had wider effects on NK cells, other than inhibition of proliferation. IL-15 stimulated NK cells upregulate CD56 on their surface (Van Acker et al., 2017) (Figure 5.9), but pre-treatment with reovirus attenuated this effect in an IFN-I dependent manner. This suggested that IFN-I could inhibit additional NK cell activatory pathways, separate to proliferation. A possible explanation could be that reovirus treated cells have attenuated responses to IL-15, due to altered signalling pathway activation. Two studies, one based on NK cells and one on T cells, were the first to show that IFN-α inhibited the proliferative effect of IL-2 (Jewett and Bonavida, 1995; Erickson et al., 1999), a cytokine with similar downstream signalling to IL-15. The T cell study also demonstrated that IFN-I blocked the accumulation of proteins required for cell cycle progression, similar to my results following reovirus treatment. These findings are consistent with an early inhibition of proliferation, potentially an inhibition of IL-2 signalling. To test whether reovirus treatment affected signalling downstream of IL-15, a panel of signalling molecules were examined for phosphorylation events associated with their activation. STAT5 phosphorylation was not significantly changed by reovirus pre-treatment, but interestingly, STAT1 phosphorylation downstream of IL-15 was significantly enhanced. In non-virus primed cells, IL-15 primarily activates STAT5 with very little STAT1 activation (chapter 3 and 5). However in virus primed cells, IL-15 appeared to enhance STAT1 activation as well as STAT5. This may be due to highly upregulated expression of total STAT1 protein during reovirus treatment (transcriptome profiling revealed 17.36 upregulation of STAT1 transcripts, FDR p value = 0.004). The balance of different STAT proteins inside the cell influences which signalling pathways become activated. For example, murine NK cells are basally high in STAT4, so initially during LCMV infection there is a strong STAT4 signal, leading to production of IFN-γ. However as more IFN-I is produced in response to virus, STAT1 levels rise leading to higher activation of STAT1 through IFN and lower activation of STAT4 (Miyagi et al., 2007). Importantly, this mechanism confines the production of IFN-γ to early in the infection. Similarly, rising levels of STAT1 protein during virus treatment may increase the probability of IL-15 signalling through STAT1.

My results on STAT5 phosphorylation are in agreement with previous studies on the effects of IFN-I: one showed that IFN-I treatment does not affect IL-7 induced STAT5 phosphorylation in T cells (Nguyen, T.P. et al., 2015) (IL-7 being another common γ chain

receptor cytokine like IL-15) and another reported that IFN-α priming triggers a modest increase in IL-15 induced STAT5 phosphorylation in NK and T cells (Hansen et al., 2011). Therefore the inhibitory effect of reovirus treatment on IL-15 induced proliferation (and the CD56 phenotype) cannot be explained by reduced STAT5 phosphorylation.

In contrast, I showed that reovirus exposure did affect NK cell Akt signalling downstream of IL-15. Expression of the IL-15 receptor was not measured, but since STAT5 phosphorylation was unaffected, it was unlikely that receptor expression would have been downregulated. In fact, analysis of the transcriptome data revealed that IL15RA – the transcript encoding the α subunit – was upregulated 4.97 fold (FDR p value = 0.014). Therefore, viral treatment selectively interfered with the Akt pathway, which has not been previously reported in NK cells. In human T cells, Nguyen et al. recently showed that IFN-α selectively inhibited Akt phosphorylation, but not STAT5 phosphorylation, in response to IL-7 or IL-2 (Nguyen, T.P. et al., 2015). They also found that IFN-α inhibited the proliferative response to both cytokines. Recently, there has been much focus on the importance of PI3K-Akt-mTOR signalling in NK cells. Experiments using inhibitors to either STAT5 or PI3K showed that IL-15 could not induce proliferation in NK cells if either of these pathways was blocked (Nandagopal et al., 2014). Therefore, the selective inhibition of Akt signalling in reovirus primed NK cells is probably at least partly responsible for the inhibition of proliferation, and potentially the inhibition of other activatory pathways. Akt signalling is also induced by other pro-proliferative cytokines, such as IL-12 (Yoo et al., 2002), which could explain why IL-12 induced proliferation was also inhibited by IFN-α (figure 5.6 and 5.7). Furthermore, these results show that reovirus priming changes the balance of signalling pathways activated by IL-15. The enhanced activation of STAT1 in response to IL-15 may contribute to enhanced cytotoxicity of reovirus primed NK cells, as NK cell intrinsic STAT1 can promote cytotoxic function during viral infection (Nguyen, K.B. et al., 2002a; Fortin et al., 2013). A previous study investigated the effect of IFN-I priming on NK cell responses to IL-15 (Hansen et al., 2011); they showed that IFN-I primed NK cells had enhanced cytotoxicity towards target cells following stimulation with IL-15. However they did not measure IL-15 induced proliferation, which would probably have been inhibited by IFN-α priming.

Although IFN-I inhibits growth in many cell lines, and NK cells in the model described here, in certain cases IFN-I can actually promote immune cell proliferation. In some cases, this can be explained by indirect effects of IFN, such as the enhancement of IL-15 *trans*-presentation by DCs, induced by IFN-I (Lucas et al., 2007). On the other hand, IFN-I can also act directly, and has an important role in the activation of T cells. Using IFN-I receptor knockout T cells, Curtsinger et al. showed that IFN acts directly on naive CD8 T cells to enhance clonal expansion (Curtsinger et al., 2005). IFN provided a third signal, after TCR stimulation and CD28 co-stimulation, to enhance expansion. Why does IFN act so differently in this situation? Importantly, the enhancing effect on expansion was mediated by STAT4 (Curtsinger et al., 2005), and STAT4 signalling promotes survival and effector differentiation pathways in T cells (Crouse et al., 2015). STAT1 signalling, on the other hand, is inhibitory to lymphocyte proliferation (Lee et al., 2000). It has since been proposed that TCR activation leads to a modulation of STAT signalling, so the IFN-I signal is directed through STAT4 rather than STAT1. Evidence for this includes the specific downregulation of STAT1 in antigen specific proliferating CD8 T cells during LCMV infection (Gil et al., 2006), and a loss of STAT1 phosphorylation in superantigen (bacterial derived antigen capable of activating up to 20% of T-cells through the TCR) activated T cells (Van de Wiele et al., 2004). This seems to be a mechanism specific to TCR activation, to allow rapid clonal expansion. Consistent with this, a recent study showed that IFN-α treatment enhanced the proliferation of superantigen activated T cells, but inhibited the proliferation of cytokine induced proliferation (Cha et al., 2014). The results in this chapter and chapter 3 showed that STAT1 signalling in NK cells was highly activated and sustained, while STAT4 phosphorylation was only transient. High levels of STAT1 phosphorylation in reovirus treated NK cells may stimulate cytotoxicity pathways, but also act to inhibit proliferation. Further experiments to inhibit STAT1 in this model could be performed, to confirm the anti-proliferative mechanism.

Ideally, the next step in the investigation would have been to measure NK cell proliferation in patients receiving reovirus therapy. Unfortunately, there were no suitable trials with patients recruited at the time. I attempted to measure NK cell proliferation from the peripheral blood of systemic lupus erythematosus (SLE) patients instead, to test the effects of high IFN-I *in vivo.* In patients with SLE, it is thought that IFN-I levels (or responsiveness to IFN-I) is chronically high, whereas during a reovirus therapy trial, IFN

response peaked and fell (El-Sherbiny et al., 2015). Although there was a slight trend towards lower proliferation in of NK cells from patients with SLE, there were no statistically significant differences. SLE is a heterogeneous disease, with some patients experiencing flares or more severe symptoms than others (Kaul et al., 2016), so many more samples would be required to make any real conclusions.

It was hypothesised that NK cells receive opposing signals during reovirus treatment: one signal to promote proliferation and a separate signal to inhibit proliferation, through IFN-I/STAT1. This could explain why reovirus treatment upregulated so many cell cycle associated transcripts, but also inhibited proliferation. When PBMC were treated with reovirus, a wide range of changes were induced in NK cells, including CD69 upregulation, IFN induced genes - including Tetherin expression - and cell cycle associated transcripts were upregulated (chapters 3 and 4). Conditioned media treatment of purified NK cells induced similar changes in CD69 and tetherin (chapter 3). However, conditioned media did not upregulate MCM4, used as a marker for cell cycle associated transcripts. This could be because CD69 and tetherin upregulation is activated by soluble factors including IFN-I, whereas cell cycle transcripts are upregulated by a separate pathway. This would make sense, as IFN present in conditioned media actually inhibited proliferation (Figure 5.5). It is unclear what the mechanism responsible for proliferative transcript upregulation is. Good candidates would be IL-2 and IL-15, which are potent inducers of NK cell proliferation. However neutralisation of IL-15 during reovirus treatment had no effect, and conditioned media – which should contain IL-2 if it were secreted by PBMC – also failed to upregulate proliferative transcripts. Additionally, STAT5 phosphorylation was not detected in this model (chapter 3), which would be expected downstream of either IL-2 or IL-15. A recent paper identified a cell contact mechanism inducing NK cell proliferation in HCV, which required OX40L expression on monocytes (Pollmann et al., 2017). Another possibility could be the direct activation of NK cell receptors by reovirus proteins, leading to proliferation. Conditioned media was filtered to remove virus particles, so direct effects of reovirus would not have been detected.

Interestingly, expansion of NK cells was detected during a clinical trial of reovirus therapy (El-Sherbiny et al., 2015), but it was unclear whether this was the result of proliferation.

The expansion happened later on in the trial, between 6 and 28 days after the first virus infusion, and some time after the peak of IFN responsiveness. It is possible that NK cell proliferation was delayed due to high levels of IFN early during treatment. Further study would be required to test this hypothesis, ideally tracking NK cell proliferation during another reovirus trial.

Chapter 6. Conclusions

In this study, I investigated the effects of the oncolytic virus (OV) reovirus on human NK cells, using an *in vitro* model. In chapter 3, I showed that, within PBMC, NK cells were activated by reovirus in a directly type I interferon (IFN-I) dependent manner. Activation of NK cells was assessed by analysing the activation marker CD69 on the cell surface; upregulated CD69 is predictive of increased NK cell cytotoxicity (Clausen et al., 2003). A directly IFN-I dependent mechanism was supported by blocking experiments, demonstrating that NK cells were activated by IFN-I present in reovirus conditioned media. Secondly, activation of both STAT1 and STAT4 was consistent with pathway activation downstream of the IFN-I receptor. Finally, gene expression profiling revealed dramatic upregulation of IFN induced genes (ISGs).

Gene expression profiling (described in chapter 4) revealed that, as well as ISGs and NK cytotoxicity associated genes, there were changes in additional NK cell functions and pathways. Non granule dependent killing strategies are likely important, especially involving the death ligand TRAIL, which was highly upregulated. Genes associated with lymph node homing and chemotaxis were significantly upregulated. However I was unable to detect the chemokine receptor CCR7 on cultured NK cells, so this could not be confirmed at the protein level. Further work to improve the detection of CCR7, and to assess NK cell chemotaxis, should be carried out to confirm the effects of reovirus treatment on NK cell migration. Increased NK cell migration to the lymph nodes during therapy, where NK cell derived IFN-γ can induce T helper cell polarisation, would likely enhance the adaptive immune response. Finally, gene expression profiling revealed the upregulation of many cell cycle associated genes, suggesting that reovirus treatment may also regulate NK cell proliferation.

Despite the upregulation of cell cycle associated transcripts, the total effect of reovirus on NK cell proliferation was actually inhibitory. The results presented in chapter 5 showed

that reovirus treatment inhibited NK cell proliferation, due to high levels of IFN-I released by virus treated PBMC. IFN-I acting through STAT1 is known to inhibit lymphocyte proliferation (Lee et al., 2000; Gil et al., 2006), but exactly how this is achieved is not well understood. I showed that pre-treatment of PBMC with reovirus selectively inhibited Akt phosphorylation downstream of IL-15, but not STAT5 phosphorylation. The inhibition of this pathway likely contributes to the inhibition of IL-15 induced proliferation in reovirus primed cells.

Together, these results show that reovirus treatment has the potential to enhance some NK cell functions while inhibiting others. High levels of IFN-I are released by reovirus treated PBMC, leading to the activation of IFN sensitive pathways, but may temporarily inhibit NK cell proliferation pathways. In Figure 6.1, the proposed model for reovirus induced NK cell activation is shown.
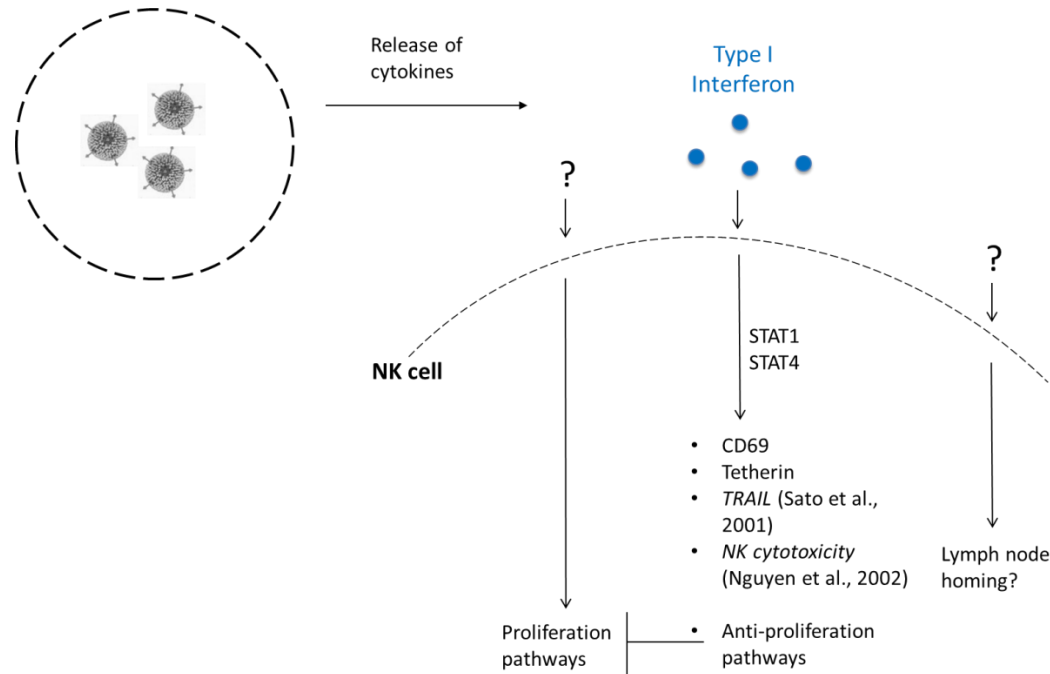
Figure 6.1 Proposed model of NK cell activation by reovirus

Detection of reovirus particles by PBMC triggers the release of cytokines, including IFN-I, which act on NK cells to induce functional changes. The diagram summarises the pathways activated within NK cells, supported by the results described in this thesis. Many functions were dependent on IFN-I in this study; for functions in italics IFN-I dependency has been shown by others. Other functions may be activated downstream of cytokines or other factors, marked as (?).

In vitro treatment of PBMC replicates many features of *in vivo* therapy. In patients treated with intravenous reovirus, a strong IFN-I response was observed within 24-48 hours, as well as CD69 and Tetherin upregulation on NK cells (El-Sherbiny et al., 2015). The same was observed within *in vitro* treated PBMC in this study. On the other hand, there are limitations of the *in vitro* model. In chapter 5, I showed that PBMC could not be cultured long term with reovirus, as it caused increased level of cell death relative to untreated cells. It is possible that, without the *in vivo* context of circulation and additional immune cell types, reovirus is capable of damaging PBMC, perhaps through overstimulation. Because a large proportion of the population has been already exposed to reovirus, neutralising antibodies present in the blood may also trigger the removal of virus particles.

In conclusion, in vitro culture of PBMC is a convenient model that accurately represents many aspects of *in vivo* therapy. Using this model, I was able to explore NK cell responses to reovirus in great detail. While previous studies have demonstrated that OVs activate NK cell granule dependent cytotoxicity, my results show that oncolytic reovirus acts on the spectrum of NK cell activity, with the potential to modulate TRAIL-mediated cytotoxicity, NK cell migration (potentially important in providing IFN-γ in lymph nodes for cytotoxic T cells), and to have effects on NK proliferation. Therefore, the results presented in this thesis add previously unknown detail to current models of reovirus therapy. Future directions could include studying samples from current clinical trials of reovirus, to confirm the findings discussed here. An important next step could be to compare the mechanisms of NK cell activation and functional effects of reovirus with other OVs, and to determine how these pathways might be enhanced or inhibited by combination therapies.

References

Adair, R.A., Roulstone, V., Scott, K.J., Morgan, R., Nuovo, G.J., Fuller, M., Beirne, D., West, E.J., Jennings, V.A., Rose, A., Kyula, J., Fraser, S., Dave, R., Anthoney, D.A., Merrick, A., Prestwich, R., Aldouri, A., Donnelly, O., Pandha, H., Coffey, M., Selby, P., Vile, R., Toogood, G., Harrington, K. and Melcher, A.A. 2012. Cell Carriage, Delivery, and Selective Replication of an Oncolytic Virus in Tumor in Patients. *Science Translational Medicine.* **4**(138), p138ra177.

Alexopoulou, L., Holt, A.C., Medzhitov, R. and Flavell, R.A. 2001. Recognition of double-stranded RNA and activation of NF-kappa B by Toll-like receptor 3. *Nature.* **413**(6857), pp.732-738.

Allan, D.S.J., Cerdeira, A.S., Ranjan, A., Kirkham, C.L., Aguilar, O.A., Tanaka, M., Childs, R.W., Dunbar, C.E., Strominger, J.L., Kopcow, H.D. and Carlyle, J.R. 2017. Transcriptome analysis reveals similarities between human blood CD3(-) CD56(bright) cells and mouse CD127(+) innate lymphoid cells. *Scientific Reports.* **7**(1), pp.1-11.

Alter, G., Malenfant, J.M. and Altfeld, M. 2004. CD107a as a functional marker for the identification of natural killer cell activity. *J Immunol Methods.* **294**(1-2), pp.15-22.

Andersson, M., Paabo, S., Nilsson, T. and Peterson, P.A. 1985. Impaired Intracellular-Transport of Class-I Mhc Antigens as a Possible Means for Adenoviruses to Evade Immune Surveillance. *Cell.* **43**(1), pp.215-222.

Arbones, M.L., Ord, D.C., Ley, K., Ratech, H., Maynardcurry, C., Otten, G., Capon, D.J. and Tedder, T.F. 1994. Lymphocyte Homing and Leukocyte Rolling and Migration Are Impaired in L-Selectin-Deficient Mice. *Immunity.* **1**(4), pp.247-260.

Athie-Morales, V., Smits, H.H., Cantrell, D.A. and Hilkens, C.M.U. 2004. Sustained IL-12 signaling is required for Th1 development. *Journal of Immunology.* **172**(1), pp.61-69.

Au, G.G., Lincz, L.F., Enno, A. and Shafren, D.R. 2007. Oncolytic Coxsackievirus A21 as a novel therapy for multiple myeloma. *British Journal of Haematology.* **137**(2), pp.133-141.

Baechler, E.C., Batliwalla, F.M., Karypis, G., Gaffney, P.M., Ortmann, W.A., Espe, K.J., Shark, K.B., Grande, W.J., Hughes, K.M., Kapur, V., Gregersen, P.K. and Behrens, T.W. 2003. Interferon-inducible gene expression signature in peripheral blood cells of patients with severe lupus. *Proc Natl Acad Sci U S A.* **100**(5), pp.2610-2615.

Baekkevold, E.S., Yamanaka, T., Palframan, R.T., Carlsen, H.S., Reinholt, F.P., von Andrian, U.H., Brandtzaeg, P. and Haraldsen, G. 2001. The CCR7 ligand ELC (CCL19) is transcytosed in high endothelial venules and mediates T cell recruitment. *Journal of Experimental Medicine.* **193**(9), pp.1105-1111.

Bar-On, Y., Charpak-Amikam, Y., Glasner, A., Isaacson, B., Duev-Cohen, A., Tsukerman, P., Varvak, A., Mandelboim, M. and Mandelboim, O. 2017. NKp46

recognizes the sigma1 protein of reovirus: Implications for reovirus-based cancer therapy. *J Virol.* **91**(19), pp.e01045-01017.

Baranek, T., Manh, T.P., Alexandre, Y., Maqbool, M.A., Cabeza, J.Z., Tomasello, E., Crozat, K., Bessou, G., Zucchini, N., Robbins, S.H., Vivier, E., Kalinke, U., Ferrier, P. and Dalod, M. 2012. Differential responses of immune cells to type I interferon contribute to host resistance to viral infection. *Cell Host Microbe.* **12**(4), pp.571-584.

Barton, E.S., Forrest, J.C., Connolly, J.L., Chappell, J.D., Liu, Y., Schnell, F.J., Nusrat, A., Parkos, C.A. and Dermody, T.S. 2001. Junction adhesion molecule is a receptor for reovirus. *Cell.* **104**(3), pp.441-451.

Baume, D.M., Robertson, M.J., Levine, H., Manley, T.J., Schow, P.W. and Ritz, J. 1992. Differential Responses to Interleukin-2 Define Functionally Distinct Subsets of Human Natural-Killer-Cells. *European Journal of Immunology.* **22**(1), pp.1-6.

Bennett, L., Palucka, A.K., Arce, E., Cantrell, V., Borvak, J., Banchereau, J. and Pascual, V. 2003. Interferon and granulopoiesis signatures in systemic lupus erythematosus blood. *J Exp Med.* **197**(6), pp.711-723.

Berahovich, R.D., Lai, N.L., Wei, Z., Lanier, L.L. and Schall, T.J. 2006. Evidence for NK cell subsets based on chemokine receptor expression. *Journal of Immunology.* **177**(11), pp.7833-7840.

Billadeau, D.D., Upshaw, J.L., Schoon, R.A., Dick, C.J. and Leibson, P.J. 2003. NKG2D-DAP10 triggers human NK cell-mediated killing via a Syk-independent regulatory pathway. *Nat Immunol.* **4**(6), pp.557-564.

Binstadt, B.A., Brumbaugh, K.M., Dick, C.J., Scharenberg, A.M., Williams, B.L., Colonna, M., Lanier, L.L., Kinet, J.P., Abraham, R.T. and Leibson, P.J. 1996. Sequential involvement of Lck and SHP-1 with MHC-recognizing receptors on NK cells inhibits FcR-initiated tyrosine kinase activation. *Immunity.* **5**(6), pp.629-638.

Biron, C.A., Byron, K.S. and Sullivan, J.L. 1989. Severe Herpesvirus Infections in an Adolescent without Natural-Killer Cells. *New England Journal of Medicine.* **320**(26), pp.1731-1735.

Bischoff, J.R., Kim, D.H., Williams, A., Heise, C., Horn, S., Muna, M., Ng, L., Nye, J.A., SampsonJohannes, A., Fattaey, A. and McCormick, F. 1996. An adenovirus mutant that replicates selectively in p53-deficient human tumor cells. *Science.* **274**(5286), pp.373-376.

Bisset, L.R., Lung, T.L., Kaelin, M., Ludwig, E. and Dubs, R.W. 2004. Reference values for peripheral blood lymphocyte phenotypes applicable to the healthy adult population in Switzerland. *European Journal of Haematology.* **72**(3), pp.203-212.

Bjorkstrom, N.K., Lindgren, T., Stoltz, M., Fauriat, C., Braun, M., Evander, M., Michaelsson, J., Malmberg, K.J., Klingstrom, J., Ahlm, C. and Ljunggren, H.G. 2011.

Rapid expansion and long-term persistence of elevated NK cell numbers in humans infected with hantavirus. *Journal of Experimental Medicine.* **208**(1), pp.13-21.

Boehm, T. 2012. Evolution of vertebrate immunity. *Curr Biol.* **22**(17), pp.R722-732.

Bottino, C., Castriconi, R., Pende, D., Rivera, P., Nanni, M., Carnemolla, B., Cantoni, C., Grassi, J., Marcenaro, S., Reymond, N., Vitale, M., Moretta, L., Lopez, M. and Moretta, A. 2003. Identification of PVR (CD155) and nectin-2 (CD112) as cell surface ligands for the human DNAM-1 (CD226) activating molecule. *Journal of Experimental Medicine.* **198**(4), pp.557-567.

Braud, V.M., Allan, D.S., O'Callaghan, C.A., Soderstrom, K., D'Andrea, A., Ogg, G.S., Lazetic, S., Young, N.T., Bell, J.I., Phillips, J.H., Lanier, L.L. and McMichael, A.J. 1998. HLA-E binds to natural killer cell receptors CD94/NKG2A, B and C. *Nature.* **391**(6669), pp.795-799.

Braun, M., Bjorkstrom, N.K., Gupta, S., Sundstrom, K., Ahlm, C., Klingstrom, J. and Ljunggren, H.G. 2014. NK Cell Activation in Human Hantavirus Infection Explained by Virus-Induced IL-15/IL15R alpha Expression. *Plos Pathogens.* **10**(11), pe1004521.

Bryceson, Y.T., March, M.E., Ljunggren, H.G. and Long, E.O. 2006. Synergy among receptors on resting NK cells for the activation of natural cytotoxicity and cytokine secretion. *Blood.* **107**(1), pp.159-166.

Bukowski, J.F., Woda, B.A., Habu, S., Okumura, K. and Welsh, R.M. 1983. Natural killer cell depletion enhances virus synthesis and virus-induced hepatitis in vivo. *J Immunol.* **131**(3), pp.1531-1538.

Burkett, P.R., Koka, R., Chien, M., Chai, S., Boone, D.L. and Ma, A. 2004. Coordinate expression and trans presentation of interleukin (IL)-15R alpha and IL-15 supports natural killer cell and memory CD8(+) T cell homeostasis. *Journal of Experimental Medicine.* **200**(7), pp.825-834.

Caligiuri, M.A., Zmuidzinas, A., Manley, T.J., Levine, H., Smith, K.A. and Ritz, J. 1990. Functional Consequences of Interleukin-2 Receptor Expression on Resting Human-Lymphocytes - Identification of a Novel Natural-Killer-Cell Subset with High-Affinity Receptors. *Journal of Experimental Medicine.* **171**(5), pp.1509-1526.

Campbell, J.J., Qin, S.X., Unutmaz, D., Soler, D., Murphy, K.E., Hodge, M.R., Wu, L.J. and Butcher, E.C. 2001. Unique subpopulations of CD56(+) NK and NK-T peripheral blood lymphocytes identified by chemokine receptor expression repertoire. *Journal of Immunology.* **166**(11), pp.6477-6482.

Carretero, M., Palmieri, G., Llano, M., Tullio, V., Santoni, A., Geraghty, D.E. and Lopez-Botet, M. 1998. Specific engagement of the CD94/NKG2-A killer inhibitory receptor by the HLA-E class Ib molecule induces SHP-1 phosphatase recruitment to tyrosine-phosphorylated NKG2-A: evidence for receptor function in heterologous transfectants. *European Journal of Immunology.* **28**(4), pp.1280-1291.

Carson, W.E., Giri, J.G., Lindemann, M.J., Linett, M.L., Ahdieh, M., Paxton, R., Anderson, D., Eisenmann, J., Grabstein, K. and Caligiuri, M.A. 1994. Interleukin (Il)-15 Is a Novel Cytokine That Activates Human Natural-Killer-Cells Via Components of the Il-2 Receptor. *Journal of Experimental Medicine.* **180**(4), pp.1395-1403.

Castleton, A., Dey, A., Beaton, B., Patel, B., Aucher, A., Davis, D.M. and Fielding, A.K. 2014. Human mesenchymal stromal cells deliver systemic oncolytic measles virus to treat acute lymphoblastic leukemia in the presence of humoral immunity. *Blood.* **123**(9), pp.1327-1335.

Cha, L., de Jong, E., French, M.A. and Fernandez, S. 2014. IFN-alpha Exerts Opposing Effects on Activation-Induced and IL-7 Induced Proliferation of T Cells That May Impair Homeostatic Maintenance of CD4(+) T Cell Numbers in Treated HIV Infection. *Journal of Immunology.* **193**(5), pp.2178-2186.

Chan, A., Hong, D.L., Atzberger, A., Kollnberger, S., Filer, A.D., Buckley, C.D., McMichael, A., Enver, T. and Bowness, P. 2007. CD56(bright) human NK cells differentiate into CD56(dim) cells: Role of contact with peripheral fibroblasts. *Journal of Immunology.* **179**(1), pp.89-94.

Chen, H.M., Tanaka, N., Mitani, Y., Oda, E., Nozawa, H., Chen, J.Z., Yanai, H., Negishi, H., Choi, M.K., Iwasaki, T., Yamamoto, H., Taniguchi, T. and Takaoka, A. 2009. Critical role for constitutive type I interferon signaling in the prevention of cellular transformation. *Cancer Sci.* **100**(3), pp.449-456.

Cibrian, D. and Sanchez-Madrid, F. 2017. CD69: from activation marker to metabolic gatekeeper. *European Journal of Immunology.* **47**(6), pp.946-953.

Clausen, J., Vergeiner, B., Enk, M., Petzer, A.L., Gastl, G. and Gunsilius, E. 2003. Functional significance of the activation-associated receptors CD25 and CD69 on human NK-cells and NK-like T-cells. *Immunobiology.* **207**(2), pp.85-93.

Cooper, M.A., Fehniger, T.A. and Caligiuri, M.A. 2001. The biology of human natural killer-cell subsets. *Trends in Immunology.* **22**(11), pp.633-640.

Cortez, V.S. and Colonna, M. 2016. Diversity and function of group 1 innate lymphoid cells. *Immunology Letters.* **179**, pp.19-24.

Coughlan, L., Vallath, S., Saha, A., Flak, M., McNeish, I.A., Vassaux, G., Marshall, J.F., Hart, I.R. and Thomas, G.J. 2009. In Vivo Retargeting of Adenovirus Type 5 to alpha v beta 6 Integrin Results in Reduced Hepatotoxicity and Improved Tumor Uptake following Systemic Delivery. *Journal of Virology.* **83**(13), pp.6416-6428.

Crouse, J., Kalinke, U. and Oxenius, A. 2015. Regulation of antiviral T cell responses by type I interferons. *Nature Reviews Immunology.* **15**(4), pp.231-242.

Crow, M.K., Kirou, K.A. and Wohlgemuth, J. 2003. Microarray analysis of interferon-regulated genes in SLE. *Autoimmunity.* **36**(8), pp.481-490.

Curtsinger, J.M., Valenzuela, J.O., Agarwal, P., Lins, D. and Mescher, M.F. 2005. Cutting edge: Type IIFNs provide a third signal to CD8 T cells to stimulate clonal expansion and differentiation. *Journal of Immunology.* **174**(8), pp.4465-4469.

Cuylen, S., Blaukopf, C., Politi, A.Z., Muller-Reichert, T., Neumann, B., Poser, I., Ellenberg, J., Hyman, A.A. and Gerlich, D.W. 2016. Ki-67 acts as a biological surfactant to disperse mitotic chromosomes. *Nature.* **535**(7611), pp.308-+.

Daniels, R.A., Turley, H., Kimberley, F.C., Liu, X.S., Mongkolsapaya, J., Ch'en, P., Xu, X.N., Jin, B.Q., Pezzella, F. and Screaton, G.R. 2005. Expression of TRAIL and TRAIL receptors in normal and malignant tissues. *Cell Research.* **15**(6), pp.430-438.

Danthi, P., Holm, G.H., Stehle, T. and Dermody, T.S. 2013. Reovirus Receptors, Cell Entry, and Proapoptotic Signaling. *Viral Entry into Host Cells.* **790**, pp.42-71.

de Andrade, L.F., Smyth, M.J. and Martinet, L. 2014. DNAM-1 control of natural killer cells functions through nectin and nectin-like proteins. *Immunology and Cell Biology.* **92**(3), pp.237-244.

Della Chiesa, M., Sivori, S., Carlomagno, S., Moretta, L. and Moretta, A. 2015. Activating KIRs and NKG2C in Viral Infections: Toward NK Cell Memory? *Front Immunol.* **6**, p573.

Der, S.D., Zhou, A., Williams, B.R. and Silverman, R.H. 1998. Identification of genes differentially regulated by interferon alpha, beta, or gamma using oligonucleotide arrays. *Proc Natl Acad Sci U S A.* **95**(26), pp.15623-15628.

Diaz, R.M., Galivo, F., Kottke, T., Wongthida, P., Qiao, J., Thompson, J., Valdes, M., Barber, G. and Vile, R.G. 2007. Oncolytic immunovirotherapy for melanoma using vesicular stomatitis virus. *Cancer Research.* **67**(6), pp.2840-2848.

Dokun, A.O., Kim, S., Smith, H.R.C., Kang, H.S.P., Chu, D.T. and Yokoyama, W.M. 2001. Specific and nonspecific NK cell activation during virus infection. *Nature Immunology.* **2**(10), pp.951-956.

Dubois, S., Mariner, J., Waldmann, T.A. and Tagaya, Y. 2002. IL-15R alpha recycles and presents IL-15 in trans to neighboring cells. *Immunity.* **17**(5), pp.537-547.

El-Sherbiny, Y.M., Holmes, T.D., Wetherill, L.F., Black, E.V., Wilson, E.B., Phillips, S.L., Scott, G.B., Adair, R.A., Dave, R., Scott, K.J., Morgan, R.S., Coffey, M., Toogood, G.J., Melcher, A.A. and Cook, G.P. 2015. Controlled infection with a therapeutic virus defines the activation kinetics of human natural killer cells in vivo. *Clin Exp Immunol.* **180**(1), pp.98-107.

Erickson, S., Sangfelt, O., Castro, J., Heyman, M., Einhorn, S. and Grander, D. 1999. Interferon-alpha inhibits proliferation in human T lymphocytes by abrogation of interleukin 2-induced changes in cell cycle-regulatory proteins. *Cell Growth & Differentiation.* **10**(8), pp.575-582.

Errington, F., Steele, L., Prestwich, R., Harrington, K.J., Pandha, H.S., Vidal, L., de Bono, J., Selby, P., Coffey, M., Vile, R. and Melcher, A. 2008. Reovirus activates human dendritic cells to promote innate antitumor immunity. *J Immunol.* **180**(9), pp.6018-6026.

Farag, S.S., Fehniger, T.A., Ruggeri, L., Velardi, A. and Caligiuri, M.A. 2002. Natural killer cell receptors: new biology and insights into the graft-versus-leukemia effect. *Blood.* **100**(6), pp.1935-1947.

Fehniger, T.A., Cooper, M.A., Nuovo, G.J., Cella, M., Facchetti, F., Colonna, M. and Caligiuri, M.A. 2003. CD56(bright) natural killer cells are present in human lymph nodes and are activated by T cell-derived IL-2: a potential new link between adaptive and innate immunity. *Blood.* **101**(8), pp.3052-3057.

Fenner, J.E., Starr, R., Cornish, A.L., Zhang, J.G., Metcalf, D., Schreiber, R.D., Sheehan, K., Hilton, D.J., Alexander, W.S. and Hertzog, P.J. 2006. Suppressor of cytokine signaling 1 regulates the immune response to infection by a unique inhibition of type I interferon activity. *Nature Immunology.* **7**(1), pp.33-39.

Fortin, C., Huang, X.P. and Yang, Y.P. 2013. Both NK Cell-Intrinsic and -Extrinsic STAT1 Signaling Are Required for NK Cell Response against Vaccinia Virus. *Journal of Immunology.* **191**(1), pp.363-368.

Frey, M., Packianathan, N.B., Fehniger, T.A., Ross, M.E., Wang, W.C., Stewart, C.C., Caligiuri, M.A. and Evans, S.S. 1998. Differential expression and function of L-selectin on CD56(bright) and CD56(dim) natural killer cell subsets. *Journal of Immunology.* **161**(1), pp.400-408.

Fueyo, J., Gomez-Manzano, C., Alemany, R., Lee, P.S.Y., McDonnell, T.J., Mitlianga, P., Shi, Y.X., Levin, V.A., Yung, W.K.A. and Kyritsis, A.P. 2000. A mutant oncolytic adenovirus targeting the Rb pathway produces anti-glioma effect in vivo. *Oncogene.* **19**(1), pp.2-12.

Geering, B., Stoeckle, C., Conus, S. and Simon, H.U. 2013. Living and dying for inflammation: neutrophils, eosinophils, basophils. *Trends Immunol.* **34**(8), pp.398-409.

Gidlund, M., Orn, A., Wigzell, H., Senik, A. and Gresser, I. 1978. Enhanced Nk Cell Activity in Mice Injected with Interferon and Interferon Inducers. *Nature.* **273**(5665), pp.759-761.

Gil, M.P., Salomon, R., Louten, J. and Biron, C.A. 2006. Modulation of STAT1 protein levels: a mechanism shaping CD8 T-cell responses in vivo. *Blood.* **107**(3), pp.987-993.

Gong, J., Sachdev, E., Mita, A.C. and Mita, M.M. 2016. Clinical development of reovirus for cancer therapy: An oncolytic virus with immune-mediated antitumor activity. *World J Methodol.* **6**(1), pp.25-42.

Goubau, D., Schlee, M., Deddouche, S., Pruijssers, A.J., Zillinger, T., Goldeck, M., Schuberth, C., Van der Veen, A.G., Fujimura, T., Rehwinkel, J., Iskarpatyoti, J.A., Barchet, W., Ludwig, J., Dermody, T.S., Hartmann, G. and Sousa, C.R.E. 2014. Antiviral

immunity via RIG-I-mediated recognition of RNA bearing 5 '-diphosphates. *Nature.* **514**(7522), pp.372-375.

Gregoire, C., Chasson, L., Luci, C., Tomasello, E., Geissmann, F., Vivier, E. and Walzer, T. 2007. The trafficking of natural killer cells. *Immunological Reviews.* **220**, pp.169-182.

Groh, V., Rhinehart, R., Secrist, H., Bauer, S., Grabstein, K.H. and Spies, T. 1999. Broad tumor-associated expression and recognition by tumor-derived gamma delta T cells of MICA and MICB. *Proceedings of the National Academy of Sciences of the United States of America.* **96**(12), pp.6879-6884.

Guermonprez, P., Valladeau, J., Zitvogel, L., Thery, C. and Amigorena, S. 2002. Antigen presentation and T cell stimulation by dendritic cells. *Annu Rev Immunol.* **20**, pp.621-667.

Guerra, N., Tan, Y.X., Joncker, N.T., Choy, A., Gallardo, F., Xiong, N., Knoblaugh, S., Cado, D., Greenberg, N.M. and Raulet, D.H. 2008. NKG2D-deficient mice are defective in tumor surveillance in models of spontaneous malignancy (vol 28, pg 571, 2008). *Immunity.* **28**(5), pp.723-723.

Guma, M., Budt, M., Saez, A., Brckalo, T., Hengel, H., Angulo, A. and Lopez-Botet, M. 2006. Expansion of CD94/NKG2C(+) NK cells in response to human cytomegalovirus-infected fibroblasts. *Blood.* **107**(9), pp.3624-3631.

Habu, S., Akamatsu, K., Tamaoki, N. and Okumura, K. 1984. In vivo significance of NK cell on resistance against virus (HSV-1) infections in mice. *J Immunol.* **133**(5), pp.2743-2747.

Hanahan, D. and Weinberg, R.A. 2011. Hallmarks of Cancer: The Next Generation. *Cell.* **144**(5), pp.646-674.

Hansen, M.L., Woetmann, A., Krejsgaard, T., Kopp, K.L.M., Sokilde, R., Litman, T., Straten, P.T., Geisler, C., Wasik, M.A., Odum, N. and Eriksen, K.W. 2011. IFN-alpha primes T- and NK-cells for IL-15-mediated signaling and cytotoxicity. *Molecular Immunology.* **48**(15-16), pp.2087-2093.

Hansmann, L., Groeger, S., von Wulffen, W., Bein, G. and Hackstein, H. 2008. Human monocytes represent a competitive source of interferon-alpha in peripheral blood. *Clin Immunol.* **127**(2), pp.252-264.

Hashiro, G., Loh, P.C. and Yau, J.T. 1977. Preferential Cytotoxicity of Reovirus for Certain Transformed-Cell Lines. *Archives of Virology.* **54**(4), pp.307-315.

Hecht, M.L., Rosental, B., Horlacher, T., Hershkovitz, O., De Paz, J.L., Noti, C., Schauer, S., Porgador, A. and Seeberger, P.H. 2009. Natural cytotoxicity receptors NKp30, NKp44 and NKp46 bind to different heparan sulfate/heparin sequences. *J Proteome Res.* **8**(2), pp.712-720.

Heim, M.H. 2012. Interferons and hepatitis C virus. *Swiss Medical Weekly.* **142**, pw13586.

Heinemann, L., Simpson, G.R., Annels, N.E., Vile, R., Melcher, A., Prestwich, R., Harrington, K.J. and Pandha, H.S. 2010. The Effect of Cell Cycle Synchronization on Tumor Sensitivity to Reovirus Oncolysis. *Molecular Therapy.* **18**(12), pp.2085-2093.

Heusel, J.W., Wesselschmidt, R.L., Shresta, S., Russell, J.H. and Ley, T.J. 1994. Cytotoxic lymphocytes require granzyme B for the rapid induction of DNA fragmentation and apoptosis in allogeneic target cells. *Cell.* **76**(6), pp.977-987.

Hokeness, K.L., Kuziel, W.A., Biron, C.A. and Salazar-Mather, T.P. 2005. Monocyte chemoattractant protein-1 and CCR2 interactions are required for IFN-alpha/beta-induced inflammatory responses and antiviral defense in liver. *Journal of Immunology.* **174**(3), pp.1549-1556.

Holmes, T.D., El-Sherbiny, Y.M., Davison, A., Clough, S.L., Blair, G.E. and Cook, G.P. 2011. A human NK cell activation/inhibition threshold allows small changes in the target cell surface phenotype to dramatically alter susceptibility to NK cells. *J Immunol.* **186**(3), pp.1538-1545.

Honda, K., Takaoka, A. and Taniguchi, T. 2006. Type I inteferon gene induction by the interferon regulatory factor family of transcription factors. *Immunity.* **25**(3), pp.349-360.

Horowitz, A., Behrens, R.H., Okell, L., Fooks, A.R. and Riley, E.M. 2010. NK Cells as Effectors of Acquired Immune Responses: Effector CD4(+) T Cell-Dependent Activation of NK Cells Following Vaccination. *Journal of Immunology.* **185**(5), pp.2808-2818.

Hozumi, N. and Tonegawa, S. 1976. Evidence for somatic rearrangement of immunoglobulin genes coding for variable and constant regions. *Proc Natl Acad Sci U S A.* **73**(10), pp.3628-3632.

Huntington, N.D., Legrand, N., Alves, N.L., Jaron, B., Weijer, K., Plet, A., Corcuff, E., Mortier, E., Jacques, Y., Spits, H. and Di Santo, J.P. 2009. IL-15 trans-presentation promotes human NK cell development and differentiation in vivo. *J Exp Med.* **206**(1), pp.25-34.

Imai, K., Matsuyama, S., Miyake, S., Suga, K. and Nakachi, K. 2000. Natural cytotoxic activity of peripheral-blood lymphocytes and cancer incidence: an 11-year follow-up study of a general population. *Lancet.* **356**(9244), pp.1795-1799.

Izaguirre, A., Barnes, B.J., Amrute, S., Yeow, W.S., Megjugorac, N., Dai, J., Feng, D., Chung, E., Pitha, P.M. and Fitzgerald-Bocarsly, P. 2003. Comparative analysis of IRF and IFN-alpha expression in human plasmacytoid and monocyte-derived dendritic cells. *J Leukoc Biol.* **74**(6), pp.1125-1138.

Jacobs, R., Hintzen, G., Kemper, A., Beul, K., Kempf, S., Behrens, G., Sykora, K.W. and Schmidt, R.E. 2001. CD56(bright) cells differ in their KIR repertoire and cytotoxic features from CD56(dim) NK cells. *European Journal of Immunology.* **31**(10), pp.3121-3127.

Jewett, A. and Bonavida, B. 1995. Interferon-Alpha Activates Cytotoxic Function but Inhibits Interleukin-2 Mediated Proliferation and Tumor-Necrosis-Factor-Alpha Secretion by Immature Human Natural-Killer-Cells. *Journal of Clinical Immunology.* **15**(1), pp.35-44.

Kagi, D., Ledermann, B., Burki, K., Seiler, P., Odermatt, B., Olsen, K.J., Podack, E.R., Zinkernagel, R.M. and Hengartner, H. 1994. Cytotoxicity Mediated by T-Cells and Natural-Killer-Cells Is Greatly Impaired in Perforin Deficient Mice. *Nature.* **369**(6475), pp.31-37.

Kaul, A., Gordon, C., Crow, M.K., Touma, Z., Urowitz, M.B., van Vollenhoven, R., Ruiz-Irastorza, G. and Hughes, G. 2016. Systemic lupus erythematosus. *Nat Rev Dis Primers.* **2**, p16039.

Keating, S.E., Zaiatz-Bittencourt, V., Loftus, R.M., Keane, C., Brennan, K., Finlay, D.K. and Gardiner, C.M. 2016. Metabolic Reprogramming Supports IFN-gamma Production by CD56(bright) NK Cells. *Journal of Immunology.* **196**(6), pp.2552-2560.

Kelly, E. and Russell, S.J. 2007. History of oncolytic viruses: Genesis to genetic engineering. *Molecular Therapy.* **15**(4), pp.651-659.

Kiessling, R., Klein, E. and Wigzell, H. 1975. Natural Killer Cells in Mouse .1. Cytotoxic Cells with Specificity for Mouse Moloney Leukemia-Cells - Specificity and Distribution According to Genotype. *European Journal of Immunology.* **5**(2), pp.112-117.

Kim, K.H., Fisher, M.J., Xu, S.Q. and El-Deiry, W.S. 2000. Molecular determinants of response to TRAIL in killing of normal and cancer cells. *Clinical Cancer Research.* **6**(2), pp.335-346.

Kim, S., Iizuka, K., Aguila, H.L., Weissman, I.L. and Yokoyama, W.M. 2000. In vivo natural killer cell activities revealed by natural killer cell-deficient mice. *Proc Natl Acad Sci U S A.* **97**(6), pp.2731-2736.

Kirou, K.A., Lee, C., George, S., Louca, K., Peterson, M.G. and Crow, M.K. 2005. Activation of the interferon-alpha pathway identifies a subgroup of systemic lupus erythematosus patients with distinct serologic features and active disease. *Arthritis Rheum.* **52**(5), pp.1491-1503.

Kundig, T.M., Schorle, H., Bachmann, M.F., Hengartner, H., Zinkernagel, R.M. and Horak, I. 1993. Immune responses in interleukin-2-deficient mice. *Science.* **262**(5136), pp.1059-1061.

Kuruppu, D. and Tanabe, K.K. 2005. Viral oncolysis by herpes simplex virus and other viruses. *Cancer Biology & Therapy.* **4**(5), pp.524-531.

Landberg, G. and Roos, G. 1991. Antibodies to Proliferating Cell Nuclear Antigen as S-Phase Probes in Flow Cytometric Cell-Cycle Analysis. *Cancer Research.* **51**(17), pp.4570-4574.

Lanier, L.L. 2015. NKG2D Receptor and Its Ligands in Host Defense. *Cancer Immunology Research.* **3**(6), pp.575-582.

Larner, A.C., Chaudhuri, A. and Darnell, J.E. 1986. Transcriptional Induction by Interferon - New Protein(S) Determine the Extent and Length of the Induction. *Journal of Biological Chemistry.* **261**(1), pp.453-459.

Lau, A.S., Hannigan, G.E., Freedman, M.H. and Williams, B.R. 1986. Regulation of interferon receptor expression in human blood lymphocytes in vitro and during interferon therapy. *J Clin Invest.* **77**(5), pp.1632-1638.

Lauwerys, B.R., Hachulla, E., Spertini, F., Lazaro, E., Jorgensen, C., Mariette, X., Haelterman, E., Grouard-Vogel, G., Fanget, B., Dhellin, O., Vandepapeliere, P. and Houssiau, F.A. 2013. Down-regulation of interferon signature in systemic lupus erythematosus patients by active immunization with interferon alpha-kinoid. *Arthritis Rheum.* **65**(2), pp.447-456.

Lee, C.K., Smith, E., Gimeno, R., Gertner, R. and Levy, D.E. 2000. STAT1 affects lymphocyte survival and proliferation partially independent of its role downstream of IFN-gamma. *Journal of Immunology.* **164**(3), pp.1286-1292.

Lemke, J., von Karstedt, S., Zinngrebe, J. and Walczak, H. 2014. Getting TRAIL back on track for cancer therapy. *Cell Death and Differentiation.* **21**(9), pp.1350-1364.

Li, H., Dutuor, A., Tao, L., Fu, X.P. and Zhang, X.L. 2007. Virotherapy with a type 2 herpes simplex virus-derived oncolytic virus induces potent antitumor immunity against neuroblastoma. *Clinical Cancer Research.* **13**(1), pp.316-322.

Li, H.T., Dutuor, A., Fu, X.P. and Zhang, X.L. 2007. Induction of strong antitumor immunity by an HSV-2-based oncolytic virus in a murine mammary tumor model. *Journal of Gene Medicine.* **9**(3), pp.161-169.

Li, S., Zhu, M.Z., Pan, R.G., Fang, T., Cao, Y.Y., Chen, S.L., Zhao, X.L., Lei, C.Q., Guo, L., Chen, Y., Li, C.M., Jokitalo, E., Yin, Y.X., Shu, H.B. and Guo, D.Y. 2016. The tumor suppressor PTEN has a critical role in antiviral innate immunity. *Nature Immunology.* **17**(3), pp.241-249.

Liu, C.C., Jiang, S., Persechini, P.M., Zychlinsky, A., Kaufmann, Y. and Young, J.D. 1989. Resistance of cytolytic lymphocytes to perforin-mediated killing. Induction of resistance correlates with increase in cytotoxicity. *J Exp Med.* **169**(6), pp.2211-2225.

Ljunggren, H.G. and Karre, K. 1985. Host resistance directed selectively against H-2-deficient lymphoma variants. Analysis of the mechanism. *J Exp Med.* **162**(6), pp.1745-1759.

Lopez-Verges, S., Milush, J.M., Schwartz, B.S., Pando, M.J., Jarjoura, J., York, V.A., Houchins, J.P., Miller, S., Kang, S.M., Norris, P.J., Nixon, D.F. and Lanier, L.L. 2011. Expansion of a unique CD57(+) NKG2C(hi) natural killer cell subset during acute human

cytomegalovirus infection. *Proceedings of the National Academy of Sciences of the United States of America.* **108**(36), pp.14725-14732.

Lucas, M., Schachterle, W., Oberle, K., Aichele, P. and Diefenbach, A. 2007. Dendritic cells prime natural killer cells by trans-presenting interleukin 15. *Immunity.* **26**(4), pp.503-517.

Ma, X.J., Chow, J.M., Gri, G., Carra, G., Gerosa, F., Wolf, S.E., Dzialo, R. and Trinchieri, G. 1996. The interleukin 12 p40 gene promoter is primed by interferon gamma in monocytic cells. *Journal of Experimental Medicine.* **183**(1), pp.147-157.

Mack, E.A., Kallal, L.E., Demers, D.A. and Biron, C.A. 2011. Type 1 interferon induction of natural killer cell gamma interferon production for defense during lymphocytic choriomeningitis virus infection. *MBio.* **2**(4), pp.e00169-00111.

Mandelboim, O., Lieberman, N., Lev, M., Paul, L., Arnon, T.I., Bushkin, Y., Davis, D.M., Strominger, J.L., Yewdell, J.W. and Porgador, A. 2001. Recognition of haemagglutinins on virus-infected cells by NKp46 activates lysis by human NK cells. *Nature.* **409**(6823), pp.1055-1060.

Marais, A., Cherfils-Vicini, J., Viant, C., Degouve, S., Viel, S., Fenis, A., Rabilloud, J., Mayol, K., Tavares, A., Bienvenu, J., Gangloff, Y.G., Gilson, E., Vivier, E. and Walzer, T. 2014. The metabolic checkpoint kinase mTOR is essential for IL-15 signaling during the development and activation of NK cells. *Nature Immunology.* **15**(8), pp.749-757.

Marquardt, N., Wilk, E., Pokoyski, C., Schmidt, R.E. and Jacobs, R. 2010. Murine CXCR3+CD27bright NK cells resemble the human CD56bright NK-cell population. *Eur J Immunol.* **40**(5), pp.1428-1439.

Martin-Fontecha, A., Thomsen, L.L., Brett, S., Gerard, C., Lipp, M., Lanzavecchia, A. and Sallusto, F. 2004. Induced recruitment of NK cells to lymph nodes provides IFN-gamma for T(H)1 priming. *Nature Immunology.* **5**(12), pp.1260-1265.

Martinez, J., Huang, X.P. and Yang, Y.P. 2008. Direct action of type IIFN on NK cells is required for their activation in response to vaccinia viral infection in vivo. *Journal of Immunology.* **180**(3), pp.1592-1597.

Matikainen, S., Paananen, A., Miettinen, M., Kurimoto, M., Timonen, T., Julkunen, I. and Sareneva, T. 2001. IFN-alpha and IL-18 synergistically enhance IFN-gamma production in human NK cells: differential regulation of Stat4 activation and IFN-gamma gene expression by IFN-alpha and IL-12. *European Journal of Immunology.* **31**(7), pp.2236-2245.

Matloubian, M., Lo, C.G., Cinamon, G., Lesneski, M.J., Xu, Y., Brinkmann, V., Allende, M.L., Proia, R.L. and Cyster, J.G. 2004. Lymphocyte egress from thymus and peripheral lymphoid organs is dependent on S1P receptor 1. *Nature.* **427**(6972), pp.355-360.

Meade, J.L., de Wynter, E.A., Brett, P., Sharif, S.M., Woods, C.G., Markham, A.F. and Cook, G.P. 2006. A family with Papillon-Lefevre syndrome reveals a requirement for

cathepsin C in granzyme B activation and NK cell cytolytic activity. *Blood.* **107**(9), pp.3665-3668.

Miller, J.F. and Sprent, J. 1971. Cell-to-cell interaction in the immune response. VI. Contribution of thymus-derived cells and antibody-forming cell precursors to immunological memory. *J Exp Med.* **134**(1), pp.66-82.

Mishra, A., Sullivan, L. and Caligiuri, M.A. 2014. Molecular Pathways: Interleukin-15 Signaling in Health and in Cancer. *Clinical Cancer Research.* **20**(8), pp.2044-2050.

Miyagi, T., Gil, M.P., Wang, X., Louten, J., Chu, W.M. and Biron, C.A. 2007. High basal STAT4 balanced by STAT1 induction to control type 1 interferon effects in natural killer cells. *J Exp Med.* **204**(10), pp.2383-2396.

Moretta, A., Vitale, M., Bottino, C., Orengo, A.M., Morelli, L., Augugliaro, R., Barbaresi, M., Ciccone, E. and Moretta, L. 1993. P58 Molecules as Putative Receptors for Major Histocompatibility Complex (Mhc) Class-I Molecules in Human Natural-Killer (Nk) Cells - Anti-P58 Antibodies Reconstitute Lysis of Mhc Class-I-Protected Cells in Nk Clones Displaying Different Specificities. *Journal of Experimental Medicine.* **178**(2), pp.597-604.

Mortier, E., Woo, T., Advincula, R., Gozalo, S. and Ma, A. 2008. IL-15R alpha chaperones IL-15 to stable dendritic cell membrane complexes that activate NK cells via trans presentation. *Journal of Experimental Medicine.* **205**(5), pp.1213-1225.

Morvan, M.G. and Lanier, L.L. 2016. NK cells and cancer: you can teach innate cells new tricks. *Nature Reviews Cancer.* **16**(1), pp.7-19.

Nandagopal, N., Ali, A.K., Komal, A.K. and Lee, S.H. 2014. The critical role of IL-15-PI3K-mTOR pathway in natural killer cell effector functions. *Frontiers in Immunology.* **5**, p187.

Neil, S.J.D., Zang, T. and Bieniasz, P.D. 2008. Tetherin inhibits retrovirus release and is antagonized by HIV-1 Vpu. *Nature.* **451**(7177), pp.425-430.

Nguyen, K.B., Salazar-Mather, T.P., Dalod, M.Y., Van Deusen, J.B., Wei, X.Q., Liew, F.Y., Caligiuri, M.A., Durbin, J.E. and Biron, C.A. 2002a. Coordinated and distinct roles for IFN-alpha beta, IL-12, and IL-15 regulation of NK cell responses to viral infection. *Journal of Immunology.* **169**(8), pp.4279-4287.

Nguyen, K.B., Watford, W.T., Salomon, R., Hofmann, S.R., Pien, G.C., Morinobu, A., Gadina, M., O'Shea, J.J. and Biron, C.A. 2002b. Critical role for STAT4 activation by type 1 interferons in the interferon-gamma response to viral infection. *Science.* **297**(5589), pp.2063-2066.

Nguyen, T.P., Bazdar, D.A., Mudd, J.C., Lederman, M.M., Harding, C.V., Hardy, G.A. and Sieg, S.F. 2015. Interferon-alpha inhibits CD4 T cell responses to interleukin-7 and interleukin-2 and selectively interferes with Akt signaling. *Journal of Leukocyte Biology.* **97**(6), pp.1139-1146.

Niu, G.D., Hu, W.P., Wang, L., Chen, X.Q. and Lin, L. 2016. Overexpression of IFIT1 suppresses proliferation and promotes apoptosis of mouse podocytes. *International Journal of Clinical and Experimental Medicine.* **9**(11), pp.21580-21584.

Norman, K.L., Hirasawa, K., Yang, A.D., Shields, M.A. and Lee, P.W.K. 2004. Reovirus oncolysis: The Ras/RalGEF/p38 pathway dictates host cell permissiveness to reovirus infection. *Proceedings of the National Academy of Sciences of the United States of America.* **101**(30), pp.11099-11104.

Nussenzweig, M.C., Steinman, R.M., Gutchinov, B. and Cohn, Z.A. 1980. Dendritic cells are accessory cells for the development of anti-trinitrophenyl cytotoxic T lymphocytes. *J Exp Med.* **152**(4), pp.1070-1084.

OConnell, J., OSullivan, G.C., Collins, J.K. and Shanahan, F. 1996. The Fas counterattack: Fas-mediated T cell killing by colon cancer cells expressing Fas ligand. *Journal of Experimental Medicine.* **184**(3), pp.1075-1082.

Okada, T., Ngo, V.N., Ekland, E.H., Forster, R., Lipp, M., Littman, D.R. and Cyster, J.G. 2002. Chemokine requirements for B cell entry to lymph nodes and Peyer's patches. *Journal of Experimental Medicine.* **196**(1), pp.65-75.

Orange, J.S. 2013. Natural killer cell deficiency. *J Allergy Clin Immunol.* **132**(3), pp.515-525.

Parrish, C., Scott, G.B., Migneco, G., Scott, K.J., Steele, L.P., Ilett, E., West, E.J., Hall, K., Selby, P.J., Buchanan, D., Varghese, A., Cragg, M.S., Coffey, M., Hillmen, P., Melcher, A.A. and Errington-Mais, F. 2015. Oncolytic reovirus enhances rituximab-mediated antibody-dependent cellular cytotoxicity against chronic lymphocytic leukaemia. *Leukemia.* **29**(9), pp.1799-1810.

Pegram, H.J., Andrews, D.M., Smyth, M.J., Darcy, P.K. and Kershaw, M.H. 2011. Activating and inhibitory receptors of natural killer cells. *Immunology and Cell Biology.* **89**(2), pp.216-224.

Pende, D., Rivera, P., Marcenaro, S., Chang, C.C., Biassoni, R., Conte, R., Kubin, M., Cosman, D., Ferrone, S., Moretta, L. and Moretta, A. 2002. Major histocompatibility complex class I-related chain a and UL16-binding protein expression on tumor cell lines of different histotypes: Analysis of tumor susceptibility to NKG2D-dependent natural killer cell cytotoxicity. *Cancer Research.* **62**(21), pp.6178-6186.

Platanias, L.C. 2005. Mechanisms of type-I- and type-II-interferon-mediated signalling. *Nature Reviews Immunology.* **5**(5), pp.375-386.

Pollmann, J., Gotz, J.J., Rupp, D., Strauss, O., Granzin, M., Grunvogel, O., Mutz, P., Kramer, C., Lasitschka, F., Lohmann, V., Bjorkstrom, N.K., Thimme, R., Bartenschlager, R. and Cerwenka, A. 2017. Hepatitis C virus-induced natural killer cell proliferation involves monocyte-derived cells and the OX40/OX40L axis. *J Hepatol.* **68**(3), pp.421-430.

Poltorak, A., He, X., Smirnova, I., Liu, M.Y., Van Huffel, C., Du, X., Birdwell, D., Alejos, E., Silva, M., Galanos, C., Freudenberg, M., Ricciardi-Castagnoli, P., Layton, B. and Beutler, B. 1998. Defective LPS signaling in C3H/HeJ and C57BL/10ScCr mice: mutations in Tlr4 gene. *Science.* **282**(5396), pp.2085-2088.

Prestwich, R.J., Errington, F., Ilett, E.J., Morgan, R.S.M., Scott, K.J., Kottke, T., Thompson, J., Morrison, E.E., Harrington, K.J., Pandha, H.S., Selby, P.J., Vile, R.G. and Melcher, A.A. 2008. Tumor Infection by Oncolytic Reovirus Primes Adaptive Antitumor Immunity. *Clinical Cancer Research.* **14**(22), pp.7358-7366.

Ranson, T., Vosshenrich, C.A.J., Corcuff, E., Richard, O., Muller, W. and Di Santo, J.P. 2003. IL-15 is an essential mediator of peripheral NK-cell homeostasis. *Blood.* **101**(12), pp.4887-4893.

Robertson, M.J., Manley, T.J., Donahue, C., Levine, H. and Ritz, J. 1993. Costimulatory Signals Are Required for Optimal Proliferation of Human Natural-Killer-Cells. *Journal of Immunology.* **150**(5), pp.1705-1714.

Roder, G., Geironson, L., Bressendorff, I. and Paulsson, K. 2008. Viral proteins interfering with antigen presentation target the major histocompatibility complex class I peptide-loading complex. *J Virol.* **82**(17), pp.8246-8252.

Romagnani, C., Della Chiesa, M., Kohler, S., Moewes, B., Radbruch, A., Moretta, L., Moretta, A. and Thiel, A. 2005. Activation of human NK cells by plasmacytoid dendritic cells and its modulation by CD4(+) T helper cells and CD4(+) CD25(hi) T regulatory cells. *European Journal of Immunology.* **35**(8), pp.2452-2458.

Sahin, E., Egger, M.E., McMasters, K.M. and Zhou, H.S. 2013. Development of Oncolytic Reovirus for Cancer Therapy. *Journal of Cancer Therapy.* **4**(6), pp.1100-1115.

Salazar-Mather, T.P., Orange, J.S. and Biron, C.A. 1998. Early murine cytomegalovirus (MCMV) infection induces liver natural killer (NK) cell inflammation and protection through macrophage inflammatory protein 1 alpha (MIP-1 alpha)-dependent pathways. *Journal of Experimental Medicine.* **187**(1), pp.1-14.

Samson, A., Bentham, M.J., Scott, K., Nuovo, G., Bloy, A., Appleton, E., Adair, R.A., Dave, R., Peckham-Cooper, A., Toogood, G., Nagamori, S., Coffey, M., Vile, R., Harrington, K., Selby, P., Errington-Mais, F., Melcher, A. and Griffin, S. 2016. Oncolytic reovirus as a combined antiviral and anti-tumour agent for the treatment of liver cancer. *Gut.* **67**(3), pp.562-573.

Sangfelt, O., Erickson, S., Castro, J., Heiden, T., Gustafsson, A., Einhorn, S. and Grander, D. 1999. Molecular mechanisms underlying interferon-alpha-induced G0/G1 arrest: CKI-mediated regulation of G1 Cdk-complexes and activation of pocket proteins. *Oncogene.* **18**(18), pp.2798-2810.

Sangfelt, O., Erickson, S., Einhorn, S. and Grander, D. 1997. Induction of Cip/Kip and Ink4 cyclin dependent kinase inhibitors by interferon-alpha in hematopoietic cell lines. *Oncogene.* **14**(4), pp.415-423.

Sangfelt, O., Erickson, S. and Grander, D. 2000. Mechanisms of interferon-induced cell cycle arrest. *Frontiers in Bioscience.* **5**, pp.D479-D487.

Santoli, D., Trinchieri, G. and Koprowski, H. 1978. Cell-Mediated Cytotoxicity against Virus-Infected Target-Cells in Humans .2. Interferon Induction and Activation of Natural Killer Cells. *Journal of Immunology.* **121**(2), pp.532-538.

Sarasin-Filipowicz, M., Wang, X.Y., Yan, M., Duong, F.H.T., Poli, V., Hilton, D.J., Zhang, D.E. and Heim, M.H. 2009. Alpha Interferon Induces Long-Lasting Refractoriness of JAK-STAT Signaling in the Mouse Liver through Induction of USP18/UBP43. *Molecular and Cellular Biology.* **29**(17), pp.4841-4851.

Sato, K., Hida, S., Takayanagi, H., Yokochi, T., Kayagaki, N., Takeda, K., Yagita, H., Okumura, K., Tanaka, N., Taniguchi, T. and Ogasawara, K. 2001. Antiviral response by natural killer cells through TRAIL gene induction by IFN-alpha/beta. *European Journal of Immunology.* **31**(11), pp.3138-3146.

Sato, M., Hata, N., Asagiri, M., Nakaya, T., Taniguchi, T. and Tanaka, N. 1998. Positive feedback regulation of type I IFN genes by the IFN-inducible transcription factor IRF-7. *Febs Letters.* **441**(1), pp.106-110.

Schatz, D.G., Oettinger, M.A. and Baltimore, D. 1989. The V(D)J recombination activating gene, RAG-1. *Cell.* **59**(6), pp.1035-1048.

Schneider, W.M., Chevillotte, M.D. and Rice, C.M. 2014. Interferon-stimulated genes: a complex web of host defenses. *Annu Rev Immunol.* **32**, pp.513-545.

Shiow, L.R., Rosen, D.B., Brdickova, N., Xu, Y., An, J., Lanier, L.L., Cyster, J.G. and Matloubian, M. 2006. CD69 acts downstream of interferon-alpha/beta to inhibit S1P1 and lymphocyte egress from lymphoid organs. *Nature.* **440**(7083), pp.540-544.

Smyth, M.J., Crowe, N.Y. and Godfrey, D.I. 2001. NK cells and NKT cells collaborate in host protection from methylcholanthrene-induced fibrosarcoma. *Int Immunol.* **13**(4), pp.459-463.

Sobecki, M., Mrouj, K., Colinge, J., Gerbe, F., Jay, P., Krasinska, L., Dulic, V. and Fisher, D. 2017. Cell-Cycle Regulation Accounts for Variability in Ki-67 Expression Levels. *Cancer Research.* **77**(10), pp.2722-2734.

Steele, L., Errington, F., Prestwich, R., Ilett, E., Harrington, K., Pandha, H., Coffey, M., Selby, P., Vile, R. and Melcher, A. 2011. Pro-inflammatory cytokine/chemokine production by reovirus treated melanoma cells is PKR/NF-kappaB mediated and supports innate and adaptive anti-tumour immune priming. *Mol Cancer.* **10**(20), pp.1-13.

Stinchcombe, J.C. and Griffiths, G.M. 2007. Secretory mechanisms in cell-mediated cytotoxicity. *Annual Review of Cell and Developmental Biology.* **23**, pp.495-517.

Strengell, M., Matikainen, S., Siren, J., Lehtonen, A., Foster, D., Julkunen, I. and Sareneva, T. 2003. IL-21 in synergy with IL-15 or IL-18 enhances IFN-gamma production in human NK and T cells. *Journal of Immunology.* **170**(11), pp.5464-5469.

Strong, J.E., Coffey, M.C., Tang, D., Sabinin, P. and Lee, P.W.K. 1998. The molecular basis of viral oncolysis: usurpation of the Ras signaling pathway by reovirus. *Embo Journal.* **17**(12), pp.3351-3362.

Sutlu, T. and Alici, E. 2009. Natural killer cell-based immunotherapy in cancer: current insights and future prospects. *Journal of Internal Medicine.* **266**(2), pp.154-181.

Sutton, V.R., Davis, J.E., Cancilla, M., Johnstone, R.W., Ruefli, A.A., Sedelies, K., Browne, K.A. and Trapani, J.A. 2000. Initiation of apoptosis by granzyme B requires direct cleavage of bid, but not direct granzyme B-mediated caspase activation. *J Exp Med.* **192**(10), pp.1403-1414.

Tagaya, Y., Bamford, R.N., DeFilippis, A.P. and Waldmann, T.A. 1996. IL-15: A pleiotropic cytokine with diverse receptor/signaling pathways whose expression is controlled at multiple levels. *Immunity.* **4**(4), pp.329-336.

Takeda, K., Cretney, E., Hayakawa, Y., Ota, T., Akiba, H., Ogasawara, K., Yagita, H., Kinoshita, K., Okumura, K. and Smyth, M.J. 2005. TRAIL identifies immature natural killer cells in newborn mice and adult mouse liver. *Blood.* **105**(5), pp.2082-2089.

Thierfelder, W.E., vanDeursen, J.M., Yamamoto, K., Tripp, R.A., Sarawar, S.R., Carson, R.T., Sangster, M.Y., Vignali, D.A.A., Doherty, P.C., Grosveld, G.C. and Ihle, J.N. 1996. Requirement for Stat4 in interleukin-12-mediated responses of natural killer and T cells. *Nature.* **382**(6587), pp.171-174.

Trapani, J.A. 2001. Granzymes: a family of lymphocyte granule serine proteases. *Genome Biol.* **2**(12), pp.3014.3011-3014.3017.

Trotta, R., Parihar, R., Yu, J.H., Becknell, B., Allard, J., Wen, J., Ding, W., Mao, H., Tridandapani, S., Carson, W.E. and Caligiuri, M.A. 2005. Differential expression of SHIP1 in CD56(bright) and CD56(dim) NK cells provides a molecular basis for distinct functional responses to monokine costimulation. *Blood.* **105**(8), pp.3011-3018.

Twigger, K., Roulstone, V., Kyula, J., Karapanagiotou, E.M., Syrigos, K.N., Morgan, R., White, C., Bhide, S., Nuovo, G., Coffey, M., Thompson, B., Jebar, A., Errington, F., Melcher, A.A., Vile, R.G., Pandha, H.S. and Harrington, K.J. 2012. Reovirus exerts potent oncolytic effects in head and neck cancer cell lines that are independent of signalling in the EGFR pathway. *BMC Cancer.* **12**(368), pp.1-16.

Van Acker, H.H., Capsomidis, A., Smits, E.L. and Van Tendeloo, V.F. 2017. CD56 in the immune System: More Than a Marker for Cytotoxicity? *Frontiers in Immunology.* **8**, p892.

Van de Wiele, C.J., Marino, J.H., Whetsell, M.E., Vo, S.S., Masengale, R.M. and Teague, T.K. 2004. Loss of interferon-induced Stat1 phosphorylation in activated T cells. *Journal of Interferon and Cytokine Research.* **24**(3), pp.169-178.

Vitale, M., Bassini, A., Secchiero, P., Mirandola, P., Ponti, C., Zamai, L., Mariani, A.R., Falconi, M. and Azzali, G. 2002. NK-active cytokines IL-2, IL-12, and IL-15 selectively modulate specific protein kinase C (PKC) isoforms in primary human NK cells. *Anatomical Record.* **266**(2), pp.87-92.

Vivier, E., Nunes, J.A. and Vely, F. 2004. Natural killer cell signaling pathways. *Science.* **306**(5701), pp.1517-1519.

Voskoboinik, I., Whisstock, J.C. and Trapani, J.A. 2015. Perforin and granzymes: function, dysfunction and human pathology. *Nat Rev Immunol.* **15**(6), pp.388-400.

Waldmann, T.A. 2015. The Shared and Contrasting Roles of IL2 and IL15 in the Life and Death of Normal and Neoplastic Lymphocytes: Implications for Cancer Therapy. *Cancer Immunology Research.* **3**(3), pp.219-227.

Walker, J.R., McGeagh, K.G., Sundaresan, P., Jorgensen, T.J., Rabkin, S.D. and Martuza, R.L. 1999. Local and systemic therapy of human prostate adenocarcinoma with the conditionally replicating herpes simplex virus vector G207. *Human Gene Therapy.* **10**(13), pp.2237-2243.

Walzer, T., Chiossone, L., Chaix, J., Calver, A., Carozzo, C., Garrigue-Antar, L., Jacques, Y., Baratin, M., Tomasello, E. and Vivier, E. 2007. Natural killer cell trafficking in vivo requires a dedicated sphingosine 1-phosphate receptor. *Nature Immunology.* **8**(12), pp.1337-1344.

Warren, H.S. and Smyth, M.J. 1999. NK cells and apoptosis. *Immunology and Cell Biology.* **77**(1), pp.64-75.

Wilson, E.B., El-Jawhari, J.J., Neilson, A.L., Hall, G.D., Melcher, A.A., Meade, J.L. and Cook, G.P. 2011. Human tumour immune evasion via TGF-beta blocks NK cell activation but not survival allowing therapeutic restoration of anti-tumour activity. *PLoS One.* **6**(9), pe22842.

Xaus, J., Cardo, M., Valledor, A.F., Soler, C., Lloberas, J. and Celada, A. 1999. Inteferon gamma induces the expression of p21(waf-1) and arrests macrophage cell cycle, preventing induction of apoptosis. *Immunity.* **11**(1), pp.103-113.

Yatim, K.M. and Lakkis, F.G. 2015. A Brief Journey through the Immune System. *Clinical Journal of the American Society of Nephrology.* **10**(7), pp.1274-1281.

Yewdell, J.W. and Hill, A.B. 2002. Viral interference with antigen presentation. *Nat Immunol.* **3**(11), pp.1019-1025.

Yoo, J.K., Cho, J.H., Lee, S.W. and Sung, Y.C. 2002. IL-12 provides proliferation and survival signals to murine CD4(+) T cells through phosphatidylinositol 3-kinase/Akt signaling pathway. *Journal of Immunology.* **169**(7), pp.3637-3643.

Ythier, A., Delmon, L., Reinherz, E., Nowill, A., Moingeon, P., Mishal, Z., Bohuon, C. and Hercend, T. 1985. Proliferative Responses of Circulating Human Nk Cells - Delineation

of a Unique Pathway Involving Both Direct and Helper Signals. *European Journal of Immunology.* **15**(12), pp.1209-1215.

Yusa, S. and Campbell, K.S. 2003. Src homology region 2-containing protein tyrosine phosphatase-2 (SHP-2) can play a direct role in the inhibitory function of killer cell Ig-like receptors in human NK cells. *J Immunol.* **170**(9), pp.4539-4547.

Zaas, A.K., Burke, T., Chen, M., McClain, M., Nicholson, B., Veldman, T., Tsalik, E.L., Fowler, V., Rivers, E.P., Otero, R., Kingsmore, S.F., Voora, D., Lucas, J., Hero, A.O., Carin, L., Woods, C.W. and Ginsburg, G.S. 2013. A host-based RT-PCR gene expression signature to identify acute respiratory viral infection. *Sci Transl Med.* **5**(203), p203ra126.

Zamai, L., Ahmad, M., Bennett, I.M., Azzoni, L., Alnemri, E.S. and Perussia, B. 1998. Natural killer (NK) cell-mediated cytotoxicity: Differential use of TRAIL and Fas ligand by immature and mature primary human NK cells. *Journal of Experimental Medicine.* **188**(12), pp.2375-2380.

Zanoni, I., Spreafico, R., Bodio, C., Di Gioia, M., Cigni, C., Broggi, A., Gorletta, T., Caccia, M., Chirico, G., Sironi, L., Collini, M., Colombo, M.P., Garbi, N. and Granucci, F. 2013. IL-15 cis Presentation Is Required for Optimal NK Cell Activation in Lipopolysaccharide-Mediated Inflammatory Conditions. *Cell Reports.* **4**(6), pp.1235-1249.

Ziegler, S.F., Ramsdell, F. and Alderson, M.R. 1994. The Activation Antigen Cd69. *Stem Cells.* **12**(5), pp.456-465.

Appendix 1

Metacore pathway enrichment

Reovirus differentially expressed genes (>1.5 fold or <-1.5 fold, FDR p value<0.05) in the *Cell cycle_S phase* process network:

Network Object Name	Gene Symbol	Unit (protein or chem)	Reo/Untreated fold change	
			Signal	FDR p-value
AHR	AHR	AHR_HUMAN	2.02	0.032744
BRIP1	BRIP1	FANCJ_HUMAN	2.42	0.021595
BUB1	BUB1	BUB1_HUMAN	3.71	0.017424
Brca2	BRCA2	BRCA2_HUMAN	6.19	0.005472
CAF-1	CHAF1A	CAF1A_HUMAN	1.51	0.046469
CAF-1	CHAF1B	CAF1B_HUMAN	-1.56	0.01233
CDC45L	CDC45	CDC45_HUMAN	1.51	0.044396
CDC7	CDC7	CDC7_HUMAN	1.94	0.009222
CDK1 (p34)	CDK1	CDK1_HUMAN	1.99	0.048162
CDK2	CDK2	CDK2_HUMAN	2.68	0.00482
CRM1	XPO1	XPO1_HUMAN	1.59	0.009648
Cyclin A	CCNA2	CCNA2_HUMAN	3.04	0.048542
DNA polymerase sigma	PAPD7	PAPD7_HUMAN	2.36	0.02835
DRF1	DBF4B	DBF4B_HUMAN	1.72	0.018988
Emi1	FBXO5	FBX5_HUMAN	1.63	0.007568
FEN1	FEN1	FEN1_HUMAN	1.58	0.033812
Geminin	GMNN	GEMI_HUMAN	1.72	0.046444
HSP90	HSP90AA1	HS90A_HUMAN	1.51	0.030584
Histone H1	HIST1H1C	H12_HUMAN	1.8	0.012946
MCM10	MCM10	MCM10_HUMAN	1.94	0.02193
MCM4	MCM4	MCM4_HUMAN	2.08	0.026898
MCM4/6/7 complex	MCM6	MCM6_HUMAN	2.06	0.02371
Nek2A	NEK2	NEK2_HUMAN	1.53	0.036101
Nibrin	NBN	NBN_HUMAN	1.56	0.01028
PCNA	PCNA	PCNA_HUMAN	3.35	0.020906
POLD reg (p68)	POLD3	DPOD3_HUMAN	2.3	0.010331
Sgo1	SGO1	SGO1_HUMAN	1.89	0.010876
TEP1	TEP1	TEP1_HUMAN	1.54	0.00344

| TOP1 | TOP1 | TOP1_HUMAN | 2.53 | 0.002621 |